Essex Finance Centre

Working Paper Series

Working Paper No10: 11-2015

"Semi-Parametric Seasonal Unit Root Tests"

"Tomas del Barrio Castro, Paulo M.M. Rodrigues, and A.M. Robert Taylor"

Essex Business School, University of Essex, Wivenhoe Park, Colchester, CO4 3SQ
Web site: http://www.essex.ac.uk/ebs/

Semi-Parametric Seasonal Unit Root Tests*

Tomás del Barrio Castro[a], Paulo M.M. Rodrigues[b] and A.M. Robert Taylor[c]

[a] Department of Applied Economics, University of the Balearic Islands

[b] Banco de Portugal and NOVA School of Business and Economics

[c] University of Essex

November 3, 2015

Abstract

It is well known that (seasonal) unit root tests can be seriously affected by the presence of weak dependence in the driving shocks when this is not accounted for. In the non-seasonal case both parametric (based around augmentation of the test regression with lagged dependent variables) and semi-parametric (based around an estimator of the long run variance of the shocks) unit root tests have been proposed. Of these, the $\mathcal{M}$ class of unit root tests introduced by Stock (1999), Perron and Ng (1996) and Ng and Perron (2001), appear to be particularly successful, showing good finite sample size control even in the most problematic (near-cancellation) case where the shocks contain a strong negative moving average component. The aim of this paper is threefold. First we show the implications that neglected weak dependence in the shocks has on lag un-augmented versions of the well known regression-based seasonal unit root tests of Hylleberg *et al.* (1990). Second, in order to complement extant parametrically augmented versions of the tests of Hylleberg *et al.* (1990), we develop semi-parametric seasonal unit root test procedures, generalising the methods developed in the non-seasonal case to our setting. Third, we compare the finite sample size and power properties of the parametric and semi-parametric seasonal unit root tests considered. Our results suggest that the superior size/power trade-off offered by the $\mathcal{M}$ approach in the non-seasonal case carries over to the seasonal case.

Keywords: Seasonal unit roots, weak dependence, lag augmentation, long run variance estimator, demodulated process.

JEL: C12, C22.

1 Introduction

Over the last three decades, a debate has been conducted in the literature as to whether the within-year variations in seasonally observed time series processes are deterministic or

*Correspondence to: Robert Taylor, Essex Business School, University of Essex, Wivenhoe Park, Colchester, CO4 3SQ, United Kingdom. Email: rtaylor@essex.ac.uk. Tomás del Barrio Castro acknowledges financial support from projects ECO2011-23934 and ECO2014-58991-C3-3-R.

attributable to unit root(s) at the seasonal frequency components of the data. This is an important question because incorrect modelling of the seasonality present in a series has serious implications for the statistical validity of any subsequent procedures. Moreover, most available seasonally adjusted data are based on filtering methods which imply the application of seasonal differencing to the data. If the data do not contain seasonal unit roots then the resulting seasonally adjusted data will contain moving average unit roots, rendering standard autoregressive modelling methods invalid. In order to formally investigate this issue, in the seminal paper in this literature, Hylleberg, Engle, Granger and Yoo (1990) [HEGY] propose a seasonal generalisation of the regression-based augmented Dickey-Fuller [ADF] unit root test, where serial correlation in the driving shocks is accounted for by the inclusion of lagged dependent variables in the test regression. This procedure allows the practitioner to test for unit root behaviour at each of the zero and seasonal frequency components of the data, either separately or via a joint test. HEGY outline their procedure for quarterly data; this has been extended to the case of monthly data by Beaulieu and Miron (1993) and to an arbitrary seasonal periodicity, say S, by Smith and Taylor (1999) and Smith *et al.* (2009).

In the non-seasonal case it is well documented that ADF-type unit root tests can suffer from a variety of drawbacks in small samples, most notably low power under the alternative, particularly where deterministic components are present in the data which need to be accounted for (de-trending), and significant size distortions under the null when strong negative moving average behaviour in the so-called near-cancellation region is present in the driving shocks. Moreover, on the one hand finite sample power is decreased, other things equal, the greater the lag augmentation length used in the test regression, but on the other hand distortions due to near-cancellations are mitigated, other things equal, the greater the lag length used, yielding the well-known trade-of between these two aspects in finite samples.

The aforementioned issues have led to a large literature aimed at developing tests which simultaneously have both good finite sample size and power properties. In relation to the former, Elliott, Rothenberg and Stock (1996) [ERS] show that near-efficient unit root tests can be obtained by the use of local GLS, rather than conventional OLS-based, de-trending of the data. For the latter, see Perron and Ng (1996) for tests based on OLS de-trending and Ng and Perron (2001) for tests based on local GLS de-trending build on the class of modified ($\mathcal{M}$) unit root tests originally proposed in Stock (1999). These are based on statistics which do not emanate from an estimated regression and so, as such, do not use parametric lag correction to correct for weak dependence in the shocks. Rather, weak dependence is shown to appear through a nuisance parameter, the long run variance, which appears in the limit distribution of the statistics. This is then corrected for via a non-parametric estimate of that parameter. Both sums-of-covariances and autoregressive spectral density estimators can be used. Ng and Perron (2001) show that the latter combined with a new information criterion, the modified Akaike information criterion [MAIC] to select the autoregressive lag length used in that estimator perform particularly well in practice even in the presence of strong negative moving average components. As a result the $\mathcal{M}$ tests have become increasingly popular in the

unit root literature; indeed, in discussing the ADF tests, Haldrup and Jansson (2006, p. 267) argue that "... practitioners ought to abandon the use of these tests..." in favour of the $\mathcal{M}$ tests because of "... the excellent size properties and 'nearly' optimal power properties" of the latter.

The HEGY tests, like ADF tests, use parametric lag augmentation, to account for weak dependence in the shocks. Focusing on the case where the shocks follow a finite-order autoregressive process of order p $[AR(p)]$, Burridge and Taylor (2001) and Smith *et al.* (2009) show that such lag augmentation can provide only a partial solution with the limiting null distributions of certain of the harmonic frequency unit root tests still depending, in general, on the parameters of the $AR(p)$ polynomial with the consequence that not all of the HEGY-type tests can be reliably used in practice. However, it has been known since the seminal work of Box and Jenkins (1976) that seasonally observed time series tend to display significant moving average behaviour. Indeed Box and Jenkins (1976) developed the well-known seasonal ARIMA factorisations, the best known example of which being the so-called *airline model*. ARMA behaviour can also be a manifestation of neglected periodic autoregressive behaviour (see, for example, Ghysels and Osborn, 2001, Chapter 6). It is therefore particularly important that any seasonal unit root test can allow for moving average behaviour. Recently, del Barrio Castro *et al.* (2012) have demonstrated that the results of Burridge and Taylor (2001) and Smith *et al.* (2009) carry over to the case where the shocks admit a stationary and invertible ARMA representation, provided the lag augmentation length increases at any appropriate rate with the sample size, analogous to the results obtained for the ADF test by Said and Dickey (1984).

Motivated by these issues and the success of the $\mathcal{M}$ unit root tests in the non-seasonal case, the purpose of this paper is to develop a new class of regression-based seasonal unit root tests based on the $\mathcal{M}$ testing approach of Stock (1999), Perron and Ng (1996) and Ng and Perron (2001). In the case of tests at the harmonic seasonal frequencies we show that this requires the use of methods based on demodulated processes. We also develop seasonal implementations of the Phillips and Perron (1998) [PP] semi-parametric unit root tests which, like the $\mathcal{M}$ tests, are based on statistics which correct for weak dependence through an estimate of the long run variance. We show how the same can be done in the seasonal case using estimates, either sum-of-covariances-based or autoregressive spectral density-based, of the spectrum at the zero and seasonal frequency components of the data. Our analysis explicitly allows for the presence of $ARMA$ shocks. Where sums-of-covariances based estimators are used, the shocks need not be invertible but must satisfy the weaker condition that they do not admit spectral zeroes at either the zero or seasonal frequencies. Invertibility is required where autoregressive spectral density estimators are used. We demonstrate that the limiting distributions of all of the resulting PP and $\mathcal{M}$ statistics are pivotal under both the null hypothesis and under near-integrated alternatives, attaining the limiting distributions achieved by their standard HEGY counterparts when the shocks are independent and identically distributed $[IID]$. Where autoregressive spectral density estimators are used, a seasonal analogue of the MAIC criterion of Ng and Perron (2001), developed in del Barrio Castro *et al.* (2012) can be used to select the autoregressive lag length.

The remainder of the paper is organised as follows. In Section 2, we review the standard seasonal autoregressive model framework, highlight the typology of seasonal deterministic trend functions relevant for the seasonal unit root literature, outline the parameter restrictions on this model which yield (near) unit roots at the zero and seasonal frequencies, and provide a basic outline of the augmented HEGY tests. In Section 3 we discuss the implications that neglecting weak dependence has on the limit distributions of the unaugmented HEGY tests and use these representations to inform us on how to develop seasonal analogues of the non-seasonal PP unit root tests, together with seasonal analogues of the $\mathcal{M}$ class of unit root tests. The large sample properties of the new seasonal PP and seasonal $\mathcal{M}$ unit root tests are detailed in Section 4. Section 5 presents a Monte Carlo comparison of the finite sample properties of the augmented HEGY tests and the new tests. As with the non-seasonal case, our results suggest that overall the seasonal unit root tests based on the $\mathcal{M}$ approach offer the best size/power trade-off available. Section 5 concludes. Mathematical proofs are contained in the appendix.

2 The Seasonal Unit Root Framework

2.1 The Seasonal Model

Consider the univariate seasonal time-series process $\{y_{Sn+s}\}$, observed with constant seasonal periodicity, S,[1] which satisfies the following data generating process [DGP]

$$y_{Sn+s} = x_{Sn+s} + \mu_{Sn+s} \tag{2.1a}$$

$$\alpha(L)x_{Sn+s} = u_{Sn+s},\ s = 1-S, ..., 0,\ \ n = 1, 2, \ldots, N \tag{2.1b}$$

where μ_{Sn+s} is a purely deterministic component, further details on which are given below, and $\alpha(z) := 1 - \sum_{j=1}^{S} \alpha_j^* z^j$, is an $AR(S)$ polynomial in the conventional lag operator, L. In what follows we define the total sample size to be $T := SN$ and the number of harmonic seasonal frequencies to be $S^* := \lfloor (S-1)/2 \rfloor$, where $\lfloor . \rfloor$ denotes the integer part of its argument.

We assume that $\{u_{Sn+s}\}$ in (2.1b) is a mean-zero covariance stationary (linear) process satisfying the following conditions:

Assumption 1: The random error term u_{Sn+s} in (2.1b) follows the linear process $u_{Sn+s} = \psi(L)\varepsilon_{Sn+s}$, where ε_{Sn+s} is $IID(0, \sigma_\varepsilon^2)$ with finite fourth order moments and where the lag polynomial $\psi(z) := 1 + \sum_{j=1}^{\infty} \psi_j z^j$ satisfies: (i) $\psi(\exp\{\pm \mathrm{i} 2\pi k/S\}) \neq 0$, $k = 0, \ldots, \lfloor S/2 \rfloor$; and (ii) $\sum_{j=1}^{\infty} j|\psi_j| < \infty$.

Assumption 1 ensures that the spectral density function of u_{Sn+s} is bounded, and that it is strictly positive at both the zero and seasonal spectral frequencies, $\omega_k := 2\pi k/S$, $k = 0, ..., \lfloor S/2 \rfloor$. Under Assumption 1 the long run variance of u_{Sn+s} may be defined as $\lambda_0^2 := \sigma_\varepsilon^2 \psi(1)^2 = \gamma_0 + 2\sum_{j=1}^{\infty} \gamma_j$, where $\gamma_j := E(u_{Sn+s}u_{Sn+s-j})$, $j = 0, 1, ...$ Notice that $\lambda_0^2 = 2\pi f_u(0)$, where $f_u(\omega)$ denotes the spectrum of $\{u_{Sn+s}\}$. Analogous quantities can be defined at the Nyquist, $\omega_{S/2} = \pi$, frequency, where S is even, as $\lambda_{S/2}^2 := \sigma_\varepsilon^2 \psi(-1)^2 = \gamma_0 +$

[1] For example, $S = 4$ yields the case of quarterly data, $S = 12$ monthly data, and $S = 1$ non-seasonal data.

$2\sum_{j=1}^{\infty}\cos[\pi j]\,\gamma_j$, and at the seasonal harmonic frequencies, $(\omega_k, 2\pi-\omega_k)$, as $\lambda_k^2 := \sigma_\varepsilon^2(a_k^2+b_k^2) = \gamma_0 + 2\sum_{j=1}^{\infty}\cos[\omega_k j]\,\gamma_j$, $k = 1, ..., S^*$, where $a_k := \mathcal{I}m(\psi[\exp(\mathrm{i}\omega_k)])$ and $b_k := \mathcal{R}e(\psi[\exp(\mathrm{i}\omega_k)])$, $k = 1, ..., S^*$, with $\mathcal{R}e(\cdot)$ and $\mathcal{I}m(\cdot)$ denoting the real and imaginary parts of their arguments, respectively. Notice that $\lambda_{S/2}^2 = 2\pi f_u(\pi)$ and $\lambda_k^2 = 2\pi f_u(2\pi k/S)$, $k = 1, ..., S^*$.

For the deterministic component in (2.1a), $\mu_{Sn+s} := \delta' z_{Sn+s,\xi}$, we consider three empirically relevant cases ($\xi = 1, 2, 3$). Here and in what follows, it is understood that terms relating to frequency π are to be omitted when S is odd and that where reference is made to the Nyquist frequency this is understood only to apply where S is even.

Case 1: Zero and seasonal frequency intercepts:

$$\begin{aligned} z_{Sn+s,1} := \quad & [1, \cos(2\pi(Sn+s)/S), \sin(2\pi(Sn+s)/S), ... \\ & ..., \cos(2\pi S^*(Sn+s)/S), \sin(2\pi S^*(Sn+s)/S), (-1)^{Sn+s}]', \end{aligned}$$

$s = 1-S, ..., 0$, $n = 1, ..., N$, with $\delta := \left(\delta_0, \delta_1', ..., \delta_{S^*}', \delta_{S/2}\right)'$ and $\delta_k := (\delta_{k,1}, \delta_{k,2})'$, $k = 1, ..., S^*$.

Case 2: Zero and seasonal frequency intercepts, and zero frequency trend:

$$z_{Sn+s,2} := \left[z_{Sn+s,1}', Sn+s\right]',$$

$s = 1-S, ..., 0$, $n = 1, ..., N$, with $\delta := \left(\delta_0, \delta_1', ..., \delta_{S^*}', \delta_{S/2}, \overline{\delta}_0\right)'$ and $\delta_k := (\delta_{k,1}, \delta_{k,2})'$, $k = 1, ..., S^*$.

Case 3: Zero and seasonal frequency intercepts and trends:

$$z_{Sn+s,3} := \left[z_{Sn+s,1}', (Sn+s)\, z_{Sn+s,1}'\right]',$$

$s = 1-S, ..., 0$, $n = 1, ..., N$, with $\delta := \left(\delta_0, \delta_1', ..., \delta_{S^*}', \delta_{S/2}, \overline{\delta}_0, \overline{\delta}_1', ..., \overline{\delta}_{S^*}', \overline{\delta}_{S/2}\right)'$ and $\overline{\delta}_k := \left(\overline{\delta}_{k,1}, \overline{\delta}_{k,2}\right)'$, $k = 1, ..., S^*$.

Following Elliot, Rothenberg and Stock (1996) and Rodrigues and Taylor (2007), the initial conditions, $x_{1-S}, ..., x_0$, are taken to be of $o_p(T^{1/2})$. Relaxing this assumption will not alter the limiting null distributions of the test statistics we outline in this paper because tests based on data which have been de-trended under Cases 1, 2 or 3 will be exact similar with respect to the initial conditions; see Smith *et al.* (2009).

2.2 The Seasonal Unit Root Hypotheses

The focus of this paper is on tests for seasonal unit roots in the Sth order polynomial $\alpha(L)$ of (2.1b). This polynomial can be factorised at the zero and seasonal spectral frequencies, ω_k, $k = 0, \ldots, \lfloor S/2 \rfloor$, so that $\alpha(L) = \prod_{k=0}^{\lfloor S/2 \rfloor} \omega_k(L)$, where $\omega_0(L) := (1-\alpha_0 L)$ associates the parameter α_0 with the zero frequency ($\omega_0 = 0$), $\omega_k(L) := \{1 - 2[\alpha_k \cos(\omega_k) - \beta_k \sin(\omega_k)]L + (\alpha_k^2+\beta_k^2)L^2\}$ corresponds to the conjugate (harmonic) seasonal frequencies $(\omega_k, 2\pi-\omega_k)$, with the associated parameters α_k and β_k, $k = 1, \ldots, S^*$, and $\omega_{S/2}(L) := \left(1+\alpha_{S/2}L\right)$ which associates the $\alpha_{S/2}$ parameter with the Nyquist frequency ($\omega_{S/2} = \pi$).

Our interest in this paper centers on testing the $(\lfloor S/2 \rfloor + 1)$ unit root null hypotheses,

$$H_{0,0} : \alpha_0 = 1, \qquad H_{0,S/2} : \alpha_{S/2} = 1, \qquad H_{0,k} : \alpha_k = 1, \quad \beta_k = 0, \quad k = 1, \ldots, S^* \tag{2.2}$$

such that $H_{0,0}$ corresponds to a unit root at the zero frequency, while $H_{0,S/2}$ yields a unit root at the Nyquist frequency, and finally $H_{0,k}$, $k = 1, \ldots, S^*$, yields a pair of complex conjugate unit roots at the harmonic seasonal frequencies $(\omega_k, 2\pi - \omega_k)$. In order to examine the asymptotic local power properties of the test procedures we discuss, we follow Rodrigues (2001) and Rodrigues and Taylor (2007) and focus attention on the alternative hypotheses of near integration at the zero, Nyquist and harmonic seasonal frequencies; that is,

$$\begin{gathered} H_{1,c_0} : \alpha_0 = \exp\left(\tfrac{c_0}{T}\right) \cong \left(1 + \tfrac{c_0}{T}\right), \qquad H_{1,c_{S/2}} : \alpha_{S/2} = \exp\left(\tfrac{c_{S/2}}{T}\right) \cong \left(1 + \tfrac{c_{S/2}}{T}\right), \\ H_{1,c_k} : \alpha_k = \exp\left(\tfrac{c_k}{T}\right) \cong \left(1 + \tfrac{c_k}{T}\right) \cap \beta_k = 0, \quad k = 1, \ldots, S^* \end{gathered} \tag{2.3}$$

where c_k, $k = 0, \ldots, \lfloor S/2 \rfloor$ are fixed constants. Under H_{1,c_k} the process $\{y_{Sn+s}\}$ admits either a single root $(k = 0, S/2)$ or a pair of complex conjugate roots $(k = 1, \ldots, S^*)$ with modulus in the neighbourhood of unity at frequency ω_k. These roots are stable for $c_k < 0$ and explosive for $c_k > 0$. Notice that H_{1,c_k} reduces to $H_{0,k}$ where $c_k = 0$, $k = 0, \ldots, \lfloor S/2 \rfloor$. In what follows, let $\mathbf{c} := (c_0, c_1, ..., c_{\lfloor S/2 \rfloor})'$ be the $(\lfloor S/2 \rfloor + 1)$-vector of non-centrality parameters and denote the lag polynomial $\alpha(L)$ under $H_{1,\mathbf{c}} := \cap_{k=0}^{\lfloor S/2 \rfloor} H_{1,c_k}$ as $\Delta_{\mathbf{c}} := 1 - \sum_{j=1}^{S} \alpha_j^{\mathbf{c}} L^j$.

2.3 The Seasonal Unit Root Test Regression and Augmented HEGY Tests

Following HEGY (1990) and Smith *et al.* (2009), among others, the regression-based approach to testing for seasonal unit roots in $\alpha(L)$ consists of two steps. In the first step one de-trends the data in order to yield tests which will be exact invariant (assuming μ_{Sn+s} is not under-specified) to the elements of δ which characterise the deterministic component μ_{Sn+s} in (2.1a). This can either be done using OLS de-trending, as in, for example, HEGY and Smith *et al.* (2009), or by local GLS de-trending as in Rodrigues and Taylor (2007). We define the resulting de-trended data series as $y_{Sn+s}^{\xi} := y_{Sn+s} - \hat{\delta}_\tau' z_{Sn+s,\xi}$ where $\xi = 1$, 2 and 3 corresponds to the deterministic kernels defined in Cases 1, 2 and 3 above, and where $\tau = 1$ indicates OLS de-trending and $\tau = 2$ local GLS de-trending.[2] That is, $\hat{\delta}_1$ is the OLS estimator obtained from regressing y_{Sn+s} onto $z_{Sn+s,\xi}$. While, as in Rodrigues and Taylor (2007), $\hat{\delta}_2$ is obtained from the OLS regression of $\mathbf{y_c}$ on $\mathbf{z_{c,\xi}}$, where

$$\begin{aligned} \mathbf{y_c} &:= (y_{1-S}, y_{2-S} - \alpha_1^{\mathbf{c}} y_{1-S}, y_{3-S} - \alpha_1^{\mathbf{c}} y_{2-S} - \alpha_2^{\mathbf{c}} y_{1-S}, ..., y_0 - \alpha_1^{\mathbf{c}} y_{-1} - \cdots - \alpha_S^{\mathbf{c}} y_{1-S}, \Delta_{\mathbf{c}} y_1, ... \Delta_{\mathbf{c}} y_T)' \\ \mathbf{z_{c,\xi}} &:= (z_{1-S,\xi}, z_{2-S,\xi} - \alpha_1^{\mathbf{c}} z_{1-S,\xi}, z_{3-S,\xi} - \alpha_1^{\mathbf{c}} z_{2-S,\xi} - \alpha_2^{\mathbf{c}} z_{1-S,\xi}, ..., z_{0,\xi} - \alpha_1^{\mathbf{c}} z_{1,\xi} - \cdots \\ &\qquad - \alpha_S^{\mathbf{c}} z_{1-S,\xi}, \Delta_{\mathbf{c}} z_{1,\xi}, ..., \Delta_{\mathbf{c}} z_{T,\xi})' \end{aligned}$$

for $\mathbf{c} = \bar{\mathbf{c}} := (\bar{c}_0, \bar{c}_1, ..., \bar{c}_{\lfloor S/2 \rfloor})'$. The local GLS de-trending parameters, $\bar{c}_k$, $k = 0, ..., \lfloor S/2 \rfloor$, are determined by the significance level that the seasonal unit root tests are to be run at and

[2] In order to economise on notation we will not introduce any specific notation to distinguish between these two different de-trending schemes.

the de-trending scheme employed; see Rodrigues and Taylor (2007, p.556). For example, under Case 1 for tests run at the 5% level, $\bar{c}_0 = \bar{c}_{S/2} = -7$ and $\bar{c}_k = -3.75$, $k = 1, ..., S^*$. The resulting de-trended series satisfies $\alpha(L)y^{\xi}_{Sn+s} = u^{\xi}_{Sn+s}$ with $u^{\xi}_{Sn+s} := \psi(L)\varepsilon^{\xi}_{Sn+s}$, where u^{ξ}_{Sn+s} and ε^{ξ}_{Sn+s} are the correspondingly de-trended versions of u_{Sn+s} and ε_{Sn+s}, respectively.

Under the additional assumption that $\psi(z)$ is invertible with (unique) inverse $\phi(z)$, such that an autoregressive approximation of order say p^* is valid, the second step is to then expand the composite $AR(p^*+S)$ polynomial $\phi^*(z) := \alpha(z)\phi(z)$ around the zero and seasonal frequency unit roots $\exp(\pm i2\pi k/S)$, $k = 0, ..., \lfloor S/2 \rfloor$, to obtain the *augmented* HEGY-type regression[3]

$$\Delta_S y^{\xi}_{Sn+s} = \sum_{k=0}^{S/2} \pi_k y^{\xi}_{k,Sn+s-1} + \sum_{j=1}^{S^*} \pi^*_j y^{*\xi}_{j,Sn+s-1} + \sum_{j=1}^{p^*} \phi^*_j \Delta_S y^{\xi}_{Sn+s-j} + u^{\xi}_{Sn+s,p^*} \tag{2.4}$$

where $\Delta_S := 1 - L^S$, and

$$y^{\xi}_{k,Sn+s} := \sum_{i=0}^{S-1} \cos[(i+1)\omega_k] y^{\xi}_{Sn+s-i}, \;\; k = 0, ..., \lfloor S/2 \rfloor \tag{2.5}$$

where $\omega_0 = 0$ and $\omega_{S/2} = \pi$; and

$$y^{*\xi}_{j,Sn+s-1} := -\sum_{i=0}^{S-1} \sin[(i+1)\omega_j] y^{\xi}_{Sn+s-i}, \tag{2.6}$$

with $\omega_j = (2\pi j)/S, j = 1, ..., S^*$. Cf. Proposition 1 of Smith *et al.* (2009, p.533).

Unit roots at the zero, Nyquist and harmonic seasonal frequencies imply that $\pi_0 = 0$, $\pi_{S/2} = 0$ and $\pi_k = \pi^*_k = 0$, $k = 1, ..., S^*$, respectively, in (2.4); see Smith *et al.* (2009). Consequently, tests for the presence or otherwise of a unit root at the zero and Nyquist frequencies are conventional lower tailed regression t-tests, denoted t_0 and $t_{S/2}$, for the exclusion of $y^{\xi}_{0,Sn+s-1}$ and $y^{\xi}_{S/2,Sn+s-1}$, respectively, from (2.4). Notice that for $S = 1$, t_0 is the standard non-seasonal ADF unit root test statistic. Similarly, the hypothesis of a pair of complex unit roots at the kth harmonic seasonal frequency may be tested by the lower-tailed t_k and two-tailed t^*_k regression t-tests from (2.4) for the exclusion of $y^{\xi}_{k,Sn+s-1}$ and $y^{*\xi}_{k,Sn+s-1}$, respectively, or by the (upper-tailed) regression F-test, denoted F_k, for the exclusion of both $y^{\xi}_{k,Sn+s-1}$ and $y^{*\xi}_{k,Sn+s-1}$ from (2.4). Ghysels *et al.* (1994) also consider the joint frequency (upper-tail) regression F-tests from (2.4), $F_{1...\lfloor S/2 \rfloor}$ for the exclusion of $y^{\xi}_{S/2,Sn+s-1}$, $\{y^{\xi}_{j,Sn+s-1}\}_{j=1}^{S^*}$ and $\{y^{*\xi}_{k,Sn+s-1}\}_{k=1}^{S^*}$, and $F_{0...\lfloor S/2 \rfloor}$ for the exclusion of $y^{\xi}_{0,Sn+s-1}$, $y^{\xi}_{S/2,Sn+s-1}$, $\{y^{\xi}_{j,Sn+s-1}\}_{j=1}^{S^*}$ and $\{y^{*\xi}_{k,Sn+s-1}\}_{k=1}^{S^*}$. The former tests the null hypothesis of unit roots at all of the seasonal frequencies, defined as $H_{0,\text{seas}} := \cap_{k=1}^{\lfloor S/2 \rfloor} H_{0,k}$, while the latter tests the null hypothesis of unit roots at the zero and all of the seasonal frequencies, defined as $H_0 := \cap_{k=0}^{\lfloor S/2 \rfloor} H_{0,k}$. Observe that $\alpha(L) = \Delta_S$ under H_0. Implementation of these tests, including relevant critical values, using OLS de-trending has been considered in, *inter alia*, HEGY, Smith *et al.* (2009) and Ghysels *et al.* (1994). Corresponding results for the case of local GLS de-trending are given in Rodrigues and Taylor (2007).

[3] In the case of OLS de-trending, an asymptotically equivalent procedure is to omit the first step and to include the relevant deterministic regressors in the auxiliary regression (2.4).

The limiting null distributions of the OLS de-trended HEGY statistics are given for the case where $\psi(z) = 1$ in (2.1b) and accordingly $p^* = 0$ in (2.4) by Smith and Taylor (1998). In the case where $\phi(z)$ is pth order, $0 \leq p < \infty$, Burridge and Taylor (2001) and Smith *et al.* (2009) show that the limiting null distributions of the OLS de-trended t_0, $t_{S/2}$ and F_k, $k = 1, ..., S^*$, statistics from (2.4), are as for $p = 0$, provided $p^* \geq p$ in (2.4). They show that this is not true, however, for the t_k and t_k^*, $k = 1, ..., S^*$, statistics whose limit distributions depend on functions of the parameters characterising the serial dependence in u_{Sn+s} in (2.1b). Representations for the corresponding limiting distributions under near seasonally integrated alternatives are given in Rodrigues and Taylor (2004) and again shown to be free of nuisance parameters with the exception of the t_k and t_k^*, $k = 1, ..., S^*$, statistics. Corresponding results for the local GLS de-trended HEGY-type statistic are given in Rodrigues and Taylor (2007) and here it is also the case that the harmonic frequency t-statistics depend on nuisance parameters arising from the serial correlation in u_{Sn+s}. Where $\phi(z)$ is (potentially) infinite-ordered, del Barrio Castro *et al.* (2012) show that provided the lag length p^* in (2.4) is such that $1/p^* + (p^*)^3/T \to 0$, as $T \to \infty$, then limiting distributions of the OLS and local GLS de-trended HEGY statistics will be of the same form as derived for those statistics under finite p.

3 Semi-Parametric Seasonal Unit Root Tests

The so-called HEGY approach outlined in section 2.3 adopts a parametric approach to modelling serial correlation present in u_{Sn+s} of (2.1b). In this section we explore two alternative non-parametric approaches to accounting for the serial correlation in u_{Sn+s}, mirroring analogous alternative approaches to the parametric ADF unit root tests developed for non-seasonal data. Accordingly, therefore, these methods will be based around corrections for weak dependence to HEGY-type statistics obtained from a lag *un-augmented* HEGY regression; that is, while the first step, in which we de-trend the data, of the two-step HEGY-type procedure remains the same as was outlined in section 2, in the second step we now expand only the polynomial $\alpha(z)$ around the zero and seasonal frequency unit roots. Doing so yields the auxiliary regression equation[4]

$$\Delta_S y_{Sn+s}^{\xi} = \sum_{k=0}^{\lfloor S/2 \rfloor} \pi_k y_{k,Sn+s-1}^{\xi} + \sum_{j=1}^{S^*} \pi_j^* y_{j,Sn+s-1}^{*\xi} + u_{Sn+s}^{\xi}. \tag{3.1}$$

Both the normalised OLS estimates of π_0, $\pi_{S/2}$, π_k and π_k^*, $k = 1, \ldots, S^*$, denoted $T\widehat{\pi}_0$, $T\widehat{\pi}_{S/2}$, $T\widehat{\pi}_k$ and $T\widehat{\pi}_k^*$, $k = 1, \ldots, S^*$, and the corresponding regression t- and F-statistics, outlined as in section 2.3 but now computed from the un-augmented HEGY regression in (3.1), will depend in general on nuisance parameters arising from any weak dependence present in u_{Sn+s}. In Theorem 3.1 we now provide representations for these limiting distributions. These representations are indexed by the parameter ζ whose value is determined by which of Cases 1-3 of μ_{Sn+s}, as outlined in section 1, holds and the frequency under test. For the zero frequency

[4] Again, for the case of OLS de-trending, an asymptotically equivalent procedure is to omit the first step and to include the relevant deterministic regressors in (3.1).

ω_0 tests: Case 1: $\zeta = 1$; Cases 2 and 3: $\zeta = 2$. For the seasonal frequency ω_k, $k = 1, ..., \lfloor S/2 \rfloor$, tests: Cases 1 and 2: $\zeta = 1$; Case 3: $\zeta = 2$.

Theorem 3.1. *Let y_{Sn+s} be generated by (2.1) under $H_{1,\mathbf{c}}$ and let Assumption 1 hold. Then the HEGY-type statistics computed from (3.1) are such that, as $T \to \infty$,*

$$T\hat{\pi}_k \Rightarrow \frac{\int_0^1 J^{\zeta}_{k,c_k}(r)dJ^{\zeta}_{k,c_k}(r) + \mathcal{D}_k \int_0^1 J^{\zeta *}_{k,c_k}(r)dJ^{\zeta *}_{k,c_k}(r) + \frac{\lambda_k^2 - \gamma_0}{2\lambda_k^2}}{\frac{(2-\mathcal{D})}{2}\left\{\int_0^1 \left[J^{\zeta}_{k,c_k}(r)\right]^2 dr + \mathcal{D}_k \int_0^1 \left[J^{\zeta *}_{k,c_k}(r)\right]^2 dr\right\}}, \quad k = 0, ..., \lfloor S/2 \rfloor \tag{3.2}$$

$$T\hat{\pi}^*_k \Rightarrow \frac{\int_0^1 J^{\zeta *}_{k,c_k}(r)dJ^{\zeta}_{k,c_k}(r) - \int_0^1 J^{\zeta}_{k,c_k}(r)dJ^{\zeta *}_{k,c_k}(r) + \frac{\lambda_k^{*2} - \gamma_0}{2\lambda_k^2}}{\frac{1}{2}\left\{\int_0^1 \left[J^{\zeta}_{k,c_k}(r)\right]^2 dr + \int_0^1 \left[J^{\zeta *}_{k,c_k}(r)\right]^2 dr\right\}}, \quad k = 1, ..., S^* \tag{3.3}$$

and

$$t_k \Rightarrow \frac{\lambda_k}{\gamma_0^{1/2}} \frac{\int_0^1 J^{\zeta}_{k,c_k}(r)dJ^{\zeta}_{k,c_k}(r) + \mathcal{D}_k \int_0^1 J^{\zeta *}_{k,c_k}(r)dJ^{\zeta *}_{k,c_k}(r) + \frac{\lambda_k^2 - \gamma_0}{2\lambda_k^2}}{\left\{\int_0^1 \left[J^{\zeta}_{k,c_k}(r)\right]^2 dr + \mathcal{D}_k \int_0^1 \left[J^{\zeta *}_{k,c_k}(r)\right]^2 dr\right\}^{1/2}} =: \Upsilon^{\zeta}_k, \; k = 0, ..., \lfloor S/2 \rfloor \tag{3.4}$$

$$t^*_k \Rightarrow \frac{\lambda_k}{\gamma_0^{1/2}} \frac{\int_0^1 J^{\zeta *}_{k,c_k}(r)dJ^{\zeta}_{k,c_k}(r) - \int_0^1 J^{\zeta}_{k,c_k}(r)dJ^{\zeta *}_{k,c_k}(r) + \frac{\left(\lambda_k^{*2} - \gamma_0\right)}{2\lambda_k^2}}{\left\{\int_0^1 \left[J^{\zeta}_{k,c_k}(r)\right]^2 dr + \int_0^1 \left[J^{\zeta *}_{k,c_k}(r)\right]^2 dr\right\}^{1/2}} =: \Upsilon^{*\zeta}_k, \quad k = 1, ..., S^* \tag{3.5}$$

where "$\Rightarrow$" is used throughout the paper to denote weak convergence in the Skorohod topology, $\mathcal{D}_k := 0$, for $k = 0$, $S/2$ and $\mathcal{D}_k := 1$, for $k = 1, ..., S^*$, $\lambda_k^{*2} := \gamma_0 + 2\sum_{i=1}^{\infty} \sin(\omega_k i)\gamma_k$, $k = 1, ..., S^*$, and where $W_0(r)$, $W_{S/2}(r)$, $W_k(r)$ and $W^*_k(r)$, $k = 1, \ldots, S^*$, are mutually independent standard Brownian motions, $J^{\zeta}_{0,c_0}(r)$, $J^{\zeta}_{S/2,c_{S/2}}(r)$, $J^{\zeta}_{k,c_k}(r)$ and $J^{\zeta *}_{k,c_k}(r)$, $k = 1, \ldots, S^*$, are mutually independent functionals of these Brownian motions whose precise form depends on the de-trending index ξ and on whether y^{ξ}_{Sn+s} is formed using OLS de-trending or local GLS de-trending. In the case of local GLS de-trending: for $\zeta = 1$ these are standard Ornstein-Uhlenbeck [OU] processes, viz.,

$$J^1_{k,c_k}(r) := \int_0^r \exp(c_k(r-s))dW_k(s), \quad k = 0, \ldots, \lfloor S/2 \rfloor$$
$$J^{1*}_{j,c_k}(r) := \int_0^r \exp(c_k(r-s))dW^*_k(s), \quad k = 1, ..., S^*,$$

while for $\zeta = 2$,

$$J^2_{k,c_k}(r) := J^1_{k,c_k}(r) - r\left\{\frac{(1-\bar{c}_k)J^1_{k,c_k}(1) + \bar{c}_k^2 \int_0^1 sJ^1_{k,c_k}(s)ds}{1 - \bar{c}_k + \bar{c}_k^2/3}\right\}, \quad k = 0, \ldots \lfloor S/2 \rfloor$$
$$J^{2*}_{k,c_k}(r) := J^{1*}_{k,c_k}(r) - r\left\{\frac{(1-\bar{c}_k)J^{1*}_{k,c_k}(1) + \bar{c}_k^2 \int_0^1 sJ^{1*}_{k,c_k}(s)ds}{1 - \bar{c}_k + \bar{c}_k^2/3}\right\}, \quad k = 1, ..., S^*.$$

For OLS de-trending they are de-meaned standard OU processes for $\zeta = 1$, so that, for example, $J^1_{0,c_0}(r) := J^0_{0,c_0}(r) - \int_0^1 J^0_{0,c_0}(s)ds$, while for $\zeta = 2$ they are de-trended OU processes, so that,

for example, J^2_{0,c_0} *is the de-meaned and de-trended standard OU process,* $J^2_{0,c_0}(r) := J^1_{0,c_0}(r) - 12\left(r - \frac{1}{2}\right)\int_0^1 \left(s - \frac{1}{2}\right) J^1_{0,c_0}(s)ds$.

Remark 3.1. Representations for the limiting distributions of the corresponding joint F statistics, F_k, $k = 1, ..., S^*$, $F_{1...\lfloor S/2 \rfloor}$ and $F_{0...\lfloor S/2 \rfloor}$ are given by the average of the squares of the limiting distributions for the t-statistics involved in their formulation given in Theorem 3.1. So that, for example, $F_k \Rightarrow \frac{1}{2}\left[(\Upsilon_k^{\zeta})^2 + (\Upsilon_k^{*\zeta})^2\right]$, $k = 1, ..., S^*$.

Remark 3.2. The results in Theorem 3.1 (and consequently also in Remark 3.1) show that the limiting distributions (under both null and local alternatives) of the uncorrected HEGY tests from (3.1) depend on nuisance parameters which arise when u_{Sn+s} is weakly dependent. When u_{Sn+s} is IID, which occurs where $\psi(z) = 1$, then the true lag order in (3.1) is $p^* = 0$, and the representations in (3.2)-(3.5) are pivotal because here $\lambda_k^2 = \gamma_0$, $k = 0, \ldots, \lfloor S/2 \rfloor$, and $\lambda_k^{*2} = \gamma_0$, $k = 1, \ldots, S^*$. Indeed, these pivotal forms, for the statistics at the zero and Nyquist frequencies and for all of the F-type tests coincide with those which obtain from the appropriately augmented HEGY tests discussed in section 2.3. Relative to these pivotal distributions, we see that in the presence of weak dependence in u_{Sn+s} the un-augmented HEGY statistics from (3.1) have limiting distributions whose numerator includes an additional term arising from the difference between the short run variance of u_{Sn+s} and the long run variance(s) of u_{Sn+s} at the frequency component relating to that statistic and, in the case of the t-statistics (and, hence, the F-statistics), are also scaled by the ratio of the long and short run variances of u_{Sn+s} at that frequency.

The representations given for the limiting distributions of the un-augmented HEGY statistics in Theorem 3.1 are useful because they enable us to see immediately how, given consistent estimators for γ_0, λ_k^2, $k = 0, \ldots, \lfloor S/2 \rfloor$, and λ_k^{*2}, $k = 1, \ldots, S^*$, these statistics can be transformed to obtain modified statistics whose limiting distributions coincide with those which obtain in the case where $\psi(z) = 1$. We now consider two possible approaches for achieving this, mirroring developments in the non-seasonal unit root literature. In section 3.1 we will first consider seasonal analogues of the non-seasonal PP tests. In section 3.2 we will subsequently propose $\mathcal{M}$-type seasonal unit root tests. As we shall see, in the case of tests at the harmonic seasonal frequencies this will necessitate the use of demodulated processes.

3.1 Phillips-Perron-Type Seasonal Unit Root Tests

Computation of seasonal versions of the non-seasonal PP unit root tests will require consistent estimators of the nuisance parameters which feature in the limit distributions of the un-augmented HEGY statistics from (3.1) given in Theorem 3.1. As we will show, under the conditions in this paper, these may be based on either sums-of-covariances (or kernel-based) estimators or autoregressive spectral density estimators.

In their original article PP consider a sums-of-covariances estimator of the long run variance, λ_0^2. In the context of correcting the un-augmented HEGY statistics, the results in Theorem

3.1 imply that we will need the following sums-of-covariances estimators (see also Breitung and Franses, 1998, and Gregoir 2006), where it is to be recalled that $\omega_k := 2\pi k/S$, $k = 0, ..., \lfloor S/2 \rfloor$:

$$\hat{\lambda}^2_{k,WA} := \sum_{j=-T+1}^{T-1} \kappa(j/m)\hat{\gamma}_j \cos(\omega_k j), \qquad k = 0, \ldots, \lfloor S/2 \rfloor \tag{3.7}$$

$$\hat{\lambda}^{*2}_{k,WA} := \sum_{j=-T+1}^{T-1} \kappa(j/m)\hat{\gamma}_j \cos(\pi/2 + \omega_k j), \qquad k = 1, \ldots, S^* \tag{3.8}$$

where $\hat{\gamma}_j$ is the sample autocovariance of order j computed from the OLS residuals from estimating (3.1). These estimators are consistent under $H_{1,\mathbf{c}}$ provided the kernel function $\kappa(\cdot)$ satisfies *e.g.* the general conditions reported in Jansson (2002, Assumption A3) and the bandwidth parameter $m \in (0, \infty)$ satisfies the rate condition $1/m + m^2/T \to 0$ as $T \to \infty$ (which corresponds to Assumption A4 of Jansson, 2002).

It is well-known that semi-parametric unit root tests based on sums-of-covariances estimators can behave quite poorly in finite samples; see, for example, Haldrup and Jansson (2006). An alterative approach, which in the non-seasonal case has been shown to deliver unit root tests with considerably better finite sample size properties, is to use the so-called autoregressive spectral density estimators of the form proposed in Berk (1974); see, in particular, Ng and Perron (2001) and Haldrup and Jansson (2006). Following the approach in Berk (1974), the autoregressive spectral density analogues of the sums-of-covariances estimators in (3.7) are given by:

$$\hat{\lambda}^2_{0,AR} := \frac{s_e^2}{\left[1 - \widehat{\phi}(1)\right]^2}, \;\; \hat{\lambda}^2_{S/2,AR} := \frac{s_e^2}{\left[1 - \widehat{\phi}(-1)\right]^2} \tag{3.9}$$

$$\hat{\lambda}^2_{k,AR} := \frac{s_e^2}{\left\{1 - \mathcal{R}e\left(\widehat{\phi}\left(e^{(\mathrm{i}\omega_k)}\right)\right)\right\}^2 + \left\{\mathcal{I}m\left(\widehat{\phi}\left(e^{(\mathrm{i}\omega_k)}\right)\right)\right\}^2}, \; k = 1, \ldots, S^* \tag{3.10}$$

while the autoregressive spectral density analogues of the estimators in (3.8) are given by

$$\hat{\lambda}^{*2}_{k,AR} := \frac{s_e^2}{\left\{1 - \sum_{j=1}^{p^*} \hat{\phi}^*_j \cos\left(\left[j\omega_k + \frac{\pi}{2}\right]\right)\right\}^2 + \left\{\sum_{j=1}^{p^*} \hat{\phi}^*_j \sin\left(\left[j\omega_k + \frac{\pi}{2}\right]\right)\right\}^2}, \; k = 1, \ldots, S^* \tag{3.11}$$

where s_e^2 and $\widehat{\phi}(L) := \sum_{i=1}^{p^*} \hat{\phi}^*_i L^i$ denote the OLS residual variance estimator and the fitted augmentation polynomial, respectively, from the augmented HEGY regression, (2.4), with $\hat{\phi}^*_j$ denoting the OLS estimator of ϕ^*_j, $j = 1, ..., p^*$, from (2.4). As with the requirements needed for the validity of the augmented HEGY tests in section 2.3, consistency of the autoregressive spectral density estimators under $H_{1,\mathbf{c}}$ requires that: (i) $(1/p^*) + (p^*)^3/T \to 0$ as $T \to \infty$, and (ii) that the lag polynomial $\psi(z)$ is invertible; see Berk (1974).

Based on the estimators $\hat{\lambda}^2_{0,h}$, $\hat{\lambda}^2_{S/2,h}$, $\hat{\lambda}^2_{k,h}$ and $\hat{\lambda}^{*2}_{k,h}$, $h = WA$, AR, $k = 1, \ldots, S^*$, defined in (3.7), (3.8), (3.9), (3.10) and (3.11), seasonal analogues of the non-seasonal PP unit root statistics can be derived from the functional forms of the limit distributions of the un-augmented

HEGY statistics from (3.1) given in Theorem 3.1, as follows:

$$Z_k := \quad T\hat{\pi}_k - \frac{\left(\hat{\lambda}^2_{k,h} - \hat{\gamma}_0\right)}{2}\left[\frac{1}{T^2}\sum_{Sn+s=1}^{T}\left(y^{\xi}_{k,Sn+s-1}\right)^2\right]^{-1}, \quad k = 0, ..., \lfloor S/2 \rfloor \tag{3.12}$$

$$Z^*_k := \quad T\hat{\pi}^*_k - \frac{\left(\hat{\lambda}^{*2}_{k,h} - \hat{\gamma}_0\right)}{2}\left[\frac{1}{T^2}\sum_{Sn+s=1}^{T}\left(y^{*\xi}_{k,Sn+s-1}\right)^2\right]^{-1}, \quad k = 1, \ldots, S^* \tag{3.13}$$

and

$$Z_{t_k} := \quad \frac{\hat{\gamma}_0^{1/2}}{\hat{\lambda}_{k,h}}t_k - \frac{\left(\hat{\lambda}^2_{k,h} - \hat{\gamma}_0\right)}{2}\left[\frac{\hat{\lambda}^2_{k,h}}{T^2}\sum_{Sn+s=1}^{T}\left(y^{\xi}_{k,Sn+s-1}\right)^2\right]^{-1/2}, \quad k = 0, ..., \lfloor S/2 \rfloor \tag{3.14}$$

$$Z_{t^*_k} := \quad \frac{\hat{\gamma}_0^{1/2}}{\hat{\lambda}_{k,h}}t^*_k - \frac{\left(\hat{\lambda}^{*2}_{k,h} - \hat{\gamma}_0\right)}{2}\left[\frac{\hat{\lambda}^2_{k,h}}{T^2}\sum_{Sn+s=1}^{T}\left(y^{*\xi}_{k,Sn+s-1}\right)^2\right]^{-1/2}, \quad k = 1, \ldots, S^* \tag{3.15}$$

where $\hat{\gamma}_0$ is the OLS residual variance estimate from (3.1).

Remark 3.3. Notice that for $S = 1$, Z_0 in (3.12) and Z_{t_0} in (3.14) reduce to the non-seasonal unit root tests proposed in PP.

Remark 3.4. PP-type analogues of the F-type statistics F_k, $k = 1, ..., S^*$, $F_{1,...,\lfloor S/2 \rfloor}$ and $F_{0,...,\lfloor S/2 \rfloor}$ discussed in section 2 can also be constructed using the corrected normalised coefficient estimate statistics in (3.12) and (3.13). With an obvious notation we will denote these statistics as $F_{PP,k}$, $k = 1, \ldots, S^*$, $F_{PP,1...\lfloor S/2 \rfloor}$, and $F_{PP,0...\lfloor S/2 \rfloor}$. These statistics can be defined generically as follows:

$$F_{PP} := \frac{1}{\upsilon}(R\mathbf{Z})'\left[R\Lambda\mathbf{Y}'\mathbf{Y}R'\right](R\mathbf{Z}) \tag{3.16}$$

where υ denotes the number of restrictions being tested; $Z := [Z_{\pi_0}, Z_{\pi_1}, Z_{\pi^*_1}, Z_{\pi_2}, Z_{\pi^*_2}, \ldots, Z_{\pi_{S^*}}, Z_{\pi^*_{S^*}}, Z_{\pi_{S/2}}]'$ is $S \times 1$; $Y := [\mathbf{y}_0|\mathbf{y}_1|\mathbf{y}^*_1|\mathbf{y}_2|\mathbf{y}^*_2| \ \ldots \ |\mathbf{y}_{S^*}|\mathbf{y}^*_{S^*}|\mathbf{y}_{S/2}]$ is a $T \times S$ matrix where $\mathbf{y}_i$, $i = 0, S/2$, are $T \times 1$ vectors with generic element $y^{\xi}_{i,Sn+s-1}$, and $\mathbf{y}_i$ and $\mathbf{y}^*_i$, $i = 1, ..., S^*$ are $T \times 1$ vectors with generic elements $y^{\xi}_{i,Sn+s-1}$ and $y^{*\xi}_{i,Sn+s-1}$, respectively; Λ is an $S \times S$ diagonal matrix such that, $\Lambda := T^{-2}diag\left\{1/\hat{\lambda}^2_{0,h}, 1/\hat{\lambda}^2_{1,h}, 1/\hat{\lambda}^2_{1,h}, 1/\hat{\lambda}^2_{2,h}, 1/\hat{\lambda}^2_{2,h} \ \ldots, 1/\hat{\lambda}^2_{S^*,h}, 1/\hat{\lambda}^2_{S^*,h}, 1/\hat{\lambda}^2_{S/2,h}\right\}$, and finally R is the relevant $\upsilon \times S$ selection matrix; for example, setting

$$R = \begin{bmatrix} 0 & 1 & 0 & 0 & \ldots & 0 \\ 0 & 0 & 1 & 0 & \ldots & 0 \end{bmatrix},$$

yields the $F_{PP,1}$ statistic, whilst setting $R = I_S$, where I_q denotes the $q \times q$ identity matrix for any positive integer q, results in $F_{PP,0...\lfloor S/2 \rfloor}$.

3.2 $\mathcal{M}$-Type Seasonal Unit Root Tests

3.2.1 Zero and Nyquist Frequency Tests

For the non-seasonal ($S = 1$) case, Perron and Ng (1996), Stock (1999) and Ng and Perron (2001) define the trinity of so-called $\mathcal{M}$ unit root test statistics as follows:

$$\mathcal{MZ}_0 := \frac{T^{-1}\left[(y^{\xi}_T)^2 - (y^{\xi}_0)^2\right] - \hat{\lambda}^2_{0,h}}{2T^{-2}\sum_{t=1}^{T}(y^{\xi}_{t-1})^2}, \quad \mathcal{MSB}_0 := \left(T^{-2}\sum_{n=1}^{T}(y^{\xi}_{t-1})^2/\hat{\lambda}^2_{0,h}\right)^{1/2} \tag{3.17}$$

and $\mathcal{MZ}_{t_0} := \mathcal{MZ}_0 \times \mathcal{MSB}_0$, where $\hat{\lambda}^2_{0,h}$ is either $\hat{\lambda}^2_{0,WA}$ of (3.7) or $\hat{\lambda}^2_{0,AR}$ of (3.9), noting that, for $S = 1$, (3.1) and (2.4) reduce to non-seasonal un-augmented and augmented Dickey-Fuller regressions, respectively. Stock (1999) shows that the first of these statistics, $\mathcal{MZ}_{\pi_0}$, can be re-written[5] as $\mathcal{MZ}_0 = Z_0 + \frac{T}{2}(\hat{\pi}_0)^2$, where Z_0 is as given in (3.12) for $S = 1$, and where $\hat{\pi}_0$ is the OLS estimate of π_0 from (3.1) when $S = 1$. It can therefore be seen to be a modified version of the PP non-seasonal unit root test statistic, Z_0. These two statistics are asymptotically equivalent under $H_{0,c}$. The second statistic, $\mathcal{MSB}_0$, can be used as a basis for a unit root test by noting that the sums of squares of an $I(1)$ series is of $O_p(T^2)$ while that of an $I(0)$ series is of $O_p(T)$. A test which rejects for small values of the $\mathcal{MSB}_0$ statistic therefore tests the unit root null hypothesis against the stationary alternative. Stock (1999) shows that $\mathcal{MSB}_0$ can be viewed as a modified version of Bhargava's (1986) R_1 statistic. Finally, because $Z_{t_0} = \mathcal{MSB}_0 \times Z_0$, Ng and Perron (1996) propose $\mathcal{MZ}_{t_0}$ as a modified version of the PP Z_{t_0} test. As with the corresponding coefficient-based modified statistics, $\mathcal{MZ}_{t_0}$ and Z_{t_0} are asymptotically equivalent under $H_{0,c}$.

Using the estimators $\hat{\lambda}^2_{k,h}$, $h = WA$, AR, $k = 0, S/2$, from section 3.1 we can generalise the principles underlying the trinity of non-seasonal $\mathcal{M}$ unit root tests to tests for unit roots at the zero and Nyquist frequencies in the seasonal case. Consider first the modified coefficient-type tests. Here, in a similar vein to the relationship that holds between $\mathcal{MZ}_0$ and Z_0 in the non-seasonal case, it is straightforward to show that $\mathcal{MZ}_k = Z_k + \frac{T}{2}(\hat{\pi}_k)^2 + o_p(1)$, $k = 0, S/2$, where for the zero ($k = 0$) and Nyquist ($k = S/2$) frequencies,

$$\mathcal{MZ}_k := \frac{T^{-1}\left[\left(y^{\xi}_{k,T}\right)^2 - \left(y^{\xi}_{k,0}\right)^2\right] - \hat{\lambda}^2_{k,h}}{2T^{-2}\sum_{Sn+s=1}^{T}\left(y^{\xi}_{k,Sn+s-1}\right)^2}, \ k = 0, S/2. \tag{3.18}$$

Noting that the HEGY transformed level variables $y^{\xi}_{0,Sn+s}$ and $y^{\xi}_{S/2,Sn+s}$, defined in (2.5) and (2.6), filter out unit roots at all but the zero and Nyquist frequency, respectively, the sums of squares of these variables can be used to form the analogues at the zero and Nyquist frequencies, respectively, of the non-seasonal $\mathcal{MSB}_0$ statistic defined in (3.17); that is,

$$\mathcal{MSB}_k := \left[\frac{1}{T^2\hat{\lambda}^2_{k,h}}\sum_{Sn+s=1}^{T}\left(y^{\xi}_{k,Sn+s-1}\right)^2\right]^{1/2}, \ k = 0, S/2. \tag{3.19}$$

Combining (3.18) and (3.19), $\mathcal{M}$ versions of the seasonal PP-type Z_{t_k}, $k = 0, S/2$ statistics can then be straightforwardly defined as follows

$$\mathcal{MZ}_{t_k} := \mathcal{MZ}_k \times \mathcal{MSB}_k, \ \ k = 0, S/2. \tag{3.20}$$

3.2.2 Harmonic Frequency Tests

In order to generalise the $\mathcal{M}$ tests to the harmonic seasonal frequencies, two possible approaches could be used. Our attention here will be focussed on tests based around the use of the demodulator operator introduced by Granger and Hatanaka (1964), subsequently used in the context

[5]The term $-T^{-1}(y^{\xi}_0)^2$ can be omitted from the numerator of $\mathcal{MZ}_0$ for the case of local GLS de-trended data; see Mueller and Elliott (2003).

of testing for harmonic frequency unit roots in Gregoir (1999, 2006, 2010). An alternative approach is to define $\mathcal{M}$ tests at the harmonic frequencies analogously to the zero and Nyquist frequency $\mathcal{MZ}_k$, $\mathcal{MSB}_k$ and $\mathcal{MZ}_{t_k}$ $k = 0, S/2$, tests outlined above, using the relevant HEGY auxiliary variables $y^{\xi}_{k,Sn+s}$ and $y^{*\xi}_{k,Sn+s}$, $k = 1, ..., S^*$ from (2.5) and (2.6). Monte Carlo simulation results reported in the accompanying working paper suggest, however, that this approach yields tests with inferior finite sample size properties than the standard augmented HEGY tests discussed in section 2.2 and so we will not discuss this approach further here.

To illustrate the principle of demodulation, consider the complex-valued process, z_{Sn+s}, near-integrated at frequency ω_k; viz.,

$$\left(1 - \left(1 + \frac{c_k}{T}\right) e^{-i\omega_k} L\right) z_{Sn+s} = u_{Sn+s} \tag{3.21}$$

where the innovation u_{Sn+s} satisfies Assumption 1. By recursive substitution it follows from (3.21) that z_{Sn+s} can be written as,

$$z_{Sn+s} = e^{-i\omega_k(Sn+s)} \left[(1 + \frac{c_k}{T})^{(Sn+s)} z_0 + \sum_{j=1}^{Sn+s} (1 + \frac{c_k}{T})^{Sn+s-j} e^{i\omega_k j} u_j \right]. \tag{3.22}$$

From the representation in (3.22) we observe that z_{Sn+s} is driven by the complex innovation $e^{i\omega_k j} u_j$. Moreover, (3.22) shows that z_{Sn+s} can be expressed as a complex-valued near-integrated process at the zero frequency, viz., $(1 + \frac{c_k}{T})^{(Sn+s)} z_0 + \sum_{j=1}^{Sn+s} (1 + \frac{c_k}{T})^{Sn+s-j} e^{i\omega_k j} u_j$, multiplied by the demodulator operator $e^{-i\omega_k(Sn+s)}$. The latter shifts the peak in the spectrum which occurs at the zero frequency with the former to a peak in the spectrum at frequency ω_k.

Hence, in order to use the demodulation-based approach just described to develop harmonic frequency $\mathcal{M}$-type tests we first need to define the demodulated complex conjugate variables,

$$y^{\xi,\mathtt{D}a}_{k,Sn+s} := e^{i\omega_k(Sn+s)} \left(1 - e^{i\omega_k} L\right) \Delta^0_k(L)\, y^{\xi}_{Sn+s} \tag{3.23}$$

$$y^{\xi,\mathtt{D}b}_{k,Sn+s} := e^{-i\omega_k(Sn+s)} \left(1 - e^{-i\omega_k} L\right) \Delta^0_k(L)\, y^{\xi}_{Sn+s} \tag{3.24}$$

in each case for $k = 1, ..., S^*$, where

$$\Delta^0_k(L) := (1 - L)(1 + L) \sum_{j \neq k, j=1}^{S^*} (1 - 2\cos[\omega_j] L + L^2) = \sin[\omega_k]^{-1} (\sum_{j=0}^{S-1} \sin[(j+1)\omega_k] L^j)$$

omitting the factor $(1 + L)$ above when S is odd. As demonstrated in the Appendix (see equation (B.24)), applying the filter $\Delta^0_k(L)$ to y^{ξ}_{Sn+s} yields a real-valued near-integrated process at frequency ω_k with associated AR(2) polynomial $(1 - 2\cos(\omega_k)(1 + \frac{c_k}{T})L + (1 + \frac{c_k}{T})^2 L^2)$. Consequently, the filters $(1 - e^{i\omega_k} L)\Delta^0_k(L)$ and $(1 - e^{-i\omega_k} L)\Delta^0_k(L)$ when applied to y^{ξ}_{Sn+s} deliver the complex-valued near-integrated processes with associated (complex) AR(1) polynomials $(1 - (1 + \frac{c_k}{T})e^{-i\omega_k} L)$ and $(1 - (1 + \frac{c_k}{T})e^{i\omega_k} L)$, respectively; see (B.26)-(B.29) in the Appendix. Finally, the demodulation by multiplication by $e^{i\omega_k(Sn+s)}$ and $e^{-i\omega_k(Sn+s)}$ in (3.23) and (3.24), respectively, yields the complex-valued near-integrated processes at the zero frequency, $y^{\xi,\mathtt{D}a}_{k,Sn+s}$ and $y^{\xi,\mathtt{D}b}_{k,Sn+s}$, associated with the filters $(1 - (1 + \frac{c_k}{T})e^{-i\omega_k} L)$ and $(1 - (1 + \frac{c_k}{T})e^{i\omega_k} L)$, respectively; see (B.30) and (B.31) in the Appendix.

The following weak convergence results for $y^{\xi,\mathtt{D}a}_{k,Sn+s}$ and $y^{\xi,\mathtt{D}b}_{k,Sn+s}$ of (3.23) and (3.24), respectively, follow straightforwardly from (B.30) and (B.31) in the Appendix,

$$T^{-1/2}y^{\xi,\mathtt{D}a}_{k,S\lfloor rN\rfloor+s} \Rightarrow \frac{\sigma\psi\left(e^{i\omega_k}\right)}{\sqrt{2}}\left[J^{\zeta}_{k,c_k}(r)+iJ^{\zeta*}_{k,c_k}(r)\right] =: \frac{\sigma\psi\left(e^{i\omega_k}\right)}{\sqrt{2}}\mathbb{J}_{k,c_k}(r) \tag{3.25}$$

$$T^{-1/2}y^{\xi,\mathtt{D}b}_{k,S\lfloor rN\rfloor+s} \Rightarrow \frac{\sigma\psi\left(e^{-i\omega_k}\right)}{\sqrt{2}}\left[J^{\zeta}_{k,c_k}(r)-iJ^{\zeta*}_{k,c_k}(r)\right] =: \frac{\sigma\psi\left(e^{-i\omega_k}\right)}{\sqrt{2}}\overline{\mathbb{J}_{k,c_k}(r)} \tag{3.26}$$

in each case for $k=1,...,S^*$. In (3.25) and (3.26), $\psi(\cdot)$ is as defined in Assumption 1, while $J^{\zeta}_{k,c_k}(r)$ and $J^{\zeta*}_{k,c_k}(r)$, $k=1,...,S^*$, are the independent OU processes of Theorem 3.1 (defined in Remark A.3 of the Appendix). Notice that $\mathbb{J}_{k,c_k}$ and $\overline{\mathbb{J}_{k,c_k}}$ in (3.25) and (3.26), respectively, form a complex conjugate pair of complex OU processes.

As the limiting representations given for $y^{\xi,\mathtt{D}a}_{k,Sn+s}$ and $y^{\xi,\mathtt{D}b}_{k,Sn+s}$ in (3.25) and (3.26) make clear, developing feasible harmonic frequency $\mathcal{M}$-type test statistics based on these demodulated variables will require taking appropriate real-valued transformations of $y^{\xi,\mathtt{D}a}_{k,Sn+s}$ and $y^{\xi,\mathtt{D}b}_{k,Sn+s}$, together with estimates of the nuisance parameters $\sigma\psi(e^{i\omega_k})$ and $\sigma\psi(e^{-i\omega_k})$ which feature in (3.25) and (3.26), respectively, which are consistent under $H_{1,\mathbf{c}}$. Given results already established in this paper, it is easily seen that the latter can be achieved, under the additional conditions stated in section 3.1, using the autoregressive spectral density estimators, $\breve{\lambda}^2_{k,AR} := s^2_e\{1-[\widehat{\phi}(e^{i\omega_k})]\}^{-2}$ and $\breve{\lambda}^{*2}_{k,AR} := s^2_e\{1-[\widehat{\phi}(e^{-i\omega_k})]\}^{-2}$, $k=1,...,S^*$, where s^2_e and $\widehat{\phi}(\cdot)$ are as defined below (3.11), such that $(\breve{\lambda}^2_{k,AR}T)^{-1/2}y^{\xi,\mathtt{D}a}_{k,S\lfloor rN\rfloor+s} \Rightarrow \frac{1}{\sqrt{2}}\mathbb{J}_{k,c_k}(r)$ and $(\breve{\lambda}^{*2}_{k,AR}T)^{-1/2}y^{\xi,\mathtt{D}b}_{k,S\lfloor rN\rfloor+s} \Rightarrow \frac{1}{\sqrt{2}}\overline{\mathbb{J}_{k,c_k}(r)}$. For the former, we take the following transformations

$$y^{\mathcal{R}e,\xi}_{k,Sn+s} := \frac{1}{2}\mathcal{R}e\left(\frac{y^{\xi,\mathtt{D}a}_{k,Sn+s}}{\breve{\lambda}_{k,AR}\sqrt{T}}+\frac{y^{\xi,\mathtt{D}b}_{k,Sn+s}}{\breve{\lambda}^{*}_{k,AR}\sqrt{T}}\right) \tag{3.27}$$

$$y^{\mathcal{I}m,\xi}_{k,Sn+s} := \frac{1}{2}\mathcal{I}m\left(\frac{y^{\xi,\mathtt{D}a}_{k,Sn+s}}{\breve{\lambda}_{k,AR}\sqrt{T}}-\frac{y^{\xi,\mathtt{D}b}_{k,Sn+s}}{\breve{\lambda}^{*}_{k,AR}\sqrt{T}}\right) \tag{3.28}$$

for $k=1,...,S^*$. Notice that the transformations in (3.27) and (3.28) are designed such that they weakly converge to $J^{\zeta}_{k,c_k}(r)$ and $J^{\zeta*}_{k,c_k}(r)$, respectively. Other transformations with this same asymptotic property could be used instead, but we found little difference even in very small samples compared to using (3.27) and (3.28).

The sequence of transformations in (3.23)-(3.24) and (3.27)-(3.28) therefore transform the original series y^{ξ}_{Sn+s} which admits a complex pair of (near-) unit roots at frequency ω_k into two (scaled) series, $y^{\mathcal{R}e,\xi}_{k,Sn+s}$ and $y^{\mathcal{I}m,\xi}_{k,Sn+s}$, each of which has a single (near-) unit root at the zero frequency. Consequently, under $H_{0,k}$ where y^{ξ}_{Sn+s} admits a pair of unit roots at frequency ω_k, then so the two demodulated series $y^{\mathcal{R}e,\xi}_{k,Sn+s}$ and $y^{\mathcal{I}m,\xi}_{k,Sn+s}$ will each contain a zero frequency unit root. Likewise, under H_{1,c_k}, $y^{\mathcal{R}e,\xi}_{k,Sn+s}$ and $y^{\mathcal{I}m,\xi}_{k,Sn+s}$ each admit either a stable ($c_k<0$) or explosive ($c_k>0$) root at frequency zero. Consequently, by analogy to the non-seasonal $\mathcal{M}$ tests in section 3.2.1, $H_{0,k}$ can therefore be tested against H_{1,c_k} using either $y^{\mathcal{R}e,\xi}_{k,Sn+s}$ or $y^{\mathcal{I}m,\xi}_{k,Sn+s}$

in the following harmonic frequency $\mathcal{M}$-type statistics, in each case for $k = 1, ..., S^*$,

$$\mathcal{K}\text{-}\mathcal{MSB}_k := \left[\frac{2}{T}\left(\sum_{Sn+s=1}^{T} y_{k,Sn+s-1}^{\mathcal{K},\xi}\right)^2\right]^{1/2} \tag{3.29}$$

$$\mathcal{K}\text{-}\mathcal{MZ}_k := \frac{\left[\left(y_{k,T}^{\mathcal{K},\xi}\right)^2 - \left(y_{k,0}^{\mathcal{K},\xi}\right)^2\right] - 1}{\left[\mathcal{K}\text{-}\mathcal{MSB}_k\right]^2} \tag{3.30}$$

$$\mathcal{K}\text{-}\mathcal{MZ}_{t_k} := \mathcal{K}\text{-}\mathcal{MZ}_k \times \mathcal{K}\text{-}\mathcal{MSB}_k \tag{3.31}$$

where setting $\mathcal{K} = \mathcal{R}e$ in (3.29)-(3.31) denotes tests based on $y_{k,Sn+s}^{\mathcal{R}e,\xi}$, while setting $\mathcal{K} = \mathcal{I}m$ denotes the corresponding tests based on $y_{k,Sn+s}^{\mathcal{I}m,\xi}$. In parallel with the $\mathcal{M}$ tests from section 3.2.1, $H_{0,k}$ is rejected in favour of H_{1,c_k} for large negative values of $\mathcal{R}e\text{-}\mathcal{MZ}_k$, $\mathcal{I}m\text{-}\mathcal{MZ}_k$, $\mathcal{R}e\text{-}\mathcal{MZ}_{t_k}$ and $\mathcal{I}m\text{-}\mathcal{MZ}_{t_k}$, and for small values of $\mathcal{R}e\text{-}\mathcal{MSB}_k$ and $\mathcal{I}m\text{-}\mathcal{MSB}_k$, $k = 1, ..., S^*$.

The harmonic frequency $\mathcal{M}$-type unit root test statistics proposed in (3.29)-(3.31) will be shown later in Theorem 4.1 to share the same limiting distributions as the corresponding $\mathcal{M}$-type tests defined for the zero and Nyquist frequencies in section 3.2.1. As a result, asymptotic critical values for the tests based on these statistics are therefore as given for the corresponding tests in the non-seasonal case. Moreover, this also implies that their asymptotic local power functions under H_{1,c_k} will be close to the power envelope for testing for a single unit root at either the zero or Nyquist frequency. This is known to lie considerably beneath the power envelope for testing $H_{0,k}$ against H_{1,c_k}; see, for example, Rodrigues and Taylor (2007). Consequently, one could consider joint tests which combine the $\mathcal{M}$-type statistics based on (3.27) and (3.28) in order to increase power. To that end we consider the test which rejects for large values of the following statistic, analogous to the F_k test statistic of HEGY from section 2.3:

$$F_{\mathcal{M},k}^{\mathtt{D}} := \frac{1}{2}\left[\left(\mathcal{R}e\text{-}\mathcal{MZ}_{t_{\pi_k}}\right)^2 + \left(\mathcal{I}m\text{-}\mathcal{MZ}_{t_{\pi_k}}\right)^2\right], \quad k = 1, ..., S^*. \tag{3.32}$$

Similarly, $\mathcal{MZ}$-type analogues of the joint frequency $F_{1,...,\lfloor S/2\rfloor}$ and $F_{0,...,\lfloor S/2\rfloor}$ HEGY tests from section 2.3 can be formed by rejecting $H_{0,\text{seas}}$ and H_0 for large values of the statistics

$$F_{\mathcal{M},1...\lfloor S/2\rfloor}^{\mathtt{D}} := \frac{1}{S-1}\left[2\sum_{k=1}^{S^*} F_{\mathcal{M},k}^{\mathtt{D}} + \left(\mathcal{MZ}_{t_{\pi_{S/2}}}\right)^2\right] \tag{3.33}$$

and

$$F_{\mathcal{M},0...\lfloor S/2\rfloor}^{\mathtt{D}} := \frac{1}{S}\left[2\sum_{k=1}^{S^*} F_{\mathcal{M},k}^{\mathtt{D}} + \left(\mathcal{MZ}_{t_{\pi_0}}\right)^2 + \left(\mathcal{MZ}_{t_{\pi_{S/2}}}\right)^2\right], \tag{3.34}$$

respectively. Analogous joint tests can also be formed by rejecting $H_{0,k}$, $H_{0,\text{seas}}$ and H_0 for small values of the $\mathcal{MSB}$-type statistics,

$$\mathcal{MSB}_k^{\mathtt{D}} := \frac{1}{2}\left[\left(\mathcal{R}e\text{-}\mathcal{MSB}_k\right)^2 + \left(\mathcal{I}m\text{-}\mathcal{MSB}_k\right)^2\right]^{1/2}, \; k = 1, ..., S^* \tag{3.35}$$

$$\mathcal{MSB}_{1...\lfloor S/2\rfloor}^{\mathtt{D}} := \frac{1}{S-1}\left\{\sum_{k=1}^{S^*}\left[\mathcal{MSB}_k^{\mathtt{D}}\right]^2 + \mathcal{MSB}_{S/2}^2\right\}^{1/2} \tag{3.36}$$

$$\mathcal{MSB}_{0...\lfloor S/2\rfloor}^{\mathtt{D}} := \frac{1}{S}\left\{\sum_{k=1}^{S^*}\left[\mathcal{MSB}_k^{\mathtt{D}}\right]^2 + \mathcal{MSB}_0^2 + \mathcal{MSB}_{S/2}^2\right\}^{1/2} \tag{3.37}$$

respectively.

Remark 3.5: A natural possible alternative to using the $F^{\mathtt{D}}_{\mathcal{M},k}$ statistic in (3.32) for testing $H_{0,k}$, $k = 1, ..., S^*$, would be to form tests based on the statistics

$$\begin{aligned}\mathcal{MZ}^{\mathtt{D}}_k &:= \frac{2\left\{\left[\left(y^{\mathcal{R}e,\xi}_{k,T}\right)^2 - \left(y^{\mathcal{R},e\xi}_{k,0}\right)^2\right] + \left[\left(y^{\mathcal{I}m,\xi}_{k,T}\right)^2 - \left(y^{\mathcal{I}m,\xi}_{k,0}\right)^2\right] - 1\right\}}{\left[2\mathcal{MSB}^{\mathtt{D}}_k\right]^2}, \quad k = 1, ..., S^* \\ \mathcal{MZ}^{\mathtt{D}}_{t_k} &:= \mathcal{MZ}^{\mathtt{D}}_k \times \mathcal{MSB}^{\mathtt{D}}_k, \quad k = 1, ..., S^*.\end{aligned}$$

In unreported Monte Carlo simulations we found these tests to display considerably worse size distortions than the standard augmented HEGY tests when MA components are present in the DGP, and so we do not recommend the use of tests based on these statistics and will therefore not consider them further. For completeness we will, however, report representations for their limiting distributions in Remark 4.6 below.

Remark 3.6: The statistics in (3.32)-(3.37) are based on the approach underlying the corresponding F-type HEGY statistics from section 2.3, whereby the joint F-statistic is formed as the average of the corresponding squared individual t-statistics involved. An alternative is to follow the approach used to develop point optimal seasonal unit root tests in Rodrigues and Taylor (2007), whereby the optimal joint tests are based on the sum of the individual optimal test statistics involved. We define these test statistics as follows,

$$\begin{aligned}S^{\mathtt{D}}_{\mathcal{M},k} &:= \mathcal{R}e\text{-}\mathcal{MZ}_{t_k} + \mathcal{I}m\text{-}\mathcal{MZ}_{t_k}, \quad k = 1, ..., S^* \\ S^{\mathtt{D}}_{\mathcal{M},1...\lfloor S/2\rfloor} &:= \sum_{k=1}^{S^*} S^{\mathtt{D}}_{\mathcal{M},k} + \mathcal{MZ}_{t_{S/2}},\ S^{\mathtt{D}}_{\mathcal{M},0...\lfloor S/2\rfloor} := \sum_{k=1}^{S^*} S^{\mathtt{D}}_{\mathcal{M},k} + \mathcal{MZ}_{t_0} + \mathcal{MZ}_{t_{S/2}}\end{aligned}$$

rejecting $H_{0,k}$ for large negative values of $S^{\mathtt{D}}_{\mathcal{M},k}$, $k = 1, ..., S^*$, and $H_{0,\text{seas}}$ and H_0 for large negative values of $S^{\mathtt{D}}_{\mathcal{M},1...\lfloor S/2\rfloor}$ and $S^{\mathtt{D}}_{\mathcal{M},0...\lfloor S/2\rfloor}$, respectively.

4 Asymptotic Results

In sections 4.1 and 4.2, respectively, we now present the large sample distributions of the seasonal PP-type and seasonal $\mathcal{M}$-type unit root test statistics proposed in section 3. In particular, we show that these have pivotal limiting distributions whose form coincides with those which obtain in the case where the shocks are serially uncorrelated. Local asymptotic power functions of these tests, together with the relevant power envelopes, are then graphed (using direct simulation methods) in section 4.3.

4.1 The PP Type Seasonal Unit root Tests

In Theorem 4.1 we now detail the limiting distributions of the new PP-type seasonal unit root test statistics proposed in section 3.1. The proof of Theorem 4.1 follows directly from the proof of Theorem 3.1 and the consistency properties of the long run variance estimators used in the construction of the PP-type statistics.

Theorem 4.1. *Let y_{Sn+s} be generated by (2.1) under $H_{1,\mathbf{c}}$ and let Assumption 1 hold. Moreover, let the additional conditions stated in section 3.1 hold such that the estimators $\hat{\lambda}^2_{0,h}$, $\hat{\lambda}^2_{S/2,h}$, $\hat{\lambda}^2_{k,h}$ and $\hat{\lambda}^{*2}_{k,h}$, $h = WA,\ AR$, $k = 1, \ldots, S^*$, are consistent. Then, as $T \to \infty$, the PP-type coefficient statistics introduced in section 3.1 and Remark 3.4 satisfy,*

$$Z_k \Rightarrow \frac{(1+\mathcal{D}_k)\left[\int_0^1 J^{\zeta}_{k,c_k}(r)dJ^{\zeta}_{k,c_k}(r) + \mathcal{D}_k \int_0^1 J^{\zeta*}_{k,c_k}(r)dJ^{\zeta*}_{k,c_k}(r)\right]}{\int_0^1 \left[J^{\zeta}_{k,c_k}(r)\right]^2 dr + \mathcal{D}_k \int_0^1 \left[J^{\zeta*}_{k,c_k}(r)\right]^2 dr}, \quad k = 0, \ldots, \lfloor S/2 \rfloor \tag{4.1}$$

$$Z^*_k \Rightarrow \frac{2\left[\int_0^1 J^{\zeta*}_{k,c_k}(r)dJ^{\zeta}_{k,c_k}(r) - \int_0^1 J^{\zeta}_{k,c_k}(r)dJ^{\zeta*}_{k,c_k}(r)\right]}{\int_0^1 \left[J^{\zeta}_{k,c_k}(r)\right]^2 dr + \int_0^1 \left[J^{\zeta*}_{k,c_k}(r)\right]^2 dr}, \quad k = 1, \ldots, S^* \tag{4.2}$$

while the corresponding t- and $F-$type statistics satisfy

$$Z_{t_k} \Rightarrow \frac{\int_0^1 J^{\zeta}_{k,c_k}(r)dJ^{\zeta}_{k,c_k}(r) + \mathcal{D}_k \int_0^1 J^{\zeta*}_{k,c_k}(r)dJ^{\zeta*}_{k,c_k}(r)}{\left\{\int_0^1 \left[J^{\zeta}_{k,c_k}(r)\right]^2 dr + \mathcal{D}_k \int_0^1 \left[J^{\zeta*}_{k,c_k}(r)\right]^2 dr\right\}^{1/2}} =: \mathcal{T}^{\zeta}_k, \quad k = 0, ..., \lfloor S/2 \rfloor \tag{4.3}$$

$$Z_{t^*_k} \Rightarrow \frac{\int_0^1 J^{\zeta*}_{k,c_k}(r)dJ^{\zeta}_{k,c_k}(r) - \int_0^1 J^{\zeta}_{k,c_k}(r)dJ^{\zeta*}_{k,c_k}(r)}{\left\{\int_0^1 \left[J^{\zeta}_{k,c_k}(r)\right]^2 dr + \int_0^1 \left[J^{\zeta*}_{k,c_k}(r)\right]^2 dr\right\}^{1/2}} =: \mathcal{T}^{*\zeta}_k, \quad k = 1, \ldots, S^* \tag{4.4}$$

$$F_{PP,k} \Rightarrow \frac{1}{2}\left[\left(\mathcal{T}^{\zeta}_k\right)^2 + \left(\mathcal{T}^{*\zeta}_k\right)^2\right], \quad k = 1, \ldots, S^* \tag{4.5}$$

$$F_{PP,j...\lfloor S/2 \rfloor} \Rightarrow \frac{1}{S-j}\left[\sum_{i=j}^{\lfloor S/2 \rfloor}\left(\mathcal{T}^{\zeta}_i\right)^2 + \sum_{k=1}^{S^*}\left(\mathcal{T}^{*\zeta}_k\right)^2\right], \ j = 0, 1 \tag{4.6}$$

where $\mathcal{D}_k = 0$, for $k = 0, S/2$ and $\mathcal{D}_k = 1$, for $k = 1, ..., S^*$. The limiting processes, $J^{\zeta}_{0,c_0}(r)$, $J^{\zeta}_{S/2,c_{S/2}}(r)$, $J^{\zeta}_{k,c_k}(r)$ and $J^{\zeta*}_{k,c_k}(r)$, $k = 1, \ldots, S^*$, are as defined in Theorem 3.1.

Remark 4.1: The limiting null distributions of the PP-type statistics from section 3.1 are obtained on setting $c_k = 0$ (so that, correspondingly, $H_{0,k}$ holds) in the representations given in Theorem 4.1. These limiting null distributions coincide with those reported in Smith *et al.* (2009) and Rodrigues and Taylor (2007), for OLS and local GLS de-trending respectively, for the corresponding HEGY statistics from (3.1) in the case where u_{Sn+s} is serially uncorrelated. Notice also that, contrary to what is shown in, *inter alia*, Burridge and Taylor (2001) and del Barrio Castro, Osborn and Taylor (2012), for the corresponding t_k and t^*_k augmented HEGY statistics from (2.4), when u_{Sn+s} is serially correlated the limiting null distributions of the harmonic frequency PP-type test statistics Z_k, Z_{t_k}, Z^*_k and $Z_{t^*_k}$, $k = 1, ..., S^*$, are free from nuisance parameters. Indeed, the asymptotic null distributions of Z^*_k and $Z_{t^*_k}$ coincide with those reported for the augmented HEGY t_k and t^*_k statistics, $k = 1, ..., S^*$, in Burridge and Taylor (2001) and del Barrio Castro, Osborn and Taylor (2012) for the case where $a_k = 0$ and $b_k = 1$; that is, in the absence of serial correlation in u_{Sn+s}. The foregoing asymptotic

equivalence results between the HEGY and corresponding PP-type statistics also hold under the local alternative, $H_{1,\mathbf{c}}$.

Remark 4.2: Selected critical values for tests based on the statistics in (4.1)-(4.4) and (4.5)-(4.6) (for the quarterly, $S = 4$, and monthly, $S = 12$, cases) are provided for the case of OLS de-trended tests in HEGY, Ghysels *et al.* (1994) and Smith and Taylor (1998), and for GLS de-trended tests in Rodrigues and Taylor (2007). Notice that the limiting null distribution in (4.1) for both $k = 0$ and $k = \lfloor S/2 \rfloor$ coincides with the limiting null distribution of the standard normalised bias statistic of Dickey and Fuller (1979), with relevant critical values provided in Fuller (1996). Furthermore, the limiting null distribution in (4.1), for $k = 1, ..., S^*$, coincides with the limiting null distribution of the Dickey *et al.* (1984) unit root test statistic, from where relevant critical values can be obtained.

4.2 The $\mathcal{M}$-Type Seasonal Unit Root Tests

In this subsection we detail the limiting distributions for the various $\mathcal{M}$-type seasonal unit root test statistics proposed in section 3.2. In Theorem 4.1 we first provide limiting representations for the single unit root $\mathcal{M}$-type statistics in (3.18)-(3.20) and (3.29)-(3.31).

Theorem 4.2. *Let the conditions of Theorem 4.1 hold. Then, as $T \to \infty$: (i) for the zero ($k = 0$) and Nyquist ($k = S/2$) frequencies, the single $\mathcal{M}$-type seasonal unit root test statistics in (3.18)-(3.20) satisfy,*

$$\mathcal{MZ}_k \Rightarrow \left\{ 2 \int_0^1 \left[J^{\zeta}_{k,c_k}(r) \right]^2 dr \right\}^{-1} \left\{ \left[J^{\zeta}_{k,c_k}(1) \right]^2 - 1 \right\}, \quad k = 0, S/2 \tag{4.7}$$

$$\mathcal{MSB}_k \Rightarrow \left\{ \int_0^1 \left[J^{\zeta}_{k,c_k}(r) \right]^2 dr \right\}^{1/2} =: \mathfrak{MSB}_k, \quad k = 0, S/2 \tag{4.8}$$

$$\mathcal{MZ}_{t_{\pi_k}} \Rightarrow \frac{1}{2} \left\{ \int_0^1 \left[J^{\zeta}_{k,c_k}(r) \right]^2 dr \right\}^{-1/2} \left\{ \left[J^{\zeta}_{k,c_k}(1) \right]^2 - 1 \right\}, \quad k = 0, S/2; \tag{4.9}$$

(ii) the harmonic frequency single unit root test statistics in (3.29)-(3.31), where it is to be recalled that setting $\mathcal{K} = \mathcal{R}e$ in what follows yields the results for statistics based on $y^{\mathcal{R}e,\xi}_{k,Sn+s}$ while setting $\mathcal{K} = \mathcal{I}m$ yields the corresponding results for the statistics based on $y^{\mathcal{I}m,\xi}_{k,Sn+s}$, satisfy

$$\mathcal{K}\text{-}\mathcal{MZ}_k \Rightarrow \left\{ 2 \int_0^1 \left[\mathcal{H}^{\zeta}_{k,c_k}(r) \right]^2 dr \right\}^{-1} \left\{ \left[\mathcal{H}^{\zeta}_{k,c_k}(1) \right]^2 - 1 \right\} =: \mathcal{MZ}^{\mathcal{K}}_k, \quad k = 1, ..., S^* \tag{4.10}$$

$$\mathcal{K}\text{-}\mathcal{MSB}_k \Rightarrow \left[\int_0^1 \left[\mathcal{H}^{\zeta}_{k,c_k}(r) \right]^2 dr \right]^{1/2} =: \mathfrak{MSB}^{\mathcal{K}}_k, \quad k = 1, ..., S^* \tag{4.11}$$

$$\mathcal{K}\text{-}\mathcal{MZ}_{t_k} \Rightarrow \mathcal{MZ}^{\mathcal{K}}_k \times \mathfrak{MSB}^{\mathcal{K}}_k =: \mathcal{K}\text{-}\mathcal{T}^{\zeta}_k, \quad k = 1, ..., S^* \tag{4.12}$$

where $\mathcal{H}^{\zeta}_{k,c_k}(r) := J^{\zeta}_{k,c_k}(r)$ if $\mathcal{K} = \mathcal{R}e$ and $\mathcal{H}^{\zeta}_{k,c_k}(r) := J^{*\zeta}_{k,c_k}(r)$ if $\mathcal{K} = \mathcal{I}m$, with $J^{\zeta}_{0,c_0}(r)$, $J^{\zeta}_{S/2,c_{S/2}}(r)$, $J^{\zeta}_{k,c_k}(r)$ and $J^{\zeta *}_{k,c_k}(r)$, $k = 1, \ldots, S^*$, $\zeta = 1, 2$, the independent (scalar) OU processes defined in Remark A.3 of the Appendix.

Remark 4.3: Using Itô's rule, the limiting distributions given for $\mathcal{MZ}_k$, $k = 0, S/2$, in (4.7), which are identical (for a given value of ζ) to and independent of those given for $\mathcal{R}e\text{-}\mathcal{MZ}_k$ and $\mathcal{I}m\text{-}\mathcal{MZ}_k$, $k = 1, ..., S^*$, in (4.10), can be seen to coincide with those given for Z_k, for $k = 0, S/2$, in (4.1). Similarly, the limiting distributions for the $\mathcal{MZ}_{t_k}$, $k = 0, S/2$, statistics of (4.9) are identical (for a given value of ζ) to and independent of those for $\mathcal{R}e\text{-}\mathcal{MZ}_{t_k}$ and $\mathcal{I}m\text{-}\mathcal{MZ}_{t_k}$ in (4.12), and coincide with those given for Z_{t_k}, for $k = 0, S/2$, in (4.3). Moreover, it is also seen from (4.8) and (4.11) that the limiting distributions of the $\mathcal{MSB}_k$, $k = 0, S/2$, $\mathcal{R}e\text{-}\mathcal{MSB}_k$ and $\mathcal{I}m\text{-}\mathcal{MSB}_k$, $k = 1, ..., S^*$, statistics are identical (again for a given value of ζ) and are mutually independent.

Remark 4.4: The limiting distributions which obtain for the seasonal $\mathcal{M}$-type statistics discussed in Theorem 4.1 coincide with those of the corresponding non-seasonal $\mathcal{M}$ statistics detailed at the start of section 3.2.1. Selected critical values for the tests based on these statistics can therefore be obtained from Table I of Elliott *et al.* (1996, p.825) and from Table 1 of Ng and Perron (2001,p.1524). Moreover, the asymptotic local power functions of these statistics also coincide with those given for the corresponding statistics in the non-seasonal case and graphed in Figures 1-3 of Elliott *et al.* (1996, pp.822-24).

In Corollary 4.1, the proof of which follows immediately from the results given in Theorem 4.1 using applications of the Continuous Mapping Theorem, we now detail the limiting distributions of the harmonic frequency $\mathcal{M}$-type $F^{\mathtt{D}}_{\mathcal{M},k}$, $\mathcal{MSB}^{\mathtt{D}}_k$ and $S^{\mathtt{D}}_{\mathcal{M},k}$, $k = 1, ..., S^*$, statistics and the joint frequency $F^{\mathtt{D}}_{\mathcal{M},j...\lfloor S/2\rfloor}$, $\mathcal{MSB}^{\mathtt{D}}_{j...\lfloor S/2\rfloor}$ and $S^{\mathtt{D}}_{\mathcal{M},j...\lfloor S/2\rfloor}$, $j = 0, 1$, statistics from section 3.2.

Corollary 4.1. *Let the conditions of Theorem 4.1 hold. Then, as $T \to \infty$,*

$$\begin{aligned}
F^{\mathtt{D}}_{\mathcal{M},k} &\Rightarrow \frac{1}{2}\left[\left(\mathcal{R}e\text{-}\mathcal{T}^{\zeta}_k\right)^2 + \left(\mathcal{I}m\text{-}\mathcal{T}^{\zeta}_k\right)^2\right] =: \mathcal{F}^{\mathtt{D}}_{\mathcal{M},k}, \quad k = 1, ..., S^* \\
F^{\mathtt{D}}_{\mathcal{M},1...\lfloor S/2\rfloor} &\Rightarrow \frac{1}{S-1}\left[2\sum_{k=1}^{S^*}\mathcal{F}^{\mathtt{D}}_{\mathcal{M},k} + \left(\mathcal{T}^{\zeta}_{S/2}\right)^2\right],\ F^{\mathtt{D}}_{\mathcal{M},0...\lfloor S/2\rfloor} \Rightarrow \frac{1}{S}\left[2\sum_{k=1}^{S^*}\mathcal{F}^{\mathtt{D}}_{\mathcal{M},k} + \left(\mathcal{T}^{\zeta}_0\right)^2 + \left(\mathcal{T}^{\zeta}_{S/2}\right)^2\right]
\end{aligned}$$

$$\begin{aligned}
\mathcal{MSB}^{\mathtt{D}}_k &\Rightarrow \frac{1}{2}\left\{\left(\mathfrak{MSB}^{\mathcal{R}e}_k\right)^2 + \left(\mathfrak{MSB}^{\mathcal{I}m}_k\right)^2\right\}^{1/2} =: \mathfrak{MSB}^{\mathtt{D}}_k, \quad k = 1, ..., S^* \\
\mathcal{MSB}^{\mathtt{D}}_{j...\lfloor S/2\rfloor} &\Rightarrow \left[\sum_{k=j}^{\lfloor S/2\rfloor}\left(\mathfrak{MSB}^{\mathtt{D}}_k\right)^2\right]^{1/2}, \quad j = 0, 1
\end{aligned}$$

and

$$\begin{aligned}
S^{\mathtt{D}}_{\mathcal{M},k} &\Rightarrow \mathcal{R}e\text{-}\mathcal{T}^{\zeta}_k + \mathcal{I}m\text{-}\mathcal{T}^{\zeta}_k, \quad k = 1, ..., S^* \\
S^{\mathtt{D}}_{\mathcal{M},1...\lfloor S/2\rfloor} &\Rightarrow \sum_{k=1}^{S^*}\left(\mathcal{R}e\text{-}\mathcal{T}^{\zeta}_k + \mathcal{I}m\text{-}\mathcal{T}^{\zeta}_k\right) + \mathcal{T}^{\zeta}_{S/2},\ S^{\mathtt{D}}_{\mathcal{M},0...\lfloor S/2\rfloor} \Rightarrow \sum_{k=1}^{S^*}\left(\mathcal{R}e\text{-}\mathcal{T}^{\zeta}_k + \mathcal{I}m\text{-}\mathcal{T}^{\zeta}_k\right) + \mathcal{T}^{\zeta}_0 + \mathcal{T}^{\zeta}_{S/2}
\end{aligned}$$

where $\mathcal{T}^{\zeta}_k$, $k = 0, S/2$, are as defined in Theorem 4.1, and $\mathcal{R}e\text{-}\mathcal{T}^{\zeta}_k$, $\mathcal{I}m\text{-}\mathcal{T}^{\zeta}_k$ and $\mathfrak{MSB}^{\mathcal{K}}_k$, $k = 1, ..., S^*$, are as defined in Theorem 4.2.

Remark 4.5: The limiting distributions which appear in Corollary 4.1 have not appeared in the literature before. Consequently, in Table 1 for the $\mathcal{S}_{\mathcal{M}}^{\mathtt{D}}$ and $\mathcal{MSB}^{\mathtt{D}}$ tests, and in Table 2 for the $F_{\mathcal{M}}^{\mathtt{D}}$ tests, we provide selected asymptotic null critical values, computed by direct simulation of the relevant limiting null distributions in Corollary 4.1, using 100,000 Monte Carlo replications and a discretisation of $N = 1000$ steps, for versions of the statistics based on either OLS de-trended data or local GLS de-trended data, the latter using the relevant values of $\bar{c}$ detailed in section 2.3. Critical values are reported for each of Cases 1–3 for the deterministic component outlined in section 1.

[Tables 1 - 2 about here]

Remark 4.6: We conclude this section by providing representations for the limiting distributions of the alternative $\mathcal{M}$-type harmonic frequency unit root tests discussed in Remark 3.5. Under the conditions of Theorem 4.1 it is straightforward to show that

$$\mathcal{MZ}_k^{\mathtt{D}} \Rightarrow \frac{\left[J_{k,c_k}^{\zeta}(1)\right]^2 + \left[J_{k,c_k}^{\zeta *}(1)\right]^2 - 2}{\int_0^1 \left[J_{k,c_k}^{\zeta}(r)\right]^2 dr + \int_0^1 \left[J_{k,c_k}^{\zeta *}(r)\right]^2 dr}, \quad k = 1, ..., S^*$$

$$\mathcal{MZ}_{t_k}^{\mathtt{D}} \Rightarrow \frac{\left[J_{k,c_k}^{\zeta}(1)\right]^2 + \left[J_{k,c_k}^{\zeta *}(1)\right]^2 - 2}{2\left\{\int_0^1 \left[J_{k,c_k}^{\zeta}(r)\right]^2 dr + \int_0^1 \left[J_{k,c_k}^{\zeta *}(r)\right]^2 dr\right\}^{1/2}}, \quad k = 1, ..., S^*.$$

4.3 Asymptotic Local Power Functions

Figures 1 and 2 graph the asymptotic local power functions of the seasonal PP-type and seasonal $\mathcal{M}$-type unit root tests proposed in section 3, together with the corresponding augmented HEGY tests of section 2 and the seasonal point optimal-based tests of Rodrigues and Taylor (2007). Results for the zero, Nyquist and harmonic frequency unit root tests (which are independent of the seasonal aspect, S) are given in Figure 1, while results for joint frequency tests for the quarterly case, $S = 4$, are given in Figure 2. In each case the tests are based on local GLS de-trending[6] with results given for $\zeta = 1$ and $\zeta = 2$, where ζ is as defined in section 4. Each graph also reports the relevant Gaussian asymptotic local power envelope as a benchmark. The local power functions were calculated using direct simulation methods using 80,000 Monte Carlo replications, discretising over $N = 1000$ steps. The horizontal axes of the graphs are indexed by c which is used generically to denote either the relevant frequency-specific non-centrality parameter, c_k, $k = 0, ..., \lfloor S/2 \rfloor$ (so that for tests at the zero frequency, for example, $c = c_0$) or, in the case of joint frequency tests, a common non-centrality parameter (for example, $c = c_1 = c_2$ in the case of the tests of the null hypothesis of unit roots at all of the seasonal frequencies).

[6]This will be the case for all of the numerical results presented in the remainder of the paper. Corresponding results for tests based on OLS de-trended data are available on request.

Consider first Figure 1(a) and 1(b) which reports results for the zero and Nyquist frequency tests. In particular results are reported for the Z_k, Z_{t_k}, $\mathcal{M}Z_k$, $\mathcal{M}Z_{t_k}$ and $\mathcal{MSB}_k$, $k = 0, S/2$, tests from section 3 together with the feasible point optimal-type tests from section 4 of Rodrigues and Taylor (2007, pp.556-558). The latter statistics will be denoted $P_{k,T}$, $k = 0, S/2$, in what follows, and are based on the local GLS de-trending parameters $\bar{c}_k$ given in section 2.3. As discussed in section 4, for a given value of ζ the large sample behaviour of a given zero frequency statistic and its Nyquist frequency analogue coincide, and coincide with the behaviour of that statistic in the non-seasonal ($S = 1$) case. This is also true of the $P_{k,T}$, $k = 0, S/2$, statistics, as demonstrated in Rodrigues and Taylor (2007).

Figures 1–2 about here

For the case of local GLS de-meaning ($\zeta = 1$) in Figure 1(a) it is seen that the asymptotic local power functions of the Z_k, Z_{t_k}, $\mathcal{M}Z_k$, $\mathcal{M}Z_{t_k}$, $\mathcal{MSB}_k$ and $P_{k,T}$, $k = 0, S/2$ tests all lie very close to the Gaussian power envelope and are almost indistinguishable from each, echoing results in Figures 1-3 of Elliott *et al.* (1996). For the local GLS de-trended ($\zeta = 2$) case in Figure 1(b), we see a decline in the power curves and the power envelope relative to the corresponding quantities in Figure 1(a), again consonant with Figures 1-3 of Elliott *et al.* (1996). In the local GLS de-trended case the tests again all lie very close to one another and again are effectively indistinguishable from the Gaussian power envelope.

Figures 1(c) and 1(d) present the corresponding results for the harmonic frequency PP-type tests, Z_k, Z_{t_k} and $F_{PP,k}$, $k \in \{1, ..., S^*\}$, together with the harmonic frequency $\mathcal{M}$-type tests of section 3.2.2 and the feasible point optimal $P_{k,T}$ test of Rodrigues and Taylor (2007). The Gaussian local power envelopes in this case are taken from Gregior (2006) and Rodrigues and Taylor (2007). For a given value of ζ the demodulated single unit root $\mathcal{M}$-type tests in (3.18)-(3.20) and (3.29)-(3.31) were all virtually indistinguishable from one another and so we plot only the local power function of $\mathcal{R}e\text{-}\mathcal{MZ}_{t_k}$ in Figures 1(c) and 1(d).

Looking first at the results for local GLS de-meaning ($\zeta = 1$) in Figure 1(c), it is seen that the local power function of the demodulated single unit root $\mathcal{M}$ test lies well below the Gaussian local power envelope and well below the power functions of the other harmonic frequency unit root tests, as would be expected given that each of the latter jointly test on both complex conjugate harmonic frequency unit roots rather than only one of the pair of roots. Of the other tests, the $P_{k,T}$, Z_k and Z_{t_k} tests display the best power and are virtually indistinguishable from one another. The $\mathcal{MSB}_k^{\mathtt{D}}$ and the $S_{\mathcal{M},k}^{\mathtt{D}}$ test of Remark 3.6 are both slightly less powerful than the aforementioned group of tests, followed by the standard HEGY F_k test (notice that F_k and the PP-type $F_{PP,k}$ test have the same asymptotic local power function) and the demodulated $F_{\mathcal{M},1}^{\mathtt{D}}$ test whose power functions lie close to one another. For the local GLS de-trended case in Figure 1(d) we see the same power ordering among the tests as was seen in Figure 1(c) but the differences between these power functions are far less pronounced, with the exception of the demodulated single unit root $\mathcal{M}$ test whose power function still lies well below those of the other tests. As with the corresponding results in Figures 1(a) and 1(b), the power functions and the power envelope again decline relative to those in Figure 1(c).

Finally in Figure 2 we graph the Gaussian power envelopes and asymptotic local power functions of the joint frequency tests discussed in this paper which obtain in the quarterly case, $S = 4$. Specifically, Figures 2(a) and 2(b) report results, for the local GLS de-meaned and de-trended cases respectively, the F_{12}, $F^{\mathtt{D}}_{\mathcal{M},12}$, $\mathcal{MSB}^{\mathtt{D}}_{12}$, $S^{\mathtt{D}}_{\mathcal{M},12}$ and the corresponding feasible point optimal test of Rodrigues and Taylor (2007), denoted $PT_{12,T}$, tests, while Figures 2(c) and 2(d) report results, again for the local GLS de-meaned and de-trended cases respectively, for the F_{012}, $F^{\mathtt{D}}_{\mathcal{M},012}$, $\mathcal{MSB}^{\mathtt{D}}_{012}$, $S^{\mathtt{D}}_{\mathcal{M},012}$ and $PT_{012,T}$ tests, the latter again denoting the relevant feasible point optimal test from Rodrigues and Taylor (2007). Recall that the asymptotic local power functions of the PP-type $F_{PP,12}$ and $F_{PP,012}$ tests of Remark 3.4 coincide with those of the HEGY F_{12} and F_{012} tests, respectively.

Consider first Figures 2(a) and 2(b) which pertain to tests of the null hypothesis of unit roots at all of the seasonal frequencies, $H_{0,\text{seas}} = \cap_{k=1}^{2} H_{0,k}$. The $S^{\mathtt{D}}_{\mathcal{M},12}$ test and the feasible point optimal $P_{12,T}$ test outperform the other tests regardless of whether de-meaning or de-trending is considered. For the de-meaned case, the $\mathcal{MSB}^{\mathtt{D}}_{12}$ test outperforms both the F_{12} and $F^{\mathtt{D}}_{\mathcal{M},12}$ tests, but for the de-trended case these three tests all perform quite similarly. Rather similar qualitative patterns are also observed in Figures 2(c) and 2(d) for the corresponding tests of the overall null hypothesis, $H_0 = \cap_{k=0}^{2} H_{0,k}$.

5 Finite Sample Results

In this section we investigate the finite sample size and (local) power properties of the new semi-parametric seasonal PP-type and seasonal $\mathcal{M}$-type unit root tests proposed in section 3, comparing them with the augmented HEGY tests of section 2 and the feasible point optimal tests of Rodrigues and Taylor (2007). Our simulations are based on the following quarterly ($S = 4$) DGP:

$$\left(1 - \left[1 + \frac{c_0}{4N}\right] L\right)\left(1 + \left[1 + \frac{c_2}{4N}\right] L\right)\left(1 + \left[1 + \frac{c_1}{4N}\right]^2 L^2\right) x_{4n+s} = u_{4n+s} \quad s = -3, ..., 0, \;\; n = 1, ..., N \tag{5.1}$$

with $x_{-3} = \cdots = x_0 = 0$ and where u_{4n+s} a stationary error whose properties will be detailed below. Results relating to finite sample size, where $c_0 = c_1 = c_2 = 0$, are reported in section 5.1, while finite sample power results, where $c_i < 0$, for some $i \in \{0, 1, 2\}$, are reported in section 5.2. Results are reported for $N = 50$ and $N = 100$ years of data, yielding total sample sizes of $T = 200$ and $T = 400$, respectively.

For the long run variance estimates needed to implement the new semi-parametric tests proposed in this paper, we explored the use of Bartlett and Quadratic Spectral kernels for the sums-of-covariances estimators $\hat{\lambda}^2_{0,WA}$, $\hat{\lambda}^2_{1,WA}$, $\hat{\lambda}^{*2}_{1,WA}$ and $\hat{\lambda}^2_{2,WA}$, and the corresponding parametric autoregressive spectral density [ASD] estimators $\hat{\lambda}^2_{0,AR}$, $\hat{\lambda}^2_{1,AR}$, $\hat{\lambda}^{*2}_{1,AR}$ and $\hat{\lambda}^2_{2,AR}$. The tests based on ASD estimates displayed considerably better finite sample behaviour than those based on sums-of-covariances estimates and so we only report results here for the former; results for the latter can be obtained from the authors on request. For the purpose of estimating $\psi\left(e^{i\omega_k}\right)$ and $\psi\left(e^{-i\omega_k}\right)$, which are necessary for the computation of the demodulated tests, as in

section 3.2.2 we use the ASD estimators $\breve{\lambda}^2_{1,AR}$ and $\breve{\lambda}^{*2}_{1,AR}$. The AR lag order used in constructing the ASD estimates was determined using the modified MAIC criteria recently proposed by del Barrio Castro, Osborn and Taylor (2016) using Schwert's rule, $k_{\max K} := \lfloor K[\frac{T}{100}]^{1/4} \rfloor$, with K a constant discussed below, to determine the maximum lag length allowed. As in Perron and Qu (2007) the $MAIC$ criteria is computed based on OLS de-trended data. Results are reported for both Case 1 (zero and seasonal frequency intercepts) and Case 3 (zero and seasonal frequency intercepts and trends). As noted before, all reported results are based on local GLS de-trending.

5.1 Empirical Size

Tables 3-5 report the results of our empirical size simulations. Table 3 reports results for tests for a unit root at frequency zero for both Cases 1 and 3. Table 4a (Case 1) and Table 4b (Case 3) report the corresponding results for the tests for a unit root at the Nyquist frequency, while Table 5a (Case 1) and Table 5b (Case 3) report results for the harmonic frequencies. Joint frequency tests are also reported, where relevant to the frequency under consideration, in the tables.

As discussed in section 1, both non-seasonal and seasonal unit root tests are most prone to the problem of over-sizing in finite samples when there is a significant MA component in the shocks which is such that it causes a near cancellation effect with the autoregressive unit root. Because the non-seasonal $\mathcal{M}$ tests have been shown to be particular effective in controlling these distortions, our focus in this subsection is to investigate whether the seasonal $\mathcal{M}$-type tests proposed in this paper are also effective against such near cancellation effects. The results in Tables 3-5 therefore pertain to the case where the error term u_{4n+s} in (5.1) follows an MA process which displays a near-cancellation region with the autoregressive polynomial $\omega_k(L)$, as defined at the start of section 2.2, at the frequency ω_k, $k = 0, 1, 2$, of interest. To that end we generate u_{4n+s} as the MA(q) process

$$u_{4n+s} = \varepsilon_{4n+s} - \theta_q \varepsilon_{4n+s-q}, \;\; \varepsilon_{4n+s} \sim NIID\,(0,1)\,, \qquad s = -3, ..., 0, \;\; n = 1, ..., N$$

initialised at $\varepsilon_j = 0$, $j \leq 0$. The order of the MA process and the range of values of the MA parameter which generate a near cancellation region vary according to the frequency of interest. For the zero frequency we consider $q = 1$ and $\theta_1 \in \{0, 0.2, 0.4, 0.6, 0.8, 0.9\}$. For the Nyquist frequency we consider $q = 1$ and $\theta_1 \in \{0, -0.2, -0.4, -0.6, -0.8, -0.9\}$. Finally, for the harmonic frequency, we consider $q = 2$ and $\theta_2 \in \{0, -0.04, -0.16, -0.36, -0.64, -0.81\}$. It can be seen that these designs generate near cancellation regions at the zero, Nyquist and harmonic frequencies, respectively. Notice also that the moduli of the resulting MA roots is the same for each of these three designs. Given the range of values of θ_q considered, we set $K = 12$ in the formula for $k_{\max K}$ above in order to allow for a reasonably long lag length in the AR approximation.

Tables 3 - 5 about here

Consider first the results in Table 3 for the zero frequency tests. Although the standard HEGY t_0 test displays reasonably good size control both when $\theta_1 = 0$ and when θ_1 is small,

its empirical size rises significantly above the nominal level as θ_1 increases. This occurs in both Cases 1 and 3 of the deterministic component, with the distortions slightly lower in general under Case 3. Although ameliorated as T increases, the empirical size of t_0 remains uncomfortably large, even for $N = 100$, for large values of θ_1. To illustrate, under Case 1 and $\theta_1 = 0.9$ the empirical size of t_0 is almost 23% for $N = 50$ reducing only to 18% for $N = 100$. The size distortions seen in the PP-type Z_0 and Z_{t_0} are significantly worse than for t_0 with these tests rejecting almost all of the time in the previous two examples. Consistent with findings for the non-seasonal case in Ng and Perron (2001), the trinity of zero frequency $\mathcal{M}$-type tests all display significantly better size control than the HEGY t_0 test, and show more pronounced improvements in relative size control than the HEGY tests as the sample size increases. In the example above, the three $\mathcal{M}$ tests all display empirical size of around 8% for $N = 50$, with no over-sizing seen for $N = 100$; indeed, again consistent with the simulation results in Ng and Perron (2001), the tests are all slightly under-sized in the latter case. As with the t_0 test, distortions tend to be lower under Case 3 (with the exception of the case where $\theta_1 = 0.9$ and $N = 50$); here the three $\mathcal{M}$ tests for $\theta_1 = 0.9$ are again slightly under-sized when $N = 100$ (compared to 17% size for t_0). The feasible point optimal $P_{0,T}$ test of Rodrigues and Taylor (2007) behaves very similarly to the trinity of $\mathcal{M}$ tests. Similar observations can be made about the joint frequency tests in Table 1. The PP-type $F_{PP,012}$ test is very badly oversized when $\theta_1 > 0$. The lowest size distortions are again displayed by the joint frequency $\mathcal{M}$-type tests from section 3 and the corresponding feasible point optimal test, $P_{012,T}$, from Rodrigues and Taylor (2007), although the latter is consistently undersized, particularly so under Case 3. In particular, the $F^{\mathtt{D}}_{\mathcal{M},012}$ test displays consistently better size control than the HEGY F_{012} test.

Turning to the results for the Nyquist frequency in Tables 4a and 4b, very similar patterns of size distortions are seen here as were observed in Table 3 as might be expected, given that an equivalent near cancellation effect is obtained here for a given value of θ_1 as for the zero frequency results. In addition to the joint tests considered in Table 3, Tables 4a and 4b also report the joint tests for testing the null hypothesis of unit roots at all of the seasonal frequencies, $H_{0,\text{seas}}$. Again the same relative behaviour is seen between the HEGY-type, $\mathcal{M}$-type and PP-type tests as is observed for the other tests.

Finally, we turn to the results for the seasonal harmonic frequency in Tables 5a and 5b. Consider first the results in Table 5a for deterministic Case 1. As with the results for the HEGY tests in Tables 3 and 4a-4b, the harmonic frequency HEGY F_1 test displays good size control for small values of θ_2 but is again rather over-sized for the larger values of θ_2 considered. For example, for $\theta_2 = 0.81$ and $N = 50$ the F_1 test has size of about 12% falling to about 8% for $N = 100$. The best size control is offered by the $F^{\mathtt{D}}_{\mathcal{M},1}$ test which displays excellent size control for all values of θ_2 considered for both $N = 50$ and $N = 100$. In the example given above $F^{\mathtt{D}}_{\mathcal{M},1}$ has empirical size of about 5% for $N = 50$ and 3% for $N = 100$. The single root demodulated tests $\mathcal{R}e\text{-}\mathcal{MZ}_1$, $\mathcal{I}m\text{-}\mathcal{MZ}_1$, $\mathcal{R}e\text{-}\mathcal{MZ}_{t_1}$, $\mathcal{I}m\text{-}\mathcal{MZ}_{t_1}$, $\mathcal{R}e\text{-}\mathcal{MSB}_1$ and $\mathcal{I}m\text{-}\mathcal{MSB}_1$, all perform quite similarly to one another but do not control size quite as well as $F^{\mathtt{D}}_{\mathcal{M},1}$, displaying significant under-size when $\theta_2 = 0.81$, and some over-sizing for $\theta_2 = 0.16$ when $N = 50$. The

$\mathcal{MSB}_1^{\mathtt{D}}$ and $P_{1,T}$ test of Rodrigues and Taylor (2007) behave similarly to one another, displaying slightly poorer size control than the HEGY F_1 test. The worst size control is displayed by the PP-type $F_{PP,1}$ test.[7] As regards the joint frequency tests, here the feasible point optimal tests of Rodrigues and Taylor (2007) appear to offer the best size control overall. The joint frequency $\mathcal{M}$-type tests perform similarly to the corresponding joint frequency HEGY tests, F_{12} and F_{012}.

The results in Table 5b for deterministic Case 3 show a similar ordering between the various tests but with an overall deterioration seen in the finite sample size control of most of the tests considered. Again the best size control among the harmonic frequency unit root tests is shown by the $F_{\mathcal{M},1}^{\mathtt{D}}$ test, which displays fairly similar size control overall to the single root demodulated tests. These tests again display considerably better size control in the near cancellation region than the HEGY F_1 test. To illustrate when $\theta_2 = 0.81$, the HEGY F_1 test has empirical size of about 25% for $N = 50$ and 16% for $N = 100$, while the empirical size of $F_{\mathcal{M},1}^{\mathtt{D}}$ in these cases are about 4% and 3%, respectively, and those of the $P_{1,T}$ test are about 20% and 7%, respectively. In the case of the joint frequency tests, the joint frequency $\mathcal{M}$-type tests display arguably the best overall size control, now notably better than the corresponding joint frequency HEGY tests. The feasible point optimal tests of Rodrigues and Taylor (2007) also avoid any over-sizing but display a stronger tendency to under-sizing than the $\mathcal{M}$-type tests.

5.2 Empirical Power

Figures 3–6 graph the finite sample (size-adjusted) power functions of the tests considered in this paper for the case where the data are generated according to (5.1) with $u_{4n+s} \sim NIID(0,1)$, with K commensurately set to zero in the formula for $k_{\max K}$. And as in Rodrigues and Taylor (2007) the power results pertain to the case where, when moving a particular non-centrality parameter c_k, $k = 0, 1, 2$ away from unity, the remaining non-centrality parameters are all held at zero. The index, c, on the horizontal axes of the graphs has the same meaning as described above for Figures 1 and 2.

Figures 3 - 6 about here

From Figure 3 we observe that the zero frequency unit root tests considered display very similar power behaviour, particularly so when local GLS de-trending (Case 3) is considered, indeed here even for $N = 50$ the power functions of the various tests are almost indistinguishable. In the case of local GLS de-meaning (Case 1) and for the smaller sample size, $N = 50$, and as we move towards the stationarity region (i.e., as c becomes more negative) we note that the point optimal test PT_0 loses some power relative to the other tests, but overall finite sample power is still basically very similar across all of the zero frequency tests reported in Figure 3. We do not report corresponding results for the Nyquist frequency unit root tests statistics here because they were almost indistinguishable from the corresponding zero frequency tests reported in Figure 3.

[7] We do not report size properties for the PP-type Z_1 and Z_{t_1} tests because these were qualitatively no different from those reported for $F_{PP,1}$.

Turning to the results for the harmonic frequency unit root tests reported in Figure 4 we see that, in line with the corresponding asymptotic local power results reported in Figure 1, there is rather more variation across the finite sample power properties of the various tests, as compared with the results for the zero frequency tests in Figure 3. Again consistent with the corresponding asymptotic local power results in Figures 1(c) and 1(d), we see in Figure 4 that the demodulated single unit root test $\mathcal{R}e-\mathcal{MZ}_{t_1}$ (again we only report one of these demodulated single unit root tests because they all displayed virtually identical power properties) displays considerably lower power than the other harmonic frequency unit root tests. As for the remaining tests, under local GLS de-meaning (Case 1) the best performing tests are PT_1, $\mathcal{MSB}_1^D$ and $\mathcal{S}_{M,1}^D$, all three of which outperform the F_1 and $F_{M,1}^D$ tests, which perform very similarly, on power. These rankings hold for both $N = 50$ and $N = 100$; indeed, the local power properties of a given test alter little between the two sample sizes, suggesting again that the asymptotic local power functions provide good predictors for the finite sample powers of the tests. Under local GLS de-trending (Case 3), roughly the same power ordering as was observed for Case 1 is seen, although again as predicted by the asymptotic local power functions, the power differentials between the tests are decreased relative to those seen under Case 1.

We turn now to the finite sample power functions of the joint seasonal unit root tests graphed in Figure 5. For both sample sizes and under both Case 1 and 3 we see that the differences across the various power functions are relatively small. In terms of relative performance, under local GLS de-meaning (Case 1) for both sample sizes considered, the highest power is delivered by PT_{12}, closely followed by $\mathcal{S}_{M,12}^D$ and $\mathcal{MSB}_{12}^D$, with the lowest power displayed by F_{12} and $F_{M,12}^D$, the latter two displaying almost identical power. Under local GLS de-trending (Case 3) we again see that the best performing tests on power are PT_{12} and $\mathcal{S}_{M,12}^D$, while the power performances of F_{12} and $F_{M,12}^D$ are now as good and sometimes superior to that of $\mathcal{MSB}_{12}^D$.

Finally, in Figure 6 we display finite sample power graphs for the tests of the null hypothesis of a unit root at both the zero and all of the seasonal frequencies. The conclusions that we can draw from these graphs are qualitatively similar to those remarked on above for the joint seasonal frequency unit root tests. The only exception is for local GLS de-trending, where it is observed that F_{012}, $F_{M,012}^D$ and $\mathcal{MSB}_{012}^D$ display almost identical finite sample power.

6 Conclusions

In this paper we have generalised the class of semi-parametric unit root tests developed for non-seasonal data by Phillips and Perron (1998) and the related so-called $\mathcal{M}$ tests of Stock (1999), Perron and Ng (1996) and Ng and Perron (2001), to allow for unit root testing at the zero and seasonal frequencies in seasonally observed data. For the case of tests involving the seasonal harmonic frequencies this was shown to necessitate the use of demodulated data in constructing the $\mathcal{M}$-type class of test statistics. In the non-seasonal case the $\mathcal{M}$ unit root tests are known to considerably superior finite sample size control than the parametric augmented Dickey-Fuller tests in the most problematic (near-cancellation) case where the shocks contain

a strong negative moving average component. Using Monte Carlo simulation methods we have shown that this result carries over to the seasonal case with the $\mathcal{M}$-type seasonal unit root tests we develop here displaying significantly better finite sample size control than the corresponding parametric HEGY seasonal unit root tests in near cancellation regions. As in the non-seasonal case, these improvements in finite sample size were shown not to come at the expense of any loss in power relative to the HEGY tests. Moreover, certain of the $\mathcal{M}$-type seasonal unit root tests were shown to achieve similar power to the feasible point optimal tests of Rodrigues and Taylor (2007).

References

del Barrio Castro, T., D. R. Osborn and A.M.R. Taylor, 2012, On Augmented Hegy Tests For Seasonal Unit Roots, Econometric Theory 28, 1121-1143.

del Barrio Castro, T., D. R. Osborn and A.M.R. Taylor, 2016, The Performance of Lag Selection and Detrending Methods for HEGY Seasonal Unit Root Tests, forthcoming in Econometric Reviews.

Beaulieu, J.J. and J.A. Miron, 1993, Seasonal unit roots in aggregate U.S. data, Journal of Econometrics 55, 305-328.

Berk, K.N., 1974, Consistent autoregressive spectral estimates, The Annals of Statistics 2, 389-502.

Bhargava, A., 1986, On the theory of testing for unit roots in observed time series, Review of Economic Studies 53, 369-384.

Boswijk, H.P., and P.H. Franses, 1996, Unit roots in periodic autoregressions, Journal of Time Series Analysis 17, 221-245.

Box, G.E.P., and G.M. Jenkins, 1976, Time Series Analysis: Forecasting and Control (revised edition). San Francisco: Holden-Day.

Breitung, J. and P.H. Franses, 1998, On Phillips-Perron type tests for seasonal unit roots, Econometric Theory 14, 200-221.

Burridge, P. and A.M.R.Taylor, 2001, On the properties of regression-based tests for seasonal unit roots in the presence of higher-order serial correlation, Journal of Business and Economic Statistics 19, 374-379.

Davis, P.J., 1979, Circulant Matrices. Wiley-Interscience: New York.

Dickey, D.A., D.P. Hasza and W.A. Fuller, 1984, Testing for unit roots in seasonal time series, Journal of the American Statistical Association 79, 355-367.

Dickey, D.A. and W.A. Fuller, 1979, Distribution of the estimators for autoregressive time series with a unit root, Journal of the American Statistical Association 74, 427-431.

Elliott, G, T.J. Rothenberg and J.H. Stock, 1996, Efficient tests for an autoregressive unit root, Econometrica 64, 813-836.

Fuller, W.A., 1996, Introduction to Statistical Time Series, Second Edition, Wiley: New York.

Ghysels, E., H.S. Lee and J. Noh, 1994, Testing for unit roots in seasonal time series: some theoretical extensions and a Monte Carlo investigation, Journal of Econometrics 62, 415-442.

Ghysels, E. and D.R. Osborn, 2001, The Econometric Analysis of Seasonal Time Series, CUP: Cambridge.

Gray, R. M., 2006, Toeplitz and Circulant Matrices, A Review. Foundation and Trends(R) in Communications and Information Theory: Now Publishers Inc.

Granger, C.W.J. and M. Hatanaka, 1964, Spectral analysis of economic time series. Princeton, NJ: Princeton University Press.

Gregoir, S., 1999, Multivariate Time Series with Various Hidden Unit Roots, Part I: Integral Operator Algebra and Representation Theory, Econometric Theory 15, 435-468.

Gregoir, S., 2006, Efficient tests for the presence of a pair of complex conjugate unit roots in real time series, Journal of Econometrics, 130, 45-100.

Gregoir, S., 2010, Fully Modified Estimation of Seasonally Cointegrated Processes, Econometric Theory 26, 1491-1528.

Haldrup, N., and M. Jansson, 2006, Improving Power and Size in Unit Root Testing. Palgrave Handbooks of Econometrics: Vol. 1 Econometric Theory, Chapter 7. T. C. Mills and K. Patterson (eds.). Palgrave MacMillan, Basingstoke.

Hall, A.R., 1994, Testing for a unit root in time series with pretest data-based model selection. Journal of Business and Economic Statistics 12, 461-70.

Hylleberg, S., R.F. Engle, C.W.J. Granger and B.S. Yoo, 1990, Seasonal integration and cointegration, Journal of Econometrics 44, 215-238.

Jansson, M., 2002, Consistent covariance matrix estimation for linear processes, Econometric Theory 18, 1449-1459.

Müller, U.K. and G. Elliott, 2003, Tests for unit roots and the initial condition, Econometrica 71, 1269-1286.

Ng, S., and P. Perron, 1995, Unit root tests in ARMA models with data dependent methods for selection of the truncation lag. Journal of the American Statistical Association 90, 268-281.

Ng, S., and P. Perron, 2001, Lag length selection and the construction of unit root tests with good size and power, Econometrica 69, 1519-1554.

Osborn, D.R. and P.M.M. Rodrigues, 2002, The Asymptotic Distributions of Seasonal Unit Root Tests: A Unifying Approach. Econometric Reviews 21, 221-241.

Perron, P. and Z. Qu, 2007, A simple modification to improve the finite sample properties of Ng and Perrons unit root tests. Economics Letters 94, 1219.

Perron P., and Ng, S., 1996, Useful modifications to some unit root tests with dependent errors and their local asymptotic properties, Review of Economic Studies 63, 435-463.

Phillips, P.C.B. and P. Perron, 1988, Testing for a unit root in time series regression, Biometrika 75, 335-346.

Phillips, P.C.B., 1988, Regression theory for near-integrated time series, Econometrica 56, 1021-43.

Rodrigues, P.M.M., 2001, Near seasonal integration, Econometric Theory 17, 70-86.

Rodrigues, P.M.M. and A.M.R. Taylor, 2004, Asymptotic distributions for regression-based seasonal unit root test statistics in a near-integrated model, Econometric Theory 20, 645-670.

Rodrigues, P.M.M., and A.M.R. Taylor, 2007, Efficient Tests of the Seasonal Unit Root Hypothesis. Journal of Econometrics 141, 548-573.

Said, S.E. and D.A. Dickey, 1984, Test for unit roots in autoreressive-moving average models of unknown order, Biometrika 71, 599-609.

Smith, R.J. and A.M.R. Taylor, 1998, Additional critical values and asymptotic representations for seasonal unit root tests, Journal of Econometrics 85, 269-288.

Smith, R.J. and A.M.R. Taylor, 1999, Likelihood ratio tests for seasonal unit roots, Journal of Time Series Analysis 20, 453-476.

Smith R.J., Taylor, A.M.R., and T. del Barrio Castro, 2009, Regression-based seasonal unit root tests. Econometric Theory 25, 527-560.

Stock, J.H., 1999, A class of tests for integration and cointegration. Engle, R.F. and White, H. (eds.), Cointegration, Causality and Forecasting. A Festschrift in Honour of Clive W.J. Granger, Oxford: Oxford University Press, 137-167.

Appendix

A Preliminary Results

Before providing the proofs of the main results given in the paper, a number of preliminary results are needed first. To that end, we first note that under (2.3), x_{Sn+s} in (2.1b) can be written as,

$$\Delta_0^{c_0}\Delta_{S/2}^{c_{S/2}}\prod_{k=1}^{S^*}\Delta_k^{c_k}x_{Sn+s}=u_{Sn+s} \tag{A.1}$$

where $\Delta_0^{c_0}:=1-\alpha_0L=1-\left(1+\frac{c_0}{SN}\right)L$, $\Delta_{S/2}^{c_{S/2}}:=1+\alpha_{S/2}L=1+\left(1+\frac{c_{S/2}}{SN}\right)L$, and $\Delta_k^{c_k}:=1-2\cos\left[\omega_k\right]\alpha_kL+\alpha_k^2L^2=1-2\cos\left[\omega_k\right]\left(1+\frac{c_k}{SN}\right)L+\left(1+\frac{c_k}{SN}\right)^2L^2$, for $k=1,...,S^*$. Consequently, (A.1) can be equivalently written as,

$$x_{Sn+s}=\left[S_{0,c_0}\left(Sn+s\right)\right]\left[S_{S/2,c_{S/2}}\left(Sn+s\right)\right]\left[\prod_{k=1}^{S^*}S_{k,c_k}\left(Sn+s\right)\right]u_{Sn+s} \tag{A.2}$$

where, for $\omega_0=0$ and $\omega_{S/2}=\pi$,

$$S_{i,c_i}\left(Sn+s\right):=\sum_{j=1}^{Sn+s}\cos\left[\left(\left(Sn+s\right)-j\right)\omega_i\right]\alpha_i^{Sn+s-j}L^{Sn+s-j},\ i=0,S/2 \tag{A.3}$$

and, for $\omega_k=(2\pi k)/S, k=1,...,S^*$,

$$\begin{aligned}S_{k,c_k}\left(Sn+s\right) &:= \sin\left[\omega_k\right]^{-1}\sum_{j=0}^{Sn+s-1}\sin\left[\left(\left(Sn+s\right)+1-j\right)\omega_k\right]\alpha_k^{Sn+s-j}L^{Sn+s-j}\\ &= \sin\left[\omega_k\right]^{-1}\left(\sin\left[\left(\left(Sn+s\right)+1\right)\omega_k\right]S_{k,c_k}^{\alpha}\left(Sn+s\right)\right.\\ &\quad\left.-\cos\left[\left(\left(Sn+s\right)+1\right)\omega_k\right]S_{k,c_k}^{\beta}\left(Sn+s\right)\right)\end{aligned}$$

with

$$\begin{aligned}S_{k,c_k}^{\alpha}\left(Sn+s\right)&:=\sum_{j=1}^{Sn+s}\cos\left[j\omega_k\right]\alpha_k^{Sn+s-j}L^{Sn+s-j}\\ S_{k,c_k}^{\beta}\left(Sn+s\right)&:=\sum_{j=1}^{Sn+s}\sin\left[j\omega_k\right]\alpha_k^{Sn+s-j}L^{Sn+s-j}.\end{aligned} \tag{A.4}$$

In view of the foregoing, the identities given in Gregoir (1999, p. 463) can be extended to the terms in (2.3) as follows,

$$\frac{\Delta_0^{c_0}}{2}+\frac{\Delta_{S/2}^{c_{S/2}}}{2} = 1+\frac{1}{2}\left(\frac{c_{S/2}-c_0}{SN}\right)L=1+O\left(1/N\right) \tag{A.5}$$

$$\begin{aligned}\frac{\Delta_k^{c_k}+\left(1-2\cos\left[\omega_k\right]+L\right)\Delta_0^{c_0}}{2\kappa(\omega_k)} &= 1-\frac{c_0}{2\kappa(\omega_k)SN}L-\frac{2\cos\left[\omega_k\right]}{2\kappa(\omega_k)}\frac{\left(c_k-c_0\right)}{SN}L\\ &\quad+\frac{\left(2c_k-c_0\right)}{2\kappa(\omega_k)SN}L^2+\frac{c_k^2}{2\kappa(\omega_k)\left(SN\right)^2}L^2\\ &= 1-O\left(\frac{1}{N}\right)-O\left(\frac{1}{N}\right)+O\left(\frac{1}{N}\right)+O\left(\frac{1}{N^2}\right)\end{aligned} \tag{A.6}$$

$$\begin{aligned}\frac{\Delta_k^{c_k}+\left(1-2\cos\left[\omega_k\right]+L\right)\Delta_{S/2}^{c_{S/2}}}{2\kappa(\omega_k)} &= 1+\frac{c_{S/2}}{2\kappa(\omega_k)SN}L-\frac{2\cos\left[\omega_k\right]}{2\kappa(\omega_k)}\frac{\left(c_{S/2}-c_k\right)}{SN}L \\ &\quad+\frac{\left(2c_k-c_{S/2}\right)}{2\kappa(\omega_k)SN}L^2+\frac{c_k^2}{2\kappa(\omega_k)\left(SN\right)^2}L^2 \\ &= 1+O\left(\frac{1}{N}\right)+O\left(\frac{1}{N}\right)+O\left(\frac{1}{N}\right)+O\left(\frac{1}{N^2}\right) \quad \text{(A.7)}\end{aligned}$$

and

$$\begin{aligned}&\frac{2\cos\left[\omega_k\right]-L}{2\kappa(\omega_{kj})}\Delta_j^{c_j}+\frac{2\cos\left[\omega_j\right]-L}{2\kappa(\omega_{kj})}\Delta_k^{c_k} \\ &= 1-\frac{4\cos\left[\omega_k\right]\cos\left[\omega_j\right]}{2\kappa(\omega_{kj})}\frac{\left(c_j-c_k\right)}{SN}L+\frac{2\left[\cos\left[\omega_k\right]\frac{c_j}{SN}-\cos\left[\omega_j\right]\frac{c_k}{SN}\right]}{2\kappa(\omega_{kj})}L^2 \\ &\quad+\frac{4\left[\cos\left[\omega_k\right]\frac{c_j}{SN}-\cos\left[\omega_j\right]\frac{c_k}{SN}\right]}{2\kappa(\omega_{kj})}L^2-\frac{2}{2\kappa(\omega_{kj})}\frac{\left(c_j-c_k\right)}{SN}L^3 \\ &\quad+\frac{2\left[\cos\left[\omega_k\right]\left(\frac{c_j}{SN}\right)^2-\cos\left[\omega_j\right]\left(\frac{c_k}{SN}\right)^2\right]}{2\kappa(\omega_{kj})}L^2-\frac{1}{2\kappa(\omega_{kj})}\frac{\left(c_j^2-c_k^2\right)}{\left(SN\right)^2}L^3 \\ &= 1-O\left(\frac{1}{N}\right)+O\left(\frac{1}{N}\right)+O\left(\frac{1}{N}\right)-O\left(\frac{1}{N}\right)+O\left(\frac{1}{N^2}\right)-O\left(\frac{1}{N^2}\right) \quad \text{(A.8)}\end{aligned}$$

where $\kappa(\omega_k) := 1-\cos\left[\omega_k\right]$ and $\kappa(\omega_{kj}) := \cos\left[\omega_k\right]-\cos\left[\omega_j\right]$, $j,k = 1,...,S^*$.

Consequently, noting that $\Delta_k^{c_k} S_{k,c_k}\left(Sn+s\right)=1$ and using (A.5)-(A.8), it follows from (A.2) after some tedious algebra and using the standard trigonometric identities, $\sin\left[\left(\left(Sn+s\right)+1\right)\omega_k\right]$ $\equiv \cos\left[\omega_k\right]\sin\left[\left(Sn+s\right)\omega_k\right]+\sin\left[\omega_k\right]\cos\left[\left(Sn+s\right)\omega_k\right]$ and $\cos\left[\left(\left(Sn+s\right)+1\right)\omega_k\right] \equiv \cos\left[\omega_k\right]\cos\left[\left(Sn+s\right)\omega_k\right]$ $-\sin\left[\omega_k\right]\sin\left[\left(Sn+s\right)\omega_k\right]$, that x_{Sn+s} can be decomposed into the sum of frequency specific partial sums plus an asymptotically negligible term (see also Gregoir, 1999); that is,

$$\begin{aligned}x_{Sn+s} &= \frac{1}{S}S_{0,c_0}\left(Sn+s\right)u_{Sn+s}+\frac{1}{S}S_{S/2,c_{S/2}}\left(Sn+s\right)u_{Sn+s} \\ &\quad+\frac{2}{S}\sum_{k=1}^{S^*}\Big[\cos\left[\left(Sn+s\right)\omega_k\right]S_{k,c_k}^{\alpha}\left(Sn+s\right)u_{Sn+s} \\ &\qquad+\sin\left[\left(Sn+s\right)\omega_k\right]S_{k,c_k}^{\beta}\left(Sn+s\right)u_{Sn+s}\Big]+o_p\left(1\right). \quad \text{(A.9)}\end{aligned}$$

It will prove convenient, for the analysis that follows, to re-write (A.9) in the so-called vector-of-seasons representation; viz.,

$$\begin{aligned}X_n &= \frac{1}{S}C_0\sum_{i=1}^{n}\exp\left(\frac{c_0}{N}\right)^{n-i}U_i+\frac{1}{S}C_{S/2}\sum_{i=1}^{n}\exp\left(\frac{c_{S/2}}{N}\right)^{n-i}U_i \\ &\quad+\frac{2}{S}\sum_{k=1}^{S^*}C_k\sum_{i=1}^{n}\exp\left(\frac{c_k}{N}\right)^{n-i}U_i+o_p\left(1\right) \quad \text{(A.10)}\end{aligned}$$

where $X_n := [x_{Sn-(S-1)}, x_{Sn-(S-2)}, ..., x_{Sn}]'$, $n = 0, ..., N$, and $U_n := [u_{Sn-(S-1)}, u_{Sn-(S-2)}, ..., u_{Sn}]'$, $n = 1, ..., N$; $C_0 := \mathsf{Circ}[1,1,1,\ldots,1]$ and $C_{S/2} := \mathsf{Circ}[1,-1,1,\ldots,-1]$ are $S\times S$ circulant matri-

ces of rank 1, while for $\omega_i = 2\pi i/S$, $C_i := \mathsf{Circ}\left[\cos\left[0\right],\ \cos\left[\omega_i\right], \cos\left[2\omega_i\right], \ldots,\ \cos\left[(S-1)\,\omega_i\right]\right]$, $i = 1, \ldots, S^*$, are $S \times S$ circulant matrices of rank 2.[8]

Remark A.1: In order to relate (A.10) to (A.9) we have made use of the fact that the circulant matrices involved can be written as $C_0 = \mathbf{v}_0\mathbf{v}_0{}'$, where $\mathbf{v}_0{}' := [1, 1, 1, ..., 1]$, $C_{S/2} = \mathbf{v}_{S/2}\mathbf{v}_{S/2}{}'$, where $\mathbf{v}_{S/2}{}' := [-1, 1, -1, ..., 1]$, and $C_j = \mathbf{v}_j\mathbf{v}_j'$ and finally the matrix $\overline{C}_j := \mathsf{Circ}\left[\sin\left[0\right],\right.$ $\left.\sin\left[(S-1)\,\omega_j\right],\ \sin\left[(S-2)\,\omega_j\right],\ \ldots,\ \sin\left[\omega_j\right]\right]$, with $\overline{C}_j = \mathbf{v}_j\mathbf{v}_j^{*\prime}$, which will be used later in lemma A.1 where

$$\mathbf{v}_j' := \begin{bmatrix} \cos\left[\omega_j\,(1-S)\right] & \cos\left[\omega_j\,(2-S)\right] & \cdots & \cos\left[0\right] \\ \sin\left[\omega_j\,(1-S)\right] & \sin\left[\omega_j\,(2-S)\right] & \cdots & \sin\left[0\right] \end{bmatrix} =: \begin{bmatrix} \mathbf{h}_j' \\ \mathbf{h}_j^{*\prime} \end{bmatrix} \tag{A.11}$$

and

$$\mathbf{v}_j^{*\prime} := \begin{bmatrix} -\sin\left[\omega_j\,(1-S)\right] & -\sin\left[\omega_j\,(2-S)\right] & \cdots & -\sin\left[0\right] \\ \cos\left[\omega_j\,(1-S)\right] & \cos\left[\omega_j\,(2-S)\right] & \cdots & \cos\left[0\right] \end{bmatrix} =: \begin{bmatrix} -\mathbf{h}_j^{*\prime} \\ \mathbf{h}_j' \end{bmatrix}, \tag{A.12}$$

$j = 1, \ldots, S^*$.

We also note that,

$$\begin{aligned} \begin{bmatrix} \sum_{j=1}^n \exp\left(\frac{c_k}{SN}\right)^{S(n-j)} u_{Sj-(S-1)} \\ \sum_{j=1}^n \exp\left(\frac{c_k}{SN}\right)^{S(n-j)} u_{Sj-(S-2)} \\ \vdots \\ \sum_{j=1}^n \exp\left(\frac{c_k}{SN}\right)^{S(n-j)} u_{Sj} \end{bmatrix} &= \begin{bmatrix} \sum_{j=1}^n \exp\left(\frac{c_k}{N}\right)^{(n-j)} u_{Sj-(S-1)} \\ \sum_{j=1}^n \exp\left(\frac{c_k}{N}\right)^{(n-j)} u_{Sj-(S-2)} \\ \vdots \\ \sum_{j=1}^n \exp\left(\frac{c_k}{N}\right)^{(n-j)} u_{Sj} \end{bmatrix} \\ &= \sum_{j=1}^{n} \exp\left(\frac{c_k}{N}\right)^{n-j} U_j. \end{aligned} \tag{A.13}$$

Remark A.2: As shown in Burridge and Taylor (2001), the error process, U_n, defined in (A.10) satisfies the vector $MA(\infty)$ representation

$$U_n = \sum_{j=0}^{\infty} \mathbf{\Psi}_j E_{n-j} \tag{A.14}$$

where $E_n := [\varepsilon_{Sn-(S-1)}, \varepsilon_{Sn-(S-2)}, ..., \varepsilon_{Sn}]'$ is a vector of IID errors, and the $S \times S$ matrices $\mathbf{\Psi}_0$, $\mathbf{\Psi}_j$, $j = 1, 2, \ldots$, are,

$$\mathbf{\Psi}_0 := \begin{bmatrix} 1 & 0 & 0 & 0 & \cdots & 0 \\ \psi_1 & 1 & 0 & 0 & \cdots & 0 \\ \psi_2 & \psi_1 & 1 & 0 & \cdots & 0 \\ \psi_3 & \psi_2 & \psi_1 & 1 & \cdots & 0 \\ \vdots & \vdots & \vdots & \vdots & \ddots & \vdots \\ \psi_{S-1} & \psi_{S-2} & \psi_{S-3} & \psi_{S-4} & \cdots & 1 \end{bmatrix}$$

[8] For further details on these circulant matrices see, for example, Osborn and Rodrigues (2002) and Smith *et al.* (2009).

and

$$\mathbf{\Psi}_j := \begin{bmatrix} \psi_{jS} & \psi_{jS-1} & \psi_{jS-2} & \psi_{jS-3} & \cdots & \psi_{jS-(S-1)} \\ \psi_{jS+1} & \psi_{jS} & \psi_{jS-1} & \psi_{jS-2} & \cdots & \psi_{jS-(S-2)} \\ \psi_{jS+2} & \psi_{jS+1} & \psi_{jS} & \psi_{jS-1} & \cdots & \psi_{jS-(S-3)} \\ \psi_{jS+3} & \psi_{jS+2} & \psi_{jS+1} & \psi_{jS} & \cdots & \psi_{jS-(S-4)} \\ \vdots & \vdots & \vdots & \vdots & \ddots & \vdots \\ \psi_{jS+S-1} & \psi_{jS+S-2} & \psi_{jS+S-3} & \psi_{jS+S-4} & \cdots & \psi_{jS} \end{bmatrix},$$

respectively. □

The following Lemma provides a multivariate invariance principle for Y_n^{ξ}, where $Y_n^{\xi} := [y^{\xi}_{Sn-(S-1)}, y^{\xi}_{Sn-(S-2)}, ..., y^{\xi}_{Sn}]'$, with $y^{\xi}_{Sn+s} = x_{Sn+s} - \hat{\gamma}' z_{Sn+s,\xi}$ and where it is recalled that the parameter $\xi \in \{1,2,3\}$ denotes the deterministic Case of interest.

Lemma A.1. *Let the conditions of Theorem 3.1 hold. Then,*

$$N^{-1/2} Y^{\xi}_{\lfloor rN \rfloor} \Rightarrow \frac{\sigma}{S} \left[\psi(1) C_0 \mathbf{J}^{\xi}_{c_0}(r) + \psi(-1) C_{S/2} \mathbf{J}^{\xi}_{c_{S/2}}(r) + 2 \sum_{i=1}^{S^*} \left(b_i C_i \mathbf{J}^{\xi}_{c_i}(r) + a_i \overline{C}_i \mathbf{J}^{\xi}_{c_i}(r) \right) \right], \; r \in [0,1] \tag{A.15}$$

where $\mathbf{J}^{\xi}_{c_k}(r) := [J^{\xi}_{c_k,1-S}(r), J^{\xi}_{c_k,2-S}(r), ..., J^{\xi}_{c_k,0}(r)]'$ *is an* $S \times 1$ *vector OU process such that* $d\mathbf{J}^{\xi}_{c_k}(r) = c\mathbf{J}^{\xi}_{c_k}(r)\,dr + d\mathbf{W}^{\xi}(r)$ *and* $\mathbf{W}^{\xi}(r)$ *is an* $S \times 1$ *vector Brownian motion process;* $a_i := \mathcal{I}m(\psi[\exp(\mathrm{i}\omega_i)])$ *and* $b_i := \mathcal{R}e(\psi[\exp(\mathrm{i}\omega_i)])$, $i = 1, ..., S^*$, *with* $\mathcal{R}e(\cdot)$ *and* $\mathcal{I}m(\cdot)$ *denoting the real and imaginary parts of their arguments, respectively; and* C_0, $C_{S/2}$, C_i *and* $\overline{C}_i$, $i = 1, \ldots, S^*$, *are* $S \times S$ *circulant matrices as defined in Remark A.1. Finally, with OLS de-trending:*

$$\begin{aligned} J^1_{c_k,s}(r) &:= J_{c_k,s}(r) - \int_0^1 J_{c_k,s}(r)\,dr \\ J^2_{c_k,s}(r) &:= J^1_{c_k,s}(r) - 12\left(r - \frac{1}{2}\right) \int_0^1 \left(r - \frac{1}{2}\right) \left[\frac{1}{S} \sum_{s=1-S}^{0} J^1_{c_k,s}(r) \right] dr \\ J^3_{c_k,s}(r) &:= J^1_{c_k,s}(r) - 12\left(r - \frac{1}{2}\right) \int_0^1 \left(r - \frac{1}{2}\right) J^1_{c_k,s}(r)\,dr \end{aligned}$$

and with local GLS de-trending:

$$\begin{aligned} J^1_{c_k,s}(r) &:= J_{c_k,s}(r) \\ J^2_{c_k,s}(r) &:= J_{c_k,s}(r) - r \left[\frac{1}{S} \sum_{s=1-S}^{0} \left(\lambda J_{c_k,s}(1) + 3(1-\lambda) \int_0^1 h J_{c_k,s}(h)\,dh \right) \right] \\ J^3_{c_k,s}(r) &:= J_{c_k,s}(r) - r \left[\lambda J_{c_k,s}(1) + 3(1-\lambda) \int_0^1 h J_{c_k,s}(h)\,dh \right] \end{aligned}$$

with $\lambda := (1 - \overline{c}) / \left(1 + \overline{c} + \overline{c}^2/3\right)$, *in all cases for the indices* $s = 1-S, ..., 0$ *and* $k = 0, ..., \lfloor S/2 \rfloor$.

Proof of Lemma A.1: Following along the same lines as for the proof of Lemma 1 in del Barrio Castro, Osborn and Taylor (2012) and Phillips (1988) it follows that,

$$\begin{aligned}\frac{1}{\sqrt{N}}\sum_{i=1}^{n}\exp\left(\frac{c_k}{N}\right)^{n-i}E_i &\Rightarrow \mathbf{J}_{c_k}(r); \qquad (A.16)\\ \frac{1}{\sqrt{N}}\sum_{i=1}^{n}\exp\left(\frac{c_k}{N}\right)^{n-i}U_i &= \mathbf{\Psi}(1)\frac{1}{\sqrt{N}}\sum_{i=1}^{n}\exp\left(\frac{c_k}{N}\right)^{n-i}E_i+o_p(1)\Rightarrow\mathbf{\Psi}(1)\mathbf{J}_{c_k}(r)\end{aligned}$$

where E_i and U_i are as defined in Remark A.2, $\mathbf{dJ}_{c_k}(r)=c_k\mathbf{J}_{c_k}(r)\,\mathbf{dr}+\mathbf{dW}(r)$, $\mathbf{W}(r)$ is an $S\times 1$ vector standard Brownian motion and $\mathbf{J}_{c_k}(r)$ is an $S\times 1$ vector standard OU process. Next observe from (A.10) and (A.14), that

$$\begin{aligned}N^{-1/2}X_n &= \frac{1}{S}C_0N^{-1/2}\sum_{i=1}^{n}\exp\left(\frac{c_0}{N}\right)^{n-i}U_i+\frac{1}{S}C_{S/2}N^{-1/2}\sum_{i=1}^{n}\exp\left(\frac{c_{S/2}}{N}\right)^{n-i}U_i\\ &\quad+\frac{2}{S}\sum_{k=1}^{S^*}C_kN^{-1/2}\sum_{i=1}^{n}\exp\left(\frac{c_k}{N}\right)^{n-i}U_i+o_p(1)\\ &= \frac{1}{S}C_0\mathbf{\Psi}(1)N^{-1/2}\sum_{i=1}^{n}\exp\left(\frac{c_0}{N}\right)^{n-i}E_i+\frac{1}{S}C_{S/2}\mathbf{\Psi}(1)N^{-1/2}\sum_{i=1}^{n}\exp\left(\frac{c_{S/2}}{N}\right)^{n-i}E_i\\ &\quad+\frac{2}{S}\sum_{k=1}^{S^*}C_k\mathbf{\Psi}(1)N^{-1/2}\sum_{i=1}^{n}\exp\left(\frac{c_k}{N}\right)^{n-i}E_i+o_p(1)\end{aligned}$$

where this approximation follows using similar arguments to those used in Boswijk and Franses (1996, p.238). Using (A.16) and the continuous mapping theorem [CMT] the result in (A.15) follows immediately. Noting that $\mathbf{\Psi}(1)$ is also a circulant matrix, then by the properties of products of circulant matrices it can be shown that $C_0\mathbf{\Psi}(1)=\psi(1)C_0$, $C_{S/2}\mathbf{\Psi}(1)=\psi(-1)C_{S/2}$, $C_j\mathbf{\Psi}(1)=b_jC_j+a_j\overline{C}_j$ and $\overline{C}_j\mathbf{\Psi}(1)=-a_jC_j+b_j\overline{C}_j$ for $j=1,\dots S^*$; see, *inter alia*, Davis (1979, Theorem 3.2.4), Gray (2006, Theorem 3.1) and Smith *et al.* (2009) for further details. The stated result then follows immediately. ■

In order to obtain results for the asymptotic distributions of the different test statistics discussed in this paper, the limiting results collected in the following Lemma will also prove useful.

Lemma A.2. *Let the conditions of Lemma A.1 hold. It then follows for* $Y_{j,n}^{\xi}:=[y_{j,Sn-(S-1)}^{\xi},\ y_{j,Sn-(S-2)}^{\xi},\dots,y_{j,Sn}^{\xi}]'$, $j=0,...,\lfloor S/2\rfloor$, *and* $Y_{i,n}^{*\xi}:=[y_{i,Sn-(S-1)}^{*\xi},y_{i,Sn-(S-2)}^{*\xi},\dots,y_{i,Sn}^{*\xi}]'$, $i=1,\dots,S^*$, *as* $T\to\infty$, *that*

$$\begin{aligned}N^{-1/2}Y_{0,\lfloor rN\rfloor}^{\xi} &\Rightarrow \sigma\,\psi(1)\,C_0\mathbf{J}_{c_0}^{\xi}(r) \qquad (A.17)\\ N^{-1/2}Y_{S/2,\lfloor rN\rfloor}^{\xi} &\Rightarrow \sigma\,\psi(-1)\,C_{S/2}\mathbf{J}_{c_{S/2}}^{\xi}(r) \qquad (A.18)\\ N^{-1/2}Y_{i,\lfloor rN\rfloor}^{\xi} &\Rightarrow \sigma\left(b_iC_i+a_i\overline{C}_i\right)\mathbf{J}_{c_i}^{\xi}(r),\ \ i=1,...,S^* \qquad (A.19)\\ N^{-1/2}Y_{i,\lfloor rN\rfloor}^{*\xi} &\Rightarrow \sigma\left(b_i\overline{C}_i-a_iC_i\right)\mathbf{J}_{c_i}^{\xi}(r),\ i=1,...,S^* \qquad (A.20)\end{aligned}$$

where the vector OU process, $\mathbf{J}_{c_i}^{\xi}(r)$, $i=0,\dots,\lfloor S/2\rfloor$, *the constants* a_i *and* b_i, $i=1,...,S^*$, *and the circulant matrices,* C_i, $i=0,...,\lfloor S/2\rfloor$, *and* $\overline{C}_j$, $j=1,\dots,S^*$ *are as defined in Lemma A.1.*

Proof of Lemma A.2: Noting that $Y_{j,n}^{\xi} = C_j Y_n^{\xi}$, $j = 0, ..., \lfloor S/2 \rfloor$, and that $Y_{i,n}^{*\xi} = \overline{C}_i Y_n^{\xi}$, $i = 1, \ldots, S^*$, the stated results follow immediately from Lemma A.1 using the following identities: $C_0 C_0 \equiv S C_0$, $C_{S/2} C_{S/2} \equiv S C_{S/2}$, $C_j C_j \equiv \frac{S}{2} C_j$, $C_j \overline{C}_j \equiv \frac{S}{2} \overline{C}_j$ and $\overline{C}_j \overline{C}_j \equiv -\frac{S}{2} C_j$, $j = 1, ..., S^*$, recalling that the matrix products between C_0, $C_{S/2}$, C_j and $\overline{C}_j$, $j = 1, \ldots, S^*$ are all zero matrices, and that multiplication between circulant matrices is commutative.

Then, using Remark A.1 and (A.17) to (A.20), for the zero and Nyquist frequencies, applications of the multivariate FCLT and CMT establish that:

$$\begin{aligned} N^{-1/2} y_{0,S\lfloor rN \rfloor + s}^{\xi} &\Rightarrow \sigma \sqrt{S} \psi(1) \mathbf{v}_1' \frac{1}{\sqrt{S}} \mathbf{J}_{c_0}^{\xi}(r) =: \sigma \sqrt{S} \psi(1) \mathbf{v}_1' \mathbf{J}_{c_0}^{\xi *}(r) \\ &= \sigma \sqrt{S} \psi(1) J_{0,c_0}^{\zeta}(r) \end{aligned} \tag{A.21}$$

$$\begin{aligned} N^{-1/2} y_{S/2,S\lfloor rN \rfloor + s}^{\xi} &\Rightarrow \sigma \sqrt{S} \psi(-1)(-1)^s \mathbf{v}_{S/2}' \frac{1}{\sqrt{S}} \mathbf{J}_{c_{S/2}}^{\xi}(r) =: \sigma \sqrt{S} \psi(-1)(-1)^s \mathbf{v}_{S/2}' \mathbf{J}_{c_{S/2}}^{\xi *}(r) \\ &= \sigma \sqrt{S} \psi(-1)(-1)^s J_{S/2,c_{S/2}}^{\zeta}(r) \end{aligned} \tag{A.22}$$

where $\mathbf{v}_1'$ and $\mathbf{v}_{S/2}'$ are defined in Remark A.1. In the case of the harmonic frequencies it follows that,

$$\begin{aligned} N^{-1/2} y_{i,S\lfloor rN \rfloor + s}^{\xi} &\Rightarrow \sigma \sqrt{S/2} b_i \left[\cos[\omega_i(s)] \mathbf{h}_i' \frac{1}{\sqrt{S/2}} \mathbf{J}_{c_i}^{\xi}(r) + \sin[\omega_i(s)] \mathbf{h}_i^{*\prime} \frac{1}{\sqrt{S/2}} \mathbf{J}_{c_i}^{\xi}(r) \right] \\ &\quad + \sigma \sqrt{S/2} a_i \left[\sin[\omega_i(s)] \mathbf{h}_i' \frac{1}{\sqrt{S/2}} \mathbf{J}_{c_i}^{\xi}(r) - \cos[\omega_i(s)] \mathbf{h}_i^{*\prime} \frac{1}{\sqrt{S/2}} \mathbf{J}_{c_i}^{\xi}(r) \right] \\ &=: \sigma \sqrt{S/2} b_i \left[\cos[\omega_i(s)] \mathbf{h}_i' \mathbf{J}_{c_i}^{\xi\dagger}(r) + \sin(\omega_i[s]) \mathbf{h}_i^{*\prime} \mathbf{J}_{c_i}^{\xi\dagger}(r) \right] \\ &\quad + \sigma \sqrt{S/2} a_i \left[\sin[\omega_i(s)] \mathbf{h}_i' \mathbf{J}_{c_i}^{\xi\dagger}(r) - \cos[\omega_i(s)] \mathbf{h}_i^{*\prime} \mathbf{J}_{c_i}^{\xi\dagger}(r) \right] \\ &= \sigma \sqrt{S/2} b_i \left[\cos[\omega_i(s)] J_{i,c_i}^{\zeta}(r) + \sin[\omega_i(s)] J_{i,c_i}^{\zeta *}(r) \right] \\ &\quad + \sigma \sqrt{S/2} a_i \left[\sin[\omega_i(s)] J_{i,c_i}^{\zeta}(r) - \cos[\omega_i(s)] J_{i,c_i}^{\zeta *}(r) \right] \end{aligned} \tag{A.23}$$

and

$$\begin{aligned} N^{-1/2} y_{i,S\lfloor rN \rfloor + s}^{*\xi} &\Rightarrow \sigma \sqrt{S/2} b_i \left[\sin[\omega_i(s)] \mathbf{h}_i' \frac{1}{\sqrt{S/2}} \mathbf{J}_{c_i}^{\xi}(r) - \cos[\omega_i(s)] \mathbf{h}_i^{*\prime} \frac{1}{\sqrt{S/2}} \mathbf{J}_{c_i}^{\xi}(r) \right] \\ &\quad - \sigma \sqrt{S/2} a_i \left[\cos[\omega_i(s)] \mathbf{h}_i' \frac{1}{\sqrt{S/2}} \mathbf{J}_{c_i}^{\xi}(r) + \sin[\omega_i(s)] \mathbf{h}_i^{*\prime} \frac{1}{\sqrt{S/2}} \mathbf{J}_{c_i}^{\xi}(r) \right] \\ &=: \sigma \sqrt{S/2} b_i \left[\sin[\omega_i(s)] \mathbf{h}_i' \mathbf{J}_{c_i}^{\xi\dagger}(r) - \cos[\omega_i(s)] \mathbf{h}_i^{*\prime} \mathbf{J}_{c_i}^{\xi\dagger}(r) \right] \\ &\quad - \sigma \sqrt{S/2} a_i \left[\cos[\omega_i(s)] \mathbf{h}_i' \mathbf{J}_{c_i}^{\xi\dagger}(r) + \sin[\omega_i(s)] \mathbf{h}_i^{*\prime} \mathbf{J}_{c_i}^{\xi\dagger}(r) \right] \\ &= \sigma \sqrt{S/2} b_i \left[\sin[\omega_i(s)] J_{i,c_i}^{\zeta}(r) - \cos[\omega_i(s)] J_{i,c_i}^{\zeta *}(r) \right] \\ &\quad - \sigma \sqrt{S/2} a_i \left[\cos[\omega_i(s)] J_{i,c_i}^{\zeta}(r) + \sin[\omega_i(s)] J_{i,c_i}^{\zeta *}(r) \right] \end{aligned} \tag{A.24}$$

for $i = 1, ..., S^*$ and where $\mathbf{h}_i'$ and $\mathbf{h}_i^{*\prime}$ are the first and second rows of $\mathbf{v}_i'$, respectively, defined in Remark A.1. ■

Remark A.3: It can be seen from the results in Lemma A.2 that the right members of (A.17)-(A.20) are formed from (orthogonal) linear combinations of S independent de-meaned or de-trended OU processes which comprise $\mathbf{J}_{c_k}^{\xi}(r)$. Recalling that C_0 and $C_{S/2}$ both have rank one, and that C_j and $\overline{C}_j$ for $j = 1, \ldots, S^*$, are all of rank two, it can be seen that each element of $C_i\mathbf{J}_{c_i}^{\xi}(r)$, $i = 0, S/2$, and of $C_j\mathbf{J}_{c_j}^{\xi}(r)$, $\overline{C}_j\mathbf{J}_{c_j}^{\xi}(r)$, $j = 1, \ldots, S^*$, is, after re-scaling, a function of a scalar standard OU process and of two standard OU processes, respectively, as indicated in (A.21)-(A.24).

Remark A.4: Note that the deterministic kernels considered for the de-meaning and de-trending of the variables, have different impacts on the frequency specific OU processes. These set of processes at each frequency for each case are summarised for convenience as follows,

$$\begin{aligned}
&\textit{Case 1 } (\xi = 1) \quad : \quad J_{0,c_0}^{1}(r),\, J_{S/2,c_{S/2}}^{1}(r),\, J_{i,c_i}^{1}(r),\, J_{i,c_i}^{1*}(r),\, i = 1, ..., S^* \\
&\textit{Case 2 } (\xi = 2) \quad : \quad J_{0,c_0}^{2}(r),\, J_{S/2,c_{S/2}}^{1}(r),\, J_{i,c_i}^{1}(r),\, J_{i,c_i}^{1*}(r),\, i = 1, ..., S^* \\
&\textit{Case 3 } (\xi = 3) \quad : \quad J_{0,c_0}^{2}(r),\, J_{S/2,c_{S/2}}^{2}(r),\, J_{i,c_i}^{2}(r),\, J_{i,c_i}^{2*}(r),\, i = 1, ..., S^*
\end{aligned}$$

where $J_{k,c_k}^{\zeta}(r)$, $k = 0, ..., \lfloor S/2 \rfloor$, and where it is to be recalled that $\zeta = 1$ and $\zeta = 2$ correspond to de-meaned and de-trended OU processes, respectively. These are defined in (A.21)-(A.24) as: $J_{0,c_0}^{\zeta}(r) := \mathbf{v}_1'\mathbf{J}_{c_0}^{\xi*}(r)$, $J_{S/2,c_{S/2}}^{\zeta}(r) := \mathbf{v}_{S/2}'\mathbf{J}_{c_{S/2}}^{\xi*}(r)$, $J_{k,c_k}^{\zeta}(r) := \mathbf{h}_k'\mathbf{J}_{c_k}^{\xi\dagger}(r)$ and $J_{k,c_k}^{\zeta *}(r) := \mathbf{h}_k^{*\prime}\mathbf{J}_{c_k}^{\xi\dagger}(r)$ for $k = 1, \ldots, S^*$.

B Proof of Main Results

B.1 Proof of Theorems 3.1 and 4.1

First re-write (3.1) in vector form, *viz*, $\mathbf{y} = \mathbf{Y}\beta_0 + \mathbf{u}$, where $\mathbf{y}$ is a $T \times 1$ vector with generic element $\Delta_S y_{Sn+s}^{\xi}$; $\mathbf{Y} := [\mathbf{y}_0|\mathbf{y}_1|\mathbf{y}_1^*|\mathbf{y}_2|\mathbf{y}_2^*| \ \ldots |\mathbf{y}_{S^*}|\mathbf{y}_{S^*}^*|\mathbf{y}_{S/2}]$ is a $T \times S$ matrix where $\mathbf{y}_i$, $i = 0, ...,$ $\lfloor S/2 \rfloor$ are $T \times 1$ vectors with generic elements $y_{i,Sn+s-1}^{\xi}$, and $\mathbf{y}_i^*$, $i = 1, ..., S^*$ are $T \times 1$ vectors with generic elements $y_{i,Sn+s-1}^{*\xi}$, respectively, and $\beta_0 := [\pi_0, \pi_1\pi_1^*, \pi_2, \pi_2^*, \ \ldots, \pi_{S^*}, \pi_{S^*}^*, \pi_{S/2,}]'$. The OLS estimator from (3.1), may then be defined via,

$$T\hat{\beta}_0 := \left[T^{-2}\mathbf{Y}'\mathbf{Y}\right]^{-1}\left[T^{-1}\mathbf{Y}'\mathbf{y}\right]. \tag{B.1}$$

Because $T^{-2}\mathbf{Y}'\mathbf{Y}$ weakly converges to an $S \times S$ diagonal matrix, this as a consequence of the asymptotic orthogonality of the HEGY auxiliary variables discussed previously, we may therefore separately derive the large sample behavior of the OLS estimators of π_j, $j = 0, ..., \lfloor S/2 \rfloor$, and π_i^*, $i = 1, ..., S^*$. To that end, the so-called *normalised bias* statistics then satisfy the following,

$$T\widehat{\pi}_j = \frac{T^{-1}\mathbf{y}_j'\mathbf{y}}{T^{-2}\mathbf{y}_j'\mathbf{y}_j} + o_p(1) = \frac{T^{-1}\sum_{n=1}^{N}\sum_{s=1-S}^{0} y_{j,Sn+s-1}^{\xi}\Delta_S y_{Sn+s}^{\xi}}{T^{-2}\sum_{n=1}^{N}\sum_{s=1-S}^{0}\left(y_{j,Sn+s-1}^{\xi}\right)^2} + o_p(1), \quad j = 0, ..., \lfloor S/2 \rfloor \tag{B.2}$$

and

$$T\widehat{\pi}_i^* = \frac{T^{-1}\mathbf{y}_i^{*\prime}\mathbf{y}}{T^{-2}\mathbf{y}_i^{*\prime}\mathbf{y}_i^*}+o_p\left(1\right) = \frac{T^{-1}\sum_{n=1}^{N}\sum_{s=1-S}^{0} y_{i,Sn+s-1}^{*\xi}\Delta_S y_{Sn+s}^{\xi}}{T^{-2}\sum_{n=1}^{N}\sum_{s=1-S}^{0}\left(y_{i,Sn+s-1}^{*\xi}\right)^2}+o_p\left(1\right), \quad i=1,...,S^*. \quad \text{(B.3)}$$

Consider first the denominators of (B.2) and (B.3). Using the results that C_0 and $C_{S/2}$ are symmetric and orthogonal both to each other and to C_i and $\overline{C}_i$, and the fact that $C_jC_jC_j \equiv S^2C_j$ for $j=0,S/2$, then appealing to the multivariate invariance principle in (A.15) and using an application of the CMT we have that

$$\begin{aligned} T^{-2}\sum_{n=1}^{N}\sum_{s=1-S}^{0}\left(y_{j,Sn+s-1}^{\xi}\right)^2 &= T^{-2}\sum_{n=1}^{N} S\left(Y_{n-1}^{\xi\prime}C_jY_{n-1}^{\xi}\right)+o_p\left(1\right) \\ &\Rightarrow \frac{\sigma_\varepsilon^2}{S^2}\frac{\psi\left(\cos[\omega_j]\right)^2}{S}\int_0^1 \mathbf{J}_{c_j}^{\xi}\left(r\right)'C_j'C_jC_j\mathbf{J}_{c_j}^{\xi}\left(r\right)dr \\ &= \sigma_\varepsilon^2\psi\left(\cos[\omega_j]\right)^2\int_0^1 \mathbf{J}_{c_j}^{\xi*}\left(r\right)'C_j\mathbf{J}_{c_j}^{\xi*}\left(r\right)dr, j=0,S/2, \quad \text{(B.4)} \end{aligned}$$

where $\omega_0=0$, $\omega_{S/2}=\pi$ and $\mathbf{J}_{c_j}^{\xi*}\left(r\right) := \frac{1}{\sqrt{S}}\mathbf{J}_{c_j}^{\xi}\left(r\right)$ for $j=0,S/2$. Next we use the result that C_i, $i=1,...,S^*$, is symmetric and that $\overline{C}_i' = -\overline{C}_i$, and note also that C_i and $\overline{C}_i$ are orthogonal to C_0 and $C_{S/2}$ and that $C_iC_iC_i \equiv \left(\frac{S}{2}\right)^2 C_i$, $C_iC_i\overline{C}_i \equiv \left(\frac{S}{2}\right)^2\overline{C}_i$, $\overline{C}_i'C_iC_i \equiv -\left(\frac{S}{2}\right)^2\overline{C}_i$ and $\overline{C}_i'C_i\overline{C}_i \equiv \left(\frac{S}{2}\right)^2 C_i$. Using these facts we have that,

$$T^{-2}\sum_{n=1}^{N}\sum_{s=1-S}^{0}\left(y_{i,Sn+s-1}^{\xi}\right)^2 = T^{-2}\sum_{n=1}^{N}\left(\frac{S}{2}\right)\left(Y_{n-1}^{\xi\prime}C_i\,Y_{n-1}^{\xi}\right)+o_p\left(1\right)$$

$$T^{-2}\sum_{n=1}^{N}\sum_{s=1-S}^{0}\left(y_{i,Sn+s-1}^{*\xi}\right)^2 = T^{-2}\sum_{n=1}^{N}\left(\frac{S}{2}\right)\left(Y_{n-1}^{\xi\prime}C_i\,Y_{n-1}^{\xi}\right)+o_p\left(1\right)$$

$$\begin{aligned} T^{-2}\sum_{n=1}^{N}\left(\frac{S}{2}\right)\left(Y_{n-1}^{\xi\prime}C_i\,Y_{n-1}^{\xi}\right) \Rightarrow \quad & \frac{\sigma_\varepsilon^2}{S^2}\left(\frac{S}{2}\right)b_i^2\left(\frac{2}{S}\right)^2\int_0^1 \mathbf{J}_{c_i}^{\xi}\left(r\right)'C_iC_iC_i\mathbf{J}_{c_i}^{\xi}\left(r\right)dr + \\ & \frac{\sigma_\varepsilon^2}{S^2}\left(\frac{S}{2}\right)b_ia_i\left(\frac{2}{S}\right)^2\int_0^1 \mathbf{J}_{c_i}^{\xi}\left(r\right)'C_iC_i\overline{C}_i\mathbf{J}_{c_i}^{\xi}\left(r\right)dr + \\ & \frac{\sigma_\varepsilon^2}{S^2}\left(\frac{S}{2}\right)b_ia_i\left(\frac{2}{S}\right)^2\int_0^1 \mathbf{J}_{c_i}^{\xi}\left(r\right)'\overline{C}_i'C_iC_i\mathbf{J}_{c_i}^{\xi}\left(r\right)dr + \\ & \frac{\sigma_\varepsilon^2}{S^2}\left(\frac{S}{2}\right)a_i^2\left(\frac{2}{S}\right)^2\int_0^1 \mathbf{J}_{c_i}^{\xi}\left(r\right)'\overline{C}_i'C_i\overline{C}_i\mathbf{J}_{c_i}^{\xi}\left(r\right)dr \quad \text{(B.5)} \\ = \quad & \frac{\sigma_\varepsilon^2\left(a_i^2+b_i^2\right)}{4}\int_0^1 \mathbf{J}_{c_i}^{\xi\dagger}\left(r\right)'C_i\mathbf{J}_{c_i}^{\xi\dagger}\left(r\right)dr, \quad i=1,\ldots,S^* \end{aligned}$$

where $\mathbf{J}_{c_i}^{\xi\dagger}\left(r\right) := \frac{1}{\sqrt{S/2}}\mathbf{J}_{c_i}^{\xi}\left(r\right)$.

Consider next the numerators of (B.2) and (B.3). For (B.2) we observe that,

$$T^{-1}\sum_{n=1}^{N}\sum_{s=1-S}^{0} y_{j,Sn+s-1}^{\xi}\Delta_S y_{Sn+s}^{\xi} = T^{-1}\sum_{n=1}^{N} Y_{n-1}^{\xi\prime}C_j\Delta_S Y_n^{\xi} + \mathbf{A}_j + o_p\left(1\right), \quad j=0,S/2 \quad \text{(B.6)}$$

where $\mathbf{A}_j := S^{-1}\sum_{i=1}^{S-1}(S-i)\cos[i\omega_j]\,N^{-1}\sum_{n=1}^{N}\left(u^{\xi}_{S-i,n}u^{\xi}_{Sn}\right)$ so that $\mathbf{A}_j \to \Psi_j := S^{-1}\sum_{i=1}^{S-1}(S-i)\cos[i\omega_j]\,\gamma_i$ for $\omega_j = \frac{2\pi j}{S}$, $j = 0, S/2$. And $\Delta_S Y^{\xi}_n := [\Delta_S y^{\xi}_{Sn-(S-1)}, \Delta_S\, y^{\xi}_{Sn-(S-2)}, ..., \Delta_S\, y^{\xi}_{Sn}]'$.

Similarly, for the numerator of (B.3) it follows that for $j = 1, \ldots, S^*$,

$$T^{-1}\sum_{n=1}^{N}\sum_{s=1-S}^{0} y^{\xi}_{j,Sn+s-1}\Delta_S y^{\xi}_{Sn+s} = T^{-1}\sum_{n=1}^{N} Y^{\xi\prime}_{n-1}C_j\Delta_S Y^{\xi}_n + \mathbf{A}_j + o_p(1) \tag{B.7}$$

$$T^{-1}\sum_{n=1}^{N}\sum_{s=1-S}^{0} y^{*\xi}_{j,Sn+s-1}\Delta_S y^{\xi}_{Sn+s} = T^{-1}\sum_{n=1}^{N} Y^{\xi\prime}_{n-1}\overline{C}_j\Delta_S Y^{\xi}_n + \overline{\mathbf{A}}_j + o_p(1) \tag{B.8}$$

where $\mathbf{A}_j := S^{-1}\sum_{i=1}^{S-1}(S-i)\cos[i\omega_j]\,N^{-1}\sum_{n=1}^{N}\left(u^{\xi}_{S-i,n}u^{\xi}_{Sn}\right)$ and $\overline{\mathbf{A}}_j := -S^{-1}\sum_{i=1}^{S-1}(S-i)\sin[i\omega_j]$ $N^{-1}\sum_{n=1}^{N}\left(u^{\xi}_{S-i,n}u^{\xi}_{Sn}\right)$. Note that $\mathbf{A}_j \to \Psi^1_j := S^{-1}\sum_{i=1}^{S-1}(S-i)\cos[i\omega_j]\,\gamma_i$ and $\overline{\mathbf{A}}_j \to \Psi^2_j := -S^{-1}\sum_{i=1}^{S-1}(S-i)\sin[i\omega_j]\,\gamma_i$ for $\omega_j = \frac{2\pi j}{S}$, $\quad j = 1, \ldots, S^*$.

Again using (A.15), applications of the CMT, the identities $C_kC_kC_k \equiv S^2C_k$ for $k = 0, S/2$, and $C'_jC_jC_j \equiv \left(\frac{S}{2}\right)^2 C_j$, $C'_jC_j\overline{C}_j \equiv \left(\frac{S}{2}\right)^2 \overline{C}_j$,$\overline{C}'_j\ C_jC_j \equiv -\left(\frac{S}{2}\right)^2 \overline{C}_j$, $\overline{C}'_j\ C_j\overline{C}_j \equiv \left(\frac{S}{2}\right)^2 C_j$, $C'_j\overline{C}_jC_j \equiv \left(\frac{S}{2}\right)^2 \overline{C}_j$, $C'_j\overline{C}_j\overline{C}_j \equiv -\left(\frac{S}{2}\right)^2 C_j$, $\overline{C}'_jC_jC_j \equiv \left(\frac{S}{2}\right)^2 C_j$ and $\overline{C}'_j\overline{C}_j\overline{C}_j \equiv \left(\frac{S}{2}\right)^2 \overline{C}_j$ for $j = 1, ..., S^*$, the orthogonality between the circulant matrices and Theorem 2.6 in Phillips (1988), the following results are consequently obtained:

i) For the zero and Nyquist frequencies ($k = 0, S/2$),

$$\begin{aligned} T^{-1}\sum_{n=1}^{N} Y^{\xi\prime}_{n-1}C_k\Delta_S Y^{\xi}_n &\Rightarrow \frac{\sigma^2_\varepsilon}{S}\frac{\psi(\cos[\omega_k])^2}{S^2}\int_0^1 \mathbf{J}^{\xi}_{c_k}(r)'\,C'_kC_kC_k\mathbf{\Psi}(1)\,d\mathbf{J}^{\xi}_{c_k}(r) + \frac{1}{S}\sum_{j=2}^{\infty} E\left(U^{\xi\prime}_1 C_kU^{\xi}_j\right) \\ &= \frac{\sigma^2_\varepsilon}{S}\psi(\cos[\omega_k])^2\int_0^1 \mathbf{J}^{\xi}_{c_k}(r)'\,C_k d\mathbf{J}^{\xi}_{c_k}(r) + \frac{1}{S}\sum_{j=2}^{\infty} E\left(U^{\xi\prime}_1 C_kU^{\xi}_j\right) \\ &= \sigma^2_\varepsilon\psi(\cos[\omega_k])^2\int_0^1 \mathbf{J}^{\xi*}_{c_k}(r)'\,C_k d\mathbf{J}^{\xi*}_{c_k}(r) + \frac{1}{S}\sum_{j=2}^{\infty} E\left(U^{\xi\prime}_1 C_kU^{\xi}_j\right) \end{aligned} \tag{B.9}$$

where $\omega_0 = 0$ and $\omega_{S/2} = \pi$.

ii) For the harmonic frequencies ($j = 1, ..., S^*$),

$$\begin{aligned} T^{-1}\sum_{n=1}^{N} Y^{\xi\prime}_{n-1}C_j\Delta_S Y^{\xi}_n &\Rightarrow \frac{\sigma^2_\varepsilon}{S}\left(\frac{2}{S}\right)^2 b_j\int_0^1 \mathbf{J}^{\xi}_{c_j}(r)'\,C'_jC_j\left(b_jC_j + a_j\overline{C}_j\right)d\mathbf{J}^{\xi}_{c_j}(r) \\ &\quad + \frac{\sigma^2_\varepsilon}{S}\left(\frac{2}{S}\right)^2 a_j\int_0^1 \mathbf{J}^{\xi}_{c_j}(r)'\,\overline{C}'_jC_j\left(b_jC_j + a_j\overline{C}_j\right)d\mathbf{J}^{\xi}_{c_j}(r) + \frac{1}{S}\sum_{k=2}^{\infty} E\left(U^{\xi\prime}_1 C_jU^{\xi}_k\right) \\ &= \frac{\sigma^2_\varepsilon}{S}b_j^2\int_0^1 \mathbf{J}^{\xi}_{c_j}(r)'\,C_j d\mathbf{J}^{\xi}_{c_j}(r) + \frac{\sigma^2_\varepsilon}{S}a_jb_j\int_0^1 \mathbf{J}^{\xi}_{c_j}(r)'\,\overline{C}_j d\mathbf{J}^{\xi}_{c_j}(r) \\ &\quad + \frac{\sigma^2_\varepsilon}{S}a_j^2\int_0^1 \mathbf{J}^{\xi}_{c_j}(r)'\,C_j d\mathbf{J}^{\xi}_{c_j}(r) - \frac{\sigma^2_\varepsilon}{S}a_jb_j\int_0^1 \mathbf{J}^{\xi}_{c_j}(r)'\,\overline{C}_j d\mathbf{J}^{\xi}_{c_j}(r) \\ &\quad + \frac{1}{S}\sum_{k=2}^{\infty} E\left(U^{\xi\prime}_1 C_jU^{\xi}_k\right) \\ &= \frac{\sigma^2_\varepsilon\left(a_j^2 + b_j^2\right)}{2}\int_0^1 \mathbf{J}^{\xi\dagger}_{c_j}(r)'\,C_j d\mathbf{J}^{\xi\dagger}_{c_j}(r) + \frac{1}{S}\sum_{k=2}^{\infty} E\left(U^{\xi\prime}_1 C_jU^{\xi}_k\right), \end{aligned} \tag{B.10}$$

$$
\begin{aligned}
T^{-1}\sum_{n=1}^{N} Y_{n-1}^{\xi\prime}\overline{C}_j\Delta_S Y_n^{\xi} \;\Rightarrow\; & \frac{\sigma_\varepsilon^2}{S}\left(\frac{2}{S}\right)^2 b_j\int_0^1 \mathbf{J}_{c_j}^{\xi}(r)'\,C_j'\overline{C}_j\left(b_jC_j+a_j\overline{C}_j\right)d\mathbf{J}_{c_j}^{\xi}(r) \\
& +\frac{\sigma_\varepsilon^2}{S}\left(\frac{2}{S}\right)^2 a_j\int_0^1 \mathbf{J}_{c_j}^{\xi}(r)'\,\overline{C}_j'\overline{C}_j\left(b_jC_j+a_j\overline{C}_j\right)d\mathbf{J}_{c_j}^{\xi}(r)+\frac{1}{S}\sum_{k=2}^{\infty}E\left(U_1^{\xi\prime}\overline{C}_jU_k^{\xi}\right) \\
= \; & \frac{\sigma_\varepsilon^2}{S}b_j^2\int_0^1 \mathbf{J}_{c_j}^{\xi}(r)'\,\overline{C}_j d\mathbf{J}_{c_j}^{\xi}(r)-\frac{\sigma_\varepsilon^2}{S}b_ja_j\int_0^1 \mathbf{J}_{c_j}^{\xi}(r)'\,C_j d\mathbf{J}_{c_j}^{\xi}(r) \\
& +\frac{\sigma_\varepsilon^2}{S}a_jb_j\int_0^1 \mathbf{J}_{c_j}^{\xi}(r)'\,C_j d\mathbf{J}_{c_j}^{\xi}(r)+\frac{\sigma_\varepsilon^2}{S}a_j^2\int_0^1 \mathbf{J}_{c_j}^{\xi}(r)'\,\overline{C}_j d\mathbf{J}_{c_j}^{\xi}(r) \\
& +\frac{1}{S}\sum_{k=2}^{\infty}E\left(U_1^{\xi\prime}C_jU_k^{\xi}\right) \\
= \; & \frac{\sigma_\varepsilon^2\left(a_j^2+b_j^2\right)}{2}\int_0^1 \mathbf{J}_{c_j}^{\xi\dagger}(r)'\,\overline{C}_j d\mathbf{J}_{c_j}^{\xi\dagger}(r)+\frac{1}{S}\sum_{k=2}^{\infty}E\left(U_1^{\xi\prime}\overline{C}_jU_k^{\xi}\right) \qquad \text{(B.11)}
\end{aligned}
$$

where $\mathbf{J}_{c_j}^{\xi\dagger}(r):=\frac{1}{\sqrt{S/2}}\mathbf{J}_{c_j}^{\xi}(r)$.

Moreover, for $k=0$ and $k=S/2$,

$$
\frac{1}{S}\sum_{j=2}^{\infty}E\left(U_1^{\xi\prime}C_kU_j^{\xi}\right)+\Psi_k=\sum_{i=1}^{\infty}\cos\left[i\omega_k\right]\gamma_i=\frac{1}{2}(\lambda_k^2-\gamma_k) \qquad \text{(B.12)}
$$

and for $j=1,2,\ldots,S^*$,

$$
\begin{aligned}
\frac{1}{S}\sum_{k=2}^{\infty}E\left(U_1^{\xi\prime}C_jU_k^{\xi}\right)+\Psi_j^1 &= \sum_{i=1}^{\infty}\cos\left[(S-i)\,\omega_j\right]\gamma_i=\frac{1}{4}(\lambda_j^2-\gamma_0) \qquad \text{(B.13)} \\
\frac{1}{S}\sum_{k=2}^{\infty}E\left(U_1^{\xi\prime}\overline{C}_jU_k^{\xi}\right)+\Psi_j^2 &= -\sum_{i=1}^{\infty}\sin\left[(S-i)\,\omega_j\right]\gamma_i=\frac{1}{4}(\lambda_j^{*2}-\gamma_0) \qquad \text{(B.14)}
\end{aligned}
$$

with $\omega_j=\frac{2\pi j}{S}$.

Combining the results in (B.6), (B.9) and (B.12) and in (B.7), (B.8) and (B.12) we establish that for $k=0$ ($\omega_0=0$) and $k=S/2$ ($\omega_{S/2}=\pi$),

$$
T\widehat{\pi}_k\Rightarrow\frac{\int_0^1 \mathbf{J}_{c_k}^{\xi*}(r)'\,C_k d\mathbf{J}_{c_k}^{\xi*}(r)+\left(\sum_{i=1}^{\infty}\cos\left[i\omega_k\right]\gamma_i\right)/\sigma_\varepsilon^2\left[\psi\left(\cos[\omega_k]\right)\right]^2}{\int_0^1 \mathbf{J}_{c_k}^{\xi*}(r)'\,C_k\mathbf{J}_{c_k}^{\xi*}(r)\,dr} \qquad \text{(B.15)}
$$

and for $j=1,...,S^*$ that,

$$
\begin{aligned}
T\widehat{\pi}_j &\Rightarrow \frac{\frac{\sigma_\varepsilon^2\left(a_j^2+b_j^2\right)}{2}\int_0^1 \mathbf{J}_{c_j}^{\xi\dagger}(r)'\,C_j d\mathbf{J}_{c_j}^{\xi\dagger}(r)+\left(\sum_{i=1}^{\infty}\cos\left[(S-i)\,\omega_j\right]\gamma_i\right)}{\frac{\sigma_\varepsilon^2\left(a_j^2+b_j^2\right)}{4}\int_0^1 \mathbf{J}_{c_j}^{\xi\dagger}(r)'\,C_j\mathbf{J}_{c_j}^{\xi\dagger}(r)\,dr} \qquad \text{(B.16)} \\
T\widehat{\pi}_j^* &\Rightarrow \frac{\frac{\sigma_\varepsilon^2\left(a_j^2+b_j^2\right)}{2}\int_0^1 \mathbf{J}_{c_j}^{\xi\dagger}(r)'\,\overline{C}_j d\mathbf{J}_{c_j}^{\xi\dagger}(r)+\left(\sum_{i=1}^{\infty}\sin\left[(S-i)\,\omega_j\right]\gamma_i\right)}{\frac{\sigma_\varepsilon^2\left(a_j^2+b_j^2\right)}{4}\int_0^1 \mathbf{J}_{c_j}^{\xi\dagger}(r)'\,C_j\mathbf{J}_{c_j}^{\xi\dagger}(r)\,dr}. \qquad \text{(B.17)}
\end{aligned}
$$

Next observe that the corresponding t-statistics from (3.1) can be written as

$$
\begin{aligned}
t_k &= \widehat{\gamma}_0^{-1/2}T\widehat{\pi}_k\left[T^{-2}\sum_{n=1}^{N}\sum_{s=1-S}^{0}\left(y_{k,Sn+s}^{\xi}\right)^2\right]^{1/2}+o_p(1),\quad k=0,...,\lfloor S/2\rfloor \qquad \text{(B.18)} \\
t_i^* &= \widehat{\gamma}_0^{-1/2}T\widehat{\pi}_i^*\left[T^{-2}\sum_{n=1}^{N}\sum_{s=1-S}^{0}\left(y_{i,Sn+s}^{*\xi}\right)^2\right]^{1/2}+o_p(1),\quad i=1,\ldots,S^* \qquad \text{(B.19)}
\end{aligned}
$$

where $\widehat{\gamma}_0$ is the usual OLS variance estimator from (3.1); that is, $\widehat{\gamma}_0 := T^{-1}\sum_{n=1}^{N}\sum_{s=1-S}^{0}(\hat{u}^{\xi}_{Sn+s})^2$. Observe from (B.15)-(B.17) we obtain that $\widehat{\pi}_j = o_p(1)$ and $\widehat{\pi}^*_j = o_p(1)$, and hence $\widehat{\gamma}_0 := T^{-1}\sum_{n=1}^{N}\sum_{s=1-S}^{0}(\Delta_S y^{\xi}_{Sn+s})^2 + o_p(1)$ so that $\widehat{\gamma}_0 \xrightarrow{p} \sigma^2_{\varepsilon}\left(1+\sum_{j=1}^{\infty}\psi_j^2\right)$.

Substituting the results that $\widehat{\gamma}_0 \xrightarrow{p} \sigma^2_{\varepsilon}\left(1+\sum_{j=1}^{\infty}\psi_j^2\right)$, the results in Remark A.1, and the results in (B.15)-(B.17) and (B.4)-(B.5) into (B.18)-(B.19) and using applications of the CMT, after some simple manipulations, we finally obtain the stated results in Theorem 4.1, where we have defined the independent standard OU processes $J^{\zeta}_{i,c_i}(r) := \mathbf{v}_i'\mathbf{J}^{\xi*}_{c_i}(r)$, $i = 0, S/2$, $J^{\zeta}_{j,c_j}(r) := \mathbf{h}_j'\mathbf{J}^{\xi\dagger}_{c_j}(r)$ and $J^{\zeta*}_{j,c_j}(r) := \mathbf{h}_j^{*\prime}\mathbf{J}^{\xi\dagger}_{c_j}(r)$ where $\mathbf{h}_j'$ and $\mathbf{h}_j^{*\prime}$ are the first and second rows of $\mathbf{v}_j'$, respectively, for $j = 1,\ldots,S^*$ (see Remarks A.1 and A.3). ■

B.2 Proof of Theorem 4.2

Observe that, using Lemma A.2, (A.21), (A.22), (A.23) and (A.24) it follows that,

$$\begin{aligned} N^{-1/2}y^{\xi}_{0,S\lfloor rN\rfloor+s} &\Rightarrow \sigma\sqrt{S}\psi(1)\,J^{\zeta}_{0,c_0}(r) \\ N^{-1/2}y^{\xi}_{S/2,S\lfloor rN\rfloor+s} &\Rightarrow \sigma\sqrt{S}\psi(-1)(-1)^s\,J^{\zeta}_{S/2,c_{S/2}}(r). \end{aligned}$$

Consequently, for the $\mathcal{MZ}_{\pi_k}$, $k = 0, S/2$ tests we obtain that,

$$(SN)^{-1/2}\,y^{\xi}_{0,SN} \Rightarrow \sigma\psi(1)\,J^{\zeta}_{0,c_0}(1) \tag{B.20}$$

$$(SN)^{-1/2}\,y^{\xi}_{S/2,SN} \Rightarrow \sigma\psi(-1)(-1)^S\,J^{\zeta}_{S/2,c_{S/2}}(1). \tag{B.21}$$

Using the results in (B.20), (B.21) and (B.4) and the fact that $\hat{\lambda}^2_0 \xrightarrow{p} \sigma^2_{\varepsilon}\psi(1)^2$ and $\hat{\lambda}^2_{S/2} \xrightarrow{p} \sigma^2_{\varepsilon}\psi(-1)^2$, it therefore follows that,

$$\mathcal{MZ}_{\pi_k} \Rightarrow \frac{\sigma^2_{\varepsilon}\psi(\cos[\omega_k])^2\,J^{\zeta}_{k,c_k}(1)^2 - \sigma^2_{\varepsilon}\psi(\cos[\omega_k])^2}{2\sigma^2_{\varepsilon}\psi(\cos[\omega_k])^2\int_0^1\left[J^{\zeta}_{k,c_k}(r)\right]^2 dr} = \frac{\left[J^{\zeta}_{k,c_k}(1)\right]^2 - 1}{2\int_0^1\left[J^{\zeta}_{k,c_k}(r)\right]^2 dr},\ k = 0, S/2 \tag{B.22}$$

where $\omega_0 = 0$ and $\omega_{S/2} = \pi$. The results for the $\mathcal{MSB}_k$, $k = 0, S/2$, statistics are easily obtained from (B.4) and (B.5). Combining the results for $\mathcal{MSB}_k$ with (B.22), the limit of $\mathcal{MZ}_{t_k}$ then follows straightforwardly.

Turning to the harmonic frequency statistics, note first that the circulant matrix associated with the filter $\Delta^0_k(L) = \sin[\omega_k]^{-1}\left(\sum_{j=0}^{S-1}\sin[(j+1)\omega_k]L^j\right)$ (see Remark 2 in Smith, Taylor and del Barrio Castro, 2009) is:

$$\begin{aligned} C^k &:= \mathsf{Circ}\left[\frac{\sin[\omega_k]}{\sin[\omega_k]}, \frac{\sin[S\omega_k]}{\sin[\omega_k]}, \frac{\sin[(S-1)\omega_k]}{\sin[\omega_k]}, \ldots, \frac{\sin[2\omega_k]}{\sin[\omega_k]}\right] \\ &= C_k + \frac{\cos[\omega_k]}{\sin[\omega_k]}\overline{C}_k \end{aligned} \tag{B.23}$$

where C_k and $\overline{C}_k$ are defined in Remark A.1. Hence, as in Lemma A.2, the effect of the filter $\Delta^0_k(L)$ on y^{ξ}_{Sn+s} can be illustrated by pre-multiplying (A.10) by the circulant matrix C^k:

$$C^k Y^{\xi}_n = \left(C_k + \frac{\cos[\omega_k]}{\sin[\omega_k]}\overline{C}_k\right)\sum_{i=1}^{n}\exp\left(\frac{c_k}{N}\right)^{n-i}U^{\xi}_i + o_p(1) \tag{B.24}$$

where $C^k := \left(C_k + \frac{\cos[\omega_k]}{\sin[\omega_k]}\overline{C}_k\right)$, $C_kC_j = C_k\overline{C}_j = 0$ for $k \neq j$ and $C_kC_k = \frac{S}{2}C_k$ and $\overline{C}_kC_k = \frac{S}{2}\overline{C}_k$. Note that for C^k it also holds (see Property 1.3 and expression (2) in Gregoir, 2006) that,

$$C^k = \frac{e^{-i\omega_k}}{e^{-i\omega_k} - e^{i\omega_k}}C_k^- + \frac{e^{i\omega_k}}{e^{i\omega_k} - e^{-i\omega_k}}C_k^+ \tag{B.25}$$

with

$$\begin{aligned} C_k^- &:= \mathsf{Circ}\left[1, e^{-i(S-1)\omega_k}, e^{-i(S-2)\omega_k}, \cdots, e^{-i\omega_k}\right] \\ C_k^+ &:= \mathsf{Circ}\left[1, e^{i(S-1)\omega_k}, e^{i(S-2)\omega_k}, \cdots, e^{i\omega_k}\right]. \end{aligned}$$

Moreover, the circulant matrices associated with the filters $\left(1 - e^{i\omega_k}L\right)$ and $\left(1 - e^{-i\omega_k}L\right)$ are given by $D_{\omega_k}^+ := \mathsf{Circ}\left[1, 0, 0, \cdots, 0, e^{i\omega_k}\right]$ and $D_{\omega_k}^- := \mathsf{Circ}\left[1, 0, 0, \cdots, 0, e^{-i\omega_k}\right]$, respectively. Hence, the effects of the filters $\left(1 - e^{-i\omega_k}L\right)\Delta_k^0(L)$ and $\left(1 - e^{-i\omega_k}L\right)\Delta_k^0(L)$ on y_{Sn+s}^ξ can be analysed by pre-multiplying $C^kY_n^\xi$ by $D_{\omega_k}^+$ and $D_{\omega_k}^-$, respectively, *i.e.*,

$$D_{\omega_k}^+C^kY_n^\xi = C_k^-\sum_{i=1}^n \exp\left(\frac{c_k}{N}\right)^{n-i}U_i^\xi + o_p(1) \tag{B.26}$$

$$D_{\omega_k}^-C^kY_n^\xi = C_k^+\sum_{i=1}^n \exp\left(\frac{c_k}{N}\right)^{n-i}U_i^\xi + o_p(1) \tag{B.27}$$

where we use the facts that $D_{\omega_k}^-C_k^- = D_{\omega_k}^+C_k^+ = 0$, that $\frac{e^{-i\omega_k}}{e^{-i\omega_k}-e^{i\omega_k}}D_{\omega_k}^+C_k^- = C_k^-$, and that $\frac{e^{i\omega_k}}{e^{i\omega_k}-e^{-i\omega_k}}D_{\omega_k}^-C_k^+ = C_k^+$, each of which follows from the properties of the product of circulant matrices. Hence, from (B.26) and (B.27) we have, as in (A.16), that,

$$\frac{1}{\sqrt{N}}D_{\omega_k}^+C^kY_{[rN]}^\xi \Rightarrow \sigma C_k^-\Psi(1)\mathbf{J}_{c_k}^\xi(r) = \sigma\psi\left(e^{i\omega_k}\right)\mathcal{E}_1^-\mathcal{E}_2^{-\prime}\mathbf{J}_{c_k}^\xi(r) \tag{B.28}$$

and

$$\frac{1}{\sqrt{N}}D_{\omega_k}^-C^kY_{[rN]}^\xi \Rightarrow \sigma C_k^+\Psi(1)\mathbf{J}_{c_k}^\xi(r) = \sigma\psi\left(e^{-i\omega_k}\right)\mathcal{E}_1^+\mathcal{E}_2^{+\prime}\mathbf{J}_{c_k}^\xi(r) \tag{B.29}$$

where $\mathcal{E}_1^- := [1, e^{-i\omega_k}, e^{-i2\omega_k}, ..., e^{-i(S-1)\omega_k}]'$, $\mathcal{E}_2^- := [1, e^{-i(S-1)\omega_k}, e^{-i(S-1)\omega_k}, ..., e^{-i\omega_k}]'$, $\mathcal{E}_1^+ := [1, e^{i\omega_k}, e^{i2\omega_k}, ..., e^{i(S-1)\omega_k}]'$, $\mathcal{E}_2^+ := [1, e^{i(S-1)\omega_k}, e^{i(S-1)\omega_k}, ..., e^{i\omega_k}]'$, and $\mathbf{J}_{c_k}^\xi(r)$ is an $S \times 1$ vector of de-meaned/de-trended OU precesses. $\Psi(1)$ is an $S \times S$ circulant matrix $\Psi(1) := \mathsf{Circ}\left[1 + \sum_{j=1}^\infty \psi_{jS}, \sum_{j=1}^\infty \psi_{j(S-1)}, \sum_{j=1}^\infty \psi_{j(S-2)}, \cdots, \sum_{j=1}^\infty \psi_j\right]$ where the ψ_j are the coefficients of the polynomial $\psi(z) := 1 + \sum_{j=1}^\infty z^j\psi_j$ and hence $\psi\left(e^{i\omega_k}\right)$ is $\psi(z)$ evaluated at $z = e^{i\omega_k}$. Notice that C_k^+ and C_k^- are circulant matrices of rank one. For a circulant matrix say $\mathbf{A} := \mathsf{Circ}[a_1, a_2, a_3, \cdots, a_S]$ of order $S \times S$ it is always possible to write $\mathbf{A} = \mathbf{F}\mathbf{\Lambda}\mathbf{F}^*$ where $\mathbf{F}$ is the matrix associated with the eigenvectors and is defined for all circulant matrices as

$$\mathbf{F} := \begin{bmatrix} 1 & 1 & 1 & \cdots & 1 \\ 1 & e^{-i\frac{2\pi}{S}} & e^{-i\frac{4\pi}{S}} & \cdots & e^{-i\frac{2(S-1)\pi}{S}} \\ 1 & e^{-i\frac{4\pi}{S}} & e^{-i\frac{8\pi}{S}} & \cdots & e^{-i\frac{4(S-1)\pi}{S}} \\ \vdots & \vdots & \vdots & \ddots & \vdots \\ 1 & e^{-i\frac{2(S-1)\pi}{S}} & e^{-i\frac{4(S-1)\pi}{S}} & \cdots & e^{-i\frac{2(S-1)^2\pi}{S}} \end{bmatrix},$$

$\mathbf{F}^*$ is the conjugate transpose of $\mathbf{F}$ and $\mathbf{\Lambda} := diag\left[\lambda_1, \lambda_2, , \lambda_3, \cdots, \lambda_S\right]$, where $\lambda_j,\ j = 1, 2, 3, \cdots, S$, are the eigenvalues of $\mathbf{A}$, which can be obtained as $\lambda_j := P_A(\exp(\frac{2\pi}{S})^{j-1})$, where $P_A(z) := \sum_{j=1}^{S} a_j z^{j-1}$ is the polynomial associated with the circulant matrix $\mathbf{A}$. Hence, based on this it can be seen that the matrices C_k^- and C_k^+ have rank one and, from Theorem 3.1.1 of Fuller (1996), that the non-zero eigenvalues of C_k^- and C_k^+, which are equal to S, are located in position $j+1$ for C_k^-, and in position $S-j+1$ for C_k^+, where j is such that $\omega_j = \frac{2\pi j}{S}$. The results in (B.28) and (B.29) then follow straightforwardly. Note also that in the case of $D_{\omega_k}^-$ the element in position $j+1$ in the principal diagonal of the matrix of eigenvalues will be zero and, similarly, in the case of $D_{\omega_k}^+$ the element in position $S-j+1$.

Next observe that the vector of seasons representations of (3.23) and (3.24) with $Y_{k,n}^{\xi,\mathtt{D}h} := \left[y_{k,Sn-(S-1)}^{\xi,\mathtt{D}h},\ y_{k,Sn-(S-2)}^{\xi,\mathtt{D}h}, \cdots, y_{k,Sn}^{\xi,\mathtt{D}h}\right]'$, $h = a$ and b based on (B.28) and (B.29) are such that

$$\begin{aligned}
\frac{1}{\sqrt{SN}} Y_{k,[rN]}^{\xi,\mathtt{D}a} \quad \Rightarrow \quad & \frac{\sigma}{\sqrt{S}}\psi\left(e^{i\omega_k}\right)\left(e^{i\omega_k}\mathbf{1}\right)\mathcal{E}_2^{-\prime}\mathbf{J}_{c_k}^{\xi}(r) = \frac{\sigma}{\sqrt{S}}\psi\left(e^{i\omega_k}\right)\mathbf{1}e^{i\omega_k}\mathcal{E}_1^{+\prime}\mathbf{J}_{c_k}^{\xi}(r) \\
= \quad & \frac{\sigma}{\sqrt{2}}\psi\left(e^{i\omega_k}\right)\mathbf{1}\left[\mathbf{h}_k'\frac{1}{\sqrt{S/2}}\mathbf{J}_{c_k}^{\xi}(r) + i\mathbf{h}_k^{*\prime}\frac{1}{\sqrt{S/2}}\mathbf{J}_{c_k}^{\xi}(r)\right] \\
= \quad & \frac{\sigma}{\sqrt{2}}\psi\left(e^{i\omega_k}\right)\mathbf{1}\left[\mathbf{h}_k'\mathbf{J}_{c_k}^{\xi\dagger}(r) + i\mathbf{h}_k^{*\prime}\mathbf{J}_{c_k}^{\xi\dagger}(r)\right] \\
= \quad & \frac{\sigma}{\sqrt{2}}\psi\left(e^{i\omega_k}\right)\mathbf{1}\left[J_{k,c_k}^{\zeta}(r) + iJ_{k,c_k}^{\zeta *}(r)\right] \qquad \text{(B.30)}
\end{aligned}$$

and

$$\begin{aligned}
\frac{1}{\sqrt{SN}} Y_{k,[rN]}^{\xi,\mathtt{D}b} \quad \Rightarrow \quad & \frac{\sigma}{\sqrt{S}}\psi\left(e^{-i\omega_k}\right)\left(e^{-i\omega_k}\mathbf{1}\right)\mathcal{E}_2^{+\prime}\mathbf{J}_{c_k}^{\xi}(r) = \frac{\sigma}{\sqrt{S}}\psi\left(e^{-i\omega_k}\right)\mathbf{1}e^{-i\omega_k}\mathcal{E}_1^{-\prime}\mathbf{J}_{c_k}^{\xi}(r) \\
= \quad & \frac{\sigma}{\sqrt{2}}\psi\left(e^{-i\omega_k}\right)\mathbf{1}\left[\mathbf{h}_k'\frac{1}{\sqrt{S/2}}\mathbf{J}_{c_k}^{\xi}(r) - i\mathbf{h}_k^{*\prime}\frac{1}{\sqrt{S/2}}\mathbf{J}_{c_k}^{\xi}(r)\right] \\
= \quad & \frac{\sigma}{\sqrt{2}}\psi\left(e^{-i\omega_k}\right)\mathbf{1}\left[\mathbf{h}_k'\mathbf{J}_{c_k}^{\xi\dagger}(r) - i\mathbf{h}_k^{*\prime}\mathbf{J}_{c_k}^{\xi\dagger}(r)\right] \\
= \quad & \frac{\sigma}{\sqrt{2}}\psi\left(e^{-i\omega_k}\right)\mathbf{1}\left[J_{k,c_k}^{\zeta}(r) - iJ_{k,c_k}^{\zeta *}(r)\right] \qquad \text{(B.31)}
\end{aligned}$$

respectively, where $\mathbf{1}$ is an $S \times 1$ vector of ones, $\mathbf{h}_k$ and $\mathbf{h}_k^*$, are defined in Remark A.1, $\mathbf{J}_{c_k}^{\xi}(r)$ and $\mathbf{J}_{c_k}^{\xi\dagger}(r)$ are defined in Lemma A.1 and finally $J_{c_k}^{\zeta}(r)$ and $J_{c_k}^{\zeta *}(r)$ are defined in (A.23), (A.24) and in Remark A.3.

Using the consistency of the estimators of $\sigma\psi\left(e^{i\omega_k}\right)$ and $\sigma\psi\left(e^{-i\omega_k}\right)$, $\breve{\lambda}_{k,AR} := s_e\{1 - [\widehat{\phi}(e^{i\omega_k})]\}^{-1}$ and $\breve{\lambda}_{k,AR}^* := s_e\{1 - [\widehat{\phi}(e^{-i\omega_k})]\}^{-1}$ it is then possible to show that,

$$(\breve{\lambda}_{k,AR}^2 T)^{-1/2} y_{k,S\lfloor rN\rfloor+s}^{\xi,\mathtt{D}a} \Rightarrow \frac{1}{\sqrt{2}}\left[J_{k,c_k}^{\zeta}(r) + iJ_{k,c_k}^{\zeta *}(r)\right] = \frac{1}{\sqrt{2}}\mathbb{J}_{k,c_k}(r)$$

$$(\breve{\lambda}_{k,AR}^{*2} T)^{-1/2} y_{k,S\lfloor rN\rfloor+s}^{\xi,\mathtt{D}b} \Rightarrow \frac{1}{\sqrt{2}}\left[J_{k,c_k}^{\zeta}(r) - iJ_{k,c_k}^{\zeta *}(r)\right] = \frac{1}{\sqrt{2}}\overline{\mathbb{J}_{k,c_k}(r)}.$$

Noting that the auxiliary variables $y_{k,Sn+s}^{\mathcal{R}e,\xi}$ and $y_{k,Sn+s}^{\mathcal{I}m,\xi}$ defined in (3.27) and (3.28) are free from nuisance parameters, it is then straightforward from here to obtain the representations given for

the asymptotic distributions of the $\mathcal{K}$-$\mathcal{MZ}_k$, $\mathcal{K}$-$\mathcal{MSB}_k$ and $\mathcal{K}$-$\mathcal{MZ}_{t_k}$ statistics in (4.10), (4.11) and (4.12), along with the results for the joint frequency statistics from section 3.2.2 given in Corollary 4.1 ■

Table 1: Asymptotic critical values for the $\mathcal{MSB}^{\mathtt{D}}$-type and $S^{\mathtt{D}}_{\mathcal{M}}$-type tests

	Case 1				**Case 2**				**Case 3**			
	0.010	0.025	0.050	0.100	0.010	0.025	0.050	0.100	0.010	0.025	0.050	0.100
OLS de-trended												
$\mathcal{MSB}^{\mathtt{D}}_{1}$	0.140	0.153	0.166	0.182	0.140	0.153	0.166	0.182	0.111	0.118	0.125	0.134
$\mathcal{MSB}^{\mathtt{D}}_{12}$	0.259	0.280	0.301	0.327	0.259	0.280	0.301	0.327	0.200	0.212	0.223	0.237
$\mathcal{MSB}^{\mathtt{D}}_{012}$	0.363	0.390	0.416	0.449	0.333	0.355	0.376	0.402	0.274	0.289	0.302	0.319
$\mathcal{S}^{\mathtt{D}}_{\mathcal{M}.1}$	-5.733	-5.312	-4.953	-4.541	-5.733	-5.312	-4.953	-4.541	-6.825	-6.419	-6.079	-5.691
$\mathcal{S}^{\mathtt{D}}_{\mathcal{M}.12}$	-7.904	-7.377	-6.939	-6.426	-7.904	-7.377	-6.939	-6.426	-9.576	-9.073	-8.653	-8.175
$\mathcal{S}^{\mathtt{D}}_{\mathcal{M}.012}$	-9.944	-9.347	-8.833	-8.250	-10.504	-9.920	-9.436	-8.847	-12.23	-11.636	-11.164	-10.615
Local GLS de-trended												
$\mathcal{MSB}^{\mathtt{D}}_{1}$	0.176	0.197	0.219	0.250	0.176	0.197	0.219	0.250	0.125	0.135	0.144	0.156
$\mathcal{MSB}^{\mathtt{D}}_{12}$	0.330	0.368	0.402	0.451	0.333	0.369	0.405	0.453	0.224	0.239	0.253	0.271
$\mathcal{MSB}^{\mathtt{D}}_{012}$	0.474	0.519	0.565	0.624	0.415	0.453	0.488	0.533	0.308	0.327	0.344	0.366
$\mathcal{S}^{\mathtt{D}}_{\mathcal{M}.1}$	-3.951	-3.506	-3.115	-2.648	-3.951	-3.506	-3.115	-2.648	-5.758	-5.350	-5.025	-4.642
$\mathcal{S}^{\mathtt{D}}_{\mathcal{M}.12}$	-5.197	-4.624	-4.168	-3.596	-5.197	-4.623	-4.167	-3.596	-8.012	-7.512	-7.106	-6.647
$\mathcal{S}^{\mathtt{D}}_{\mathcal{M}.012}$	-6.307	-5.679	-5.137	-4.496	-7.245	-6.648	-6.121	-5.519	-10.136	-9.603	-9.134	-8.614

Notes: Case 1 indicates that the deterministic component used consists of a zero and seasonal frequency intercepts; Case 2 indicates that zero and seasonal frequency intercepts and a zero frequency trend were used; and Case 3 indicates that zero and seasonal frequency intercepts and trends were used.

Table 2: Asymptotic critical values for the $F^{\mathtt{D}}_{\mathcal{M}}$-type tests

	Case 1				**Case 2**				**Case 3**			
	0.900	0.950	0.975	0.990	0.900	0.950	0.975	0.990	0.900	0.950	0.975	0.990
OLS de-trended												
$F^{\mathtt{D}}_{\mathcal{M}.1}$	5.540	6.555	7.496	8.648	5.540	6.555	7.496	8.648	8.420	9.615	10.667	12.028
$F^{\mathtt{D}}_{\mathcal{M}.12}$	5.087	5.867	6.592	7.498	2.333	2.869	3.384	4.064	7.847	8.778	9.607	10.682
$F^{\mathtt{D}}_{\mathcal{M}.012}$	6.403	7.278	8.083	9.063	7.338	8.261	9.081	10.069	10.010	11.039	11.967	13.182
Local GLS de-trended												
$F^{\mathtt{D}}_{\mathcal{M}.1}$	2.555	3.259	3.961	4.880	2.555	3.259	3.961	4.880	5.731	6.695	7.565	8.765
$F^{\mathtt{D}}_{\mathcal{M}.12}$	2.352	2.880	3.414	4.052	2.333	2.869	3.384	4.064	5.343	6.089	6.782	7.648
$F^{\mathtt{D}}_{\mathcal{M}.012}$	2.208	2.647	3.073	3.616	3.956	4.620	5.249	6.035	5.099	5.723	6.318	7.016

Note: See notes to Table 1

Table 3: Empirical size of zero frequency unit root tests. MAIC lag selection. DGP (5.1) with $c = 0$ and $u_{4n+s} = \varepsilon_{4n+s} - \theta_1 \varepsilon_{4n+s-1}$.

Case 1: Local GLS de-trended data

N	θ_1	t_0	Z_0	Z_{t_0}	$\mathcal{MZ}_0$	$\mathcal{MZ}_{t_0}$	$\mathcal{MSB}_0$	$P_{0.T}$	F_{012}	$F_{PP.012}$	$F^{\mathtt{D}}_{\mathcal{M}.012}$	$\mathcal{MSB}^{\mathtt{D}}_{012}$	$P_{012.T}$	$S^{\mathtt{D}}_{\mathcal{M}.012}$
50	0.0	0.068	0.076	0.077	0.079	0.083	0.077	0.067	0.065	0.081	0.064	0.117	0.042	0.115
	0.2	0.073	0.091	0.094	0.094	0.098	0.087	0.079	0.068	0.104	0.064	0.119	0.046	0.111
	0.4	0.086	0.117	0.132	0.105	0.111	0.100	0.091	0.075	0.183	0.069	0.123	0.046	0.108
	0.6	0.102	0.218	0.287	0.108	0.115	0.100	0.096	0.076	0.333	0.073	0.131	0.051	0.116
	0.8	0.133	0.652	0.809	0.062	0.069	0.053	0.064	0.086	0.796	0.068	0.099	0.043	0.105
	0.9	0.227	0.953	0.994	0.081	0.086	0.074	0.082	0.151	0.993	0.102	0.061	0.027	0.110
100	0.0	0.063	0.065	0.067	0.066	0.069	0.064	0.061	0.060	0.065	0.052	0.073	0.034	0.072
	0.2	0.064	0.073	0.073	0.073	0.073	0.073	0.065	0.056	0.072	0.054	0.079	0.032	0.069
	0.4	0.070	0.085	0.089	0.079	0.079	0.077	0.074	0.057	0.115	0.057	0.077	0.036	0.072
	0.6	0.079	0.142	0.183	0.078	0.080	0.077	0.072	0.060	0.195	0.060	0.076	0.033	0.075
	0.8	0.103	0.502	0.665	0.046	0.050	0.040	0.050	0.070	0.639	0.050	0.071	0.032	0.069
	0.9	0.182	0.885	0.968	0.028	0.031	0.025	0.032	0.109	0.964	0.056	0.048	0.024	0.066

Case 3: Local GLS de-trended data

N	θ_1	t_0	Z_0	Z_{t_0}	$\mathcal{MZ}_0$	$\mathcal{MZ}_{t_0}$	$\mathcal{MSB}_0$	$P_{0.T}$	F_{012}	$F_{PP.012}$	$F^{\mathtt{D}}_{\mathcal{M}.012}$	$\mathcal{MSB}^{\mathtt{D}}_{012}$	$P_{012.T}$	$S^{\mathtt{D}}_{\mathcal{M}.012}$
50	0.0	0.045	0.048	0.060	0.042	0.045	0.049	0.040	0.067	0.092	0.026	0.039	0.019	0.033
	0.2	0.053	0.074	0.093	0.059	0.065	0.067	0.057	0.069	0.124	0.028	0.038	0.019	0.033
	0.4	0.063	0.131	0.180	0.079	0.084	0.088	0.076	0.069	0.225	0.025	0.033	0.015	0.027
	0.6	0.079	0.325	0.521	0.080	0.084	0.089	0.074	0.092	0.547	0.034	0.031	0.017	0.037
	0.8	0.117	0.886	0.985	0.063	0.067	0.071	0.059	0.121	0.984	0.042	0.015	0.010	0.035
	0.9	0.232	0.998	1.000	0.137	0.140	0.145	0.133	0.205	1.000	0.101	0.006	0.003	0.062
100	0.0	0.042	0.042	0.048	0.040	0.041	0.041	0.046	0.057	0.063	0.032	0.042	0.021	0.036
	0.2	0.045	0.057	0.064	0.051	0.052	0.051	0.056	0.056	0.077	0.031	0.043	0.021	0.036
	0.4	0.060	0.092	0.120	0.065	0.067	0.063	0.072	0.061	0.158	0.034	0.043	0.020	0.038
	0.6	0.065	0.224	0.367	0.056	0.059	0.057	0.065	0.067	0.373	0.042	0.051	0.026	0.048
	0.8	0.082	0.825	0.966	0.020	0.022	0.019	0.027	0.077	0.960	0.034	0.023	0.013	0.033
	0.9	0.165	0.997	1.000	0.023	0.025	0.022	0.029	0.127	1.000	0.041	0.007	0.005	0.033

Notes: Case 1 indicates that the deterministic component used consists of zero and seasonal frequency intercepts; Case 3 indicates that zero and seasonal frequency intercepts and trends were used.

Table 4.a: Empirical size of Nyquist frequency unit root tests. MAIC lag selection. DGP (5.1) with $c = 0$ and $u_{4n+s} = \varepsilon_{4n+s} + \theta_1 \varepsilon_{4n+s-1}$. Local GLS de-trended data; Case 1 (zero and seasonal frequency intercepts).

N	θ_1	t_2	Z_2	Z_{t_2}	$\mathcal{MZ}_2$	$\mathcal{MZ}_{t_2}$	$\mathcal{MSB}_2$	$F_{PP.12}$	$F_{PP.012}$	F_{12}	F_{012}
50	0.0	0.043	0.042	0.052	0.035	0.040	0.034	0.080	0.092	0.062	0.069
	0.2	0.054	0.077	0.094	0.063	0.067	0.058	0.116	0.114	0.062	0.070
	0.4	0.068	0.135	0.191	0.084	0.088	0.081	0.204	0.195	0.061	0.072
	0.6	0.076	0.319	0.518	0.076	0.082	0.071	0.524	0.500	0.082	0.090
	0.8	0.121	0.893	0.986	0.068	0.072	0.064	0.988	0.985	0.112	0.122
	0.9	0.228	0.998	1.000	0.133	0.136	0.130	1.000	1.000	0.202	0.207
100	0.0	0.049	0.050	0.054	0.047	0.048	0.047	0.060	0.066	0.054	0.060
	0.2	0.051	0.062	0.070	0.057	0.058	0.056	0.079	0.077	0.054	0.058
	0.4	0.059	0.094	0.120	0.067	0.069	0.066	0.120	0.111	0.052	0.055
	0.6	0.065	0.238	0.373	0.059	0.061	0.058	0.363	0.346	0.065	0.062
	0.8	0.081	0.827	0.963	0.018	0.019	0.017	0.960	0.956	0.071	0.073
	0.9	0.166	0.996	1.000	0.025	0.026	0.023	1.000	1.000	0.130	0.125

N	θ_1	$F^{\mathtt{D}}_{\mathcal{M}.12}$	$F^{\mathtt{D}}_{\mathcal{M}.012}$	$\mathcal{MSB}^{\mathtt{D}}_{12}$	$\mathcal{MSB}^{\mathtt{D}}_{012}$	$P_{2.T}$	$P_{12.T}$	$P_{012.T}$	$S^{\mathtt{D}}_{\mathcal{M}.12}$	$S^{\mathtt{D}}_{\mathcal{M}.012}$
50	0.0	0.063	0.070	0.092	0.121	0.067	0.041	0.051	0.060	0.118
	0.2	0.057	0.065	0.093	0.116	0.080	0.043	0.047	0.056	0.106
	0.4	0.060	0.070	0.096	0.123	0.089	0.042	0.048	0.058	0.110
	0.6	0.067	0.076	0.108	0.129	0.092	0.050	0.051	0.067	0.117
	0.8	0.066	0.076	0.079	0.096	0.062	0.044	0.046	0.067	0.115
	0.9	0.086	0.097	0.060	0.055	0.079	0.036	0.028	0.071	0.108
100	0.0	0.056	0.054	0.063	0.073	0.063	0.030	0.032	0.040	0.068
	0.2	0.050	0.055	0.069	0.077	0.068	0.035	0.030	0.043	0.072
	0.4	0.059	0.056	0.075	0.079	0.073	0.036	0.035	0.045	0.071
	0.6	0.055	0.057	0.072	0.077	0.072	0.035	0.035	0.047	0.075
	0.8	0.048	0.052	0.060	0.070	0.045	0.031	0.034	0.042	0.071
	0.9	0.052	0.058	0.035	0.041	0.032	0.024	0.022	0.042	0.065

Table 4.b: Empirical size of Nyquist frequency unit root tests. MAIC lag selection. DGP (5.1) with $c = 0$ and $u_{4n+s} = \varepsilon_{4n+s} + \theta_1 \varepsilon_{4n+s-1}$. Local GLS de-trended data; Case 3 (zero and seasonal frequency intercepts and trends).

N	θ_1	t_2	Z_2	Z_{t_2}	$\mathcal{MZ}_2$	$\mathcal{MZ}_{\pi_2}$	$\mathcal{MSB}_2$	$F_{PP.12}$	$F_{PP.012}$	F_{12}	F_{012}
50	0.0	0.043	0.042	0.052	0.035	0.040	0.034	0.080	0.092	0.062	0.069
	0.2	0.054	0.077	0.094	0.063	0.067	0.058	0.116	0.114	0.062	0.070
	0.4	0.068	0.135	0.191	0.084	0.088	0.081	0.204	0.195	0.061	0.072
	0.6	0.076	0.319	0.518	0.076	0.082	0.071	0.524	0.500	0.082	0.090
	0.8	0.121	0.893	0.986	0.068	0.072	0.064	0.988	0.985	0.112	0.122
	0.9	0.228	0.998	1.000	0.133	0.136	0.130	1.000	1.000	0.202	0.207
100	0.0	0.049	0.050	0.054	0.047	0.048	0.047	0.060	0.066	0.054	0.060
	0.2	0.051	0.062	0.070	0.057	0.058	0.056	0.079	0.077	0.054	0.058
	0.4	0.059	0.094	0.120	0.067	0.069	0.066	0.120	0.111	0.052	0.055
	0.6	0.065	0.238	0.373	0.059	0.061	0.058	0.363	0.346	0.065	0.062
	0.8	0.081	0.827	0.963	0.018	0.019	0.017	0.960	0.956	0.071	0.073
	0.9	0.166	0.996	1.000	0.025	0.026	0.023	1.000	1.000	0.130	0.125

N	θ_1	$F^{\mathtt{D}}_{\mathcal{M}.12}$	$F^{\mathtt{D}}_{\mathcal{M}.012}$	$\mathcal{MSB}^{\mathtt{D}}_{12}$	$\mathcal{MSB}^{\mathtt{D}}_{012}$	$P_{2.T}$	$P_{12.T}$	$P_{012.T}$	$S^{\mathtt{D}}_{\mathcal{M}.12}$	$S^{\mathtt{D}}_{\mathcal{M}.012}$
50	0.0	0.031	0.027	0.038	0.035	0.041	0.023	0.019	0.037	0.033
	0.2	0.037	0.026	0.048	0.036	0.067	0.027	0.018	0.039	0.030
	0.4	0.042	0.029	0.056	0.037	0.090	0.033	0.018	0.044	0.031
	0.6	0.049	0.031	0.062	0.032	0.088	0.041	0.017	0.054	0.033
	0.8	0.066	0.046	0.048	0.015	0.077	0.035	0.011	0.063	0.038
	0.9	0.124	0.098	0.055	0.007	0.142	0.030	0.004	0.101	0.058
100	0.0	0.039	0.037	0.039	0.044	0.052	0.020	0.023	0.041	0.041
	0.2	0.038	0.035	0.049	0.044	0.062	0.025	0.021	0.041	0.039
	0.4	0.044	0.035	0.054	0.041	0.073	0.028	0.021	0.048	0.039
	0.6	0.055	0.041	0.059	0.044	0.065	0.034	0.022	0.058	0.044
	0.8	0.039	0.033	0.025	0.023	0.025	0.018	0.013	0.043	0.033
	0.9	0.052	0.042	0.017	0.006	0.029	0.013	0.004	0.046	0.031

Table 5a: Empirical size of harmonic frequency unit root tests. MAIC lag selection. Order selection based on MAIC.
DGP (5.1) with $c = 0$ and $u_{4n+s} = \varepsilon_{4n+s} + \theta_2 \varepsilon_{4n+s-2}$. Local GLS de-trended data; Case 1 (zero and seasonal frequency intercepts).

N	θ_2	F_1	F_{12}	F_{012}	$F_{PP.1}$	$F_{PP.12}$	$F_{PP.012}$	$\mathcal{MSB}_1^{\mathtt{D}}$	$\mathcal{MSB}_{12}^{\mathtt{D}}$	$\mathcal{MSB}_{012}^{\mathtt{D}}$	$P_{1.T}$	$P_{12.T}$	$P_{012.T}$
50	0.00	0.055	0.065	0.071	0.063	0.077	0.086	0.075	0.096	0.115	0.067	0.040	0.047
	0.04	0.053	0.057	0.063	0.062	0.070	0.074	0.080	0.092	0.112	0.072	0.043	0.043
	0.16	0.052	0.054	0.054	0.076	0.078	0.080	0.104	0.099	0.118	0.093	0.047	0.046
	0.36	0.051	0.061	0.071	0.210	0.217	0.229	0.105	0.124	0.154	0.100	0.061	0.067
	0.64	0.069	0.068	0.067	0.949	0.943	0.942	0.123	0.131	0.156	0.127	0.064	0.069
	0.81	0.116	0.119	0.120	1.000	1.000	1.000	0.121	0.135	0.163	0.146	0.080	0.084
100	0.00	0.044	0.050	0.051	0.048	0.053	0.056	0.060	0.062	0.072	0.056	0.031	0.032
	0.04	0.050	0.048	0.050	0.054	0.053	0.055	0.067	0.060	0.068	0.064	0.030	0.031
	0.16	0.046	0.049	0.050	0.059	0.063	0.066	0.069	0.069	0.077	0.064	0.033	0.034
	0.36	0.042	0.047	0.050	0.170	0.163	0.159	0.074	0.072	0.081	0.071	0.038	0.039
	0.64	0.055	0.052	0.053	0.987	0.985	0.983	0.092	0.087	0.094	0.092	0.045	0.046
	0.81	0.082	0.077	0.076	1.000	1.000	1.000	0.081	0.090	0.094	0.100	0.050	0.049

N	θ_2	$\mathcal{R}$e-$\mathcal{MZ}_1$	$\mathcal{R}$e-$\mathcal{MSB}_1$	$\mathcal{R}$e-$\mathcal{MZ}_{t_1}$	$\mathcal{I}$m-$\mathcal{MZ}_1$	$\mathcal{I}$m-$\mathcal{MSB}_1$	$\mathcal{I}$m-$\mathcal{MZ}_{t_1}$	$F_{\mathcal{M}.1}^{\mathtt{D}}$	$F_{\mathcal{M}.12}^{\mathtt{D}}$	$F_{\mathcal{M}.012}^{\mathtt{D}}$	$S_{\mathcal{M}.1}^{\mathtt{D}}$	$S_{\mathcal{M}.12}^{\mathtt{D}}$	$S_{\mathcal{M}.012}^{\mathtt{D}}$
50	0.00	0.052	0.052	0.052	0.055	0.054	0.058	0.048	0.058	0.061	0.062	0.055	0.109
	0.04	0.062	0.062	0.062	0.057	0.057	0.059	0.054	0.060	0.059	0.069	0.063	0.114
	0.16	0.070	0.069	0.070	0.073	0.073	0.075	0.064	0.067	0.066	0.090	0.070	0.122
	0.36	0.065	0.063	0.066	0.064	0.066	0.065	0.060	0.080	0.093	0.090	0.087	0.159
	0.64	0.046	0.043	0.048	0.050	0.052	0.044	0.049	0.070	0.086	0.095	0.091	0.168
	0.81	0.035	0.032	0.038	0.036	0.039	0.031	0.050	0.094	0.124	0.093	0.105	0.196
100	0.00	0.053	0.051	0.052	0.050	0.050	0.051	0.048	0.049	0.051	0.052	0.039	0.064
	0.04	0.055	0.055	0.055	0.053	0.054	0.055	0.052	0.051	0.051	0.060	0.044	0.070
	0.16	0.052	0.052	0.054	0.050	0.049	0.051	0.049	0.053	0.053	0.058	0.047	0.075
	0.36	0.055	0.056	0.056	0.058	0.059	0.058	0.056	0.063	0.068	0.065	0.053	0.084
	0.64	0.050	0.046	0.053	0.049	0.049	0.047	0.046	0.056	0.062	0.073	0.057	0.094
	0.81	0.017	0.014	0.020	0.018	0.021	0.014	0.025	0.045	0.060	0.058	0.052	0.091

Table 5b: Empirical size of harmonic frequency unit root tests. MAIC lag selection. Order selection based on MAIC.
DGP (5.1) with $c = 0$ and $u_{4n+s} = \varepsilon_{4n+s} + \theta_2 \varepsilon_{4n+s-2}$. Local GLS de-trended data; Case 3 (zero and seasonal frequency intercepts and trends).

N	θ_2	F_1	F_{12}	F_{012}	$F_{PP.1}$	$F_{PP.12}$	$F_{PP.012}$	$\mathcal{MSB}_1^{\mathtt{D}}$	$\mathcal{MSB}_{12}^{\mathtt{D}}$	$\mathcal{MSB}_{012}^{\mathtt{D}}$	$P_{1.T}$	$P_{12.T}$	$P_{012.T}$
50	0.00	0.048	0.059	0.068	0.059	0.078	0.091	0.033	0.034	0.037	0.044	0.021	0.022
	0.04	0.063	0.068	0.070	0.076	0.085	0.093	0.045	0.036	0.032	0.060	0.021	0.019
	0.16	0.067	0.070	0.069	0.123	0.122	0.118	0.067	0.044	0.032	0.085	0.030	0.020
	0.36	0.070	0.090	0.109	0.364	0.360	0.365	0.081	0.066	0.068	0.101	0.043	0.043
	0.64	0.113	0.122	0.130	0.989	0.988	0.986	0.106	0.061	0.047	0.133	0.044	0.027
	0.81	0.246	0.250	0.259	1.000	1.000	1.000	0.174	0.043	0.030	0.202	0.036	0.018
100	0.00	0.046	0.052	0.057	0.048	0.058	0.062	0.039	0.042	0.044	0.044	0.023	0.022
	0.04	0.052	0.053	0.054	0.059	0.060	0.059	0.052	0.041	0.038	0.054	0.023	0.021
	0.16	0.053	0.060	0.064	0.085	0.090	0.091	0.059	0.056	0.052	0.065	0.031	0.028
	0.36	0.054	0.060	0.063	0.309	0.287	0.276	0.066	0.059	0.060	0.072	0.033	0.033
	0.64	0.079	0.079	0.081	0.999	0.998	0.999	0.062	0.059	0.056	0.076	0.034	0.032
	0.81	0.160	0.146	0.143	1.000	1.000	1.000	0.052	0.040	0.034	0.066	0.023	0.017

N	θ_2	$\mathcal{R}e$-$\mathcal{MZ}_1$	$\mathcal{R}e$-$\mathcal{MSB}_1$	$\mathcal{R}e$-$\mathcal{MZ}_{t_1}$	$\mathcal{I}m$-$\mathcal{MZ}_1$	$\mathcal{I}m$-$\mathcal{MSB}_1$	$\mathcal{I}m$-$\mathcal{MZ}_{t_1}$	$F_{\mathcal{M}.1}^{\mathtt{D}}$	$F_{\mathcal{M}.12}^{\mathtt{D}}$	$F_{\mathcal{M}.012}^{\mathtt{D}}$	$S_{\mathcal{M}.1}^{\mathtt{D}}$	$S_{\mathcal{M}.12}^{\mathtt{D}}$	$S_{\mathcal{M}.012}^{\mathtt{D}}$
50	0.00	0.031	0.030	0.032	0.031	0.031	0.031	0.028	0.028	0.026	0.028	0.032	0.032
	0.04	0.037	0.036	0.037	0.036	0.037	0.036	0.042	0.035	0.028	0.042	0.040	0.033
	0.16	0.044	0.043	0.045	0.045	0.047	0.044	0.056	0.046	0.037	0.059	0.051	0.042
	0.36	0.041	0.039	0.042	0.040	0.042	0.038	0.059	0.063	0.064	0.066	0.072	0.074
	0.64	0.034	0.032	0.035	0.039	0.040	0.037	0.072	0.072	0.069	0.085	0.078	0.070
	0.81	0.035	0.034	0.036	0.037	0.039	0.036	0.036	0.036	0.036	0.036	0.039	0.042
100	0.00	0.035	0.034	0.036	0.037	0.039	0.036	0.036	0.036	0.036	0.036	0.039	0.042
	0.04	0.040	0.039	0.040	0.040	0.039	0.040	0.043	0.041	0.034	0.045	0.044	0.038
	0.16	0.041	0.040	0.042	0.040	0.040	0.039	0.047	0.049	0.049	0.050	0.054	0.053
	0.36	0.047	0.046	0.049	0.046	0.047	0.045	0.055	0.057	0.057	0.060	0.062	0.062
	0.64	0.021	0.019	0.023	0.019	0.020	0.018	0.041	0.047	0.049	0.050	0.053	0.052
	0.81	0.013	0.013	0.014	0.012	0.013	0.012	0.031	0.044	0.045	0.039	0.042	0.038

Figure 1: Gaussian asymptotic local power envelopes and asymptotic local power functions of zero, Nyquist and harmonic frequency local GLS de-trended unit root tests

(a) de-meaned zero ($k = 0$) and Nyquist ($k = S/2$) frequency tests

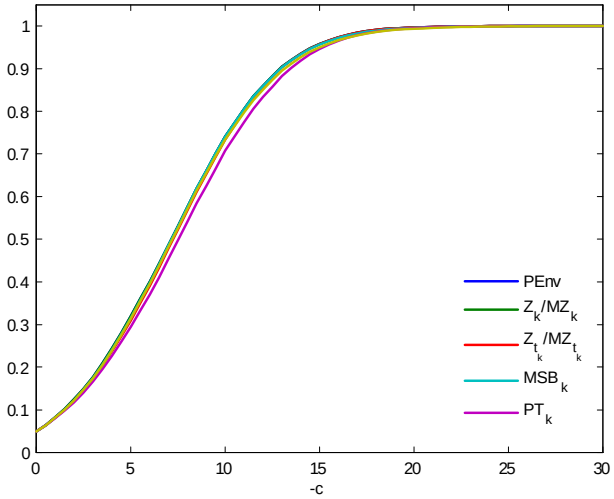

(b) de-trended zero ($k = 0$) and Nyquist ($k = S/2$) frequency tests

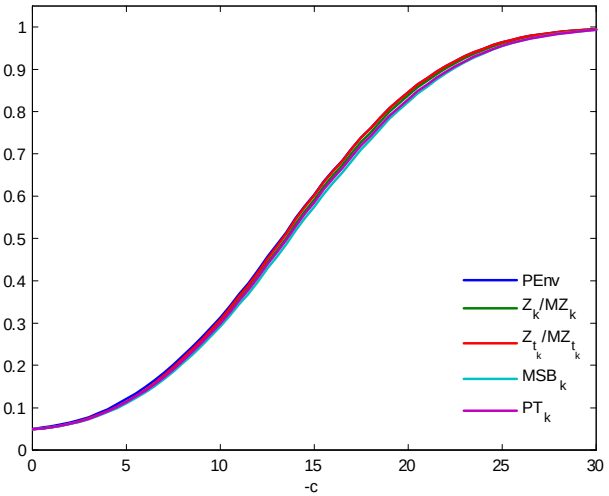

(c) de-meaned harmonic frequency tests ($k \in \{1, ..., S^*\}$)

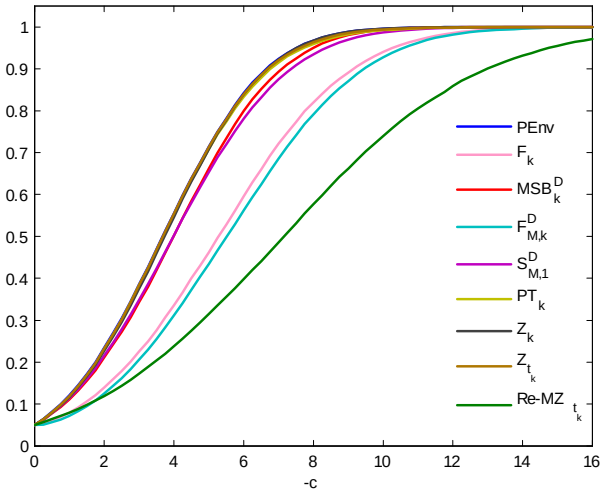

(d) de-trended harmonic frequency tests ($k \in \{1, ..., S^*\}$)

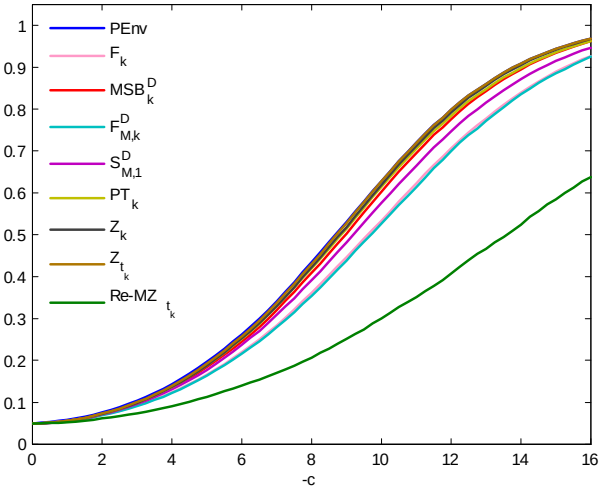

Figure 2: Gaussian asymptotic local power envelopes and asymptotic local power functions of joint frequency local GLS de-trended unit root tests for the quarterly case ($S = 4$)

(a) de-meaned joint seasonal frequency tests

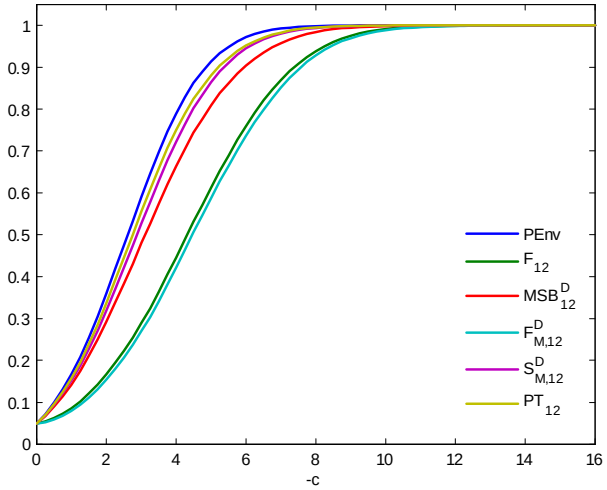

(b) de-trended joint seasonal frequency tests

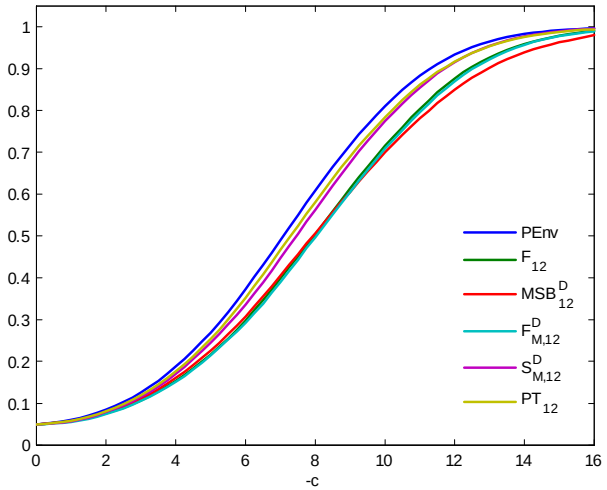

(c) de-meaned joint zero and seasonal frequency tests

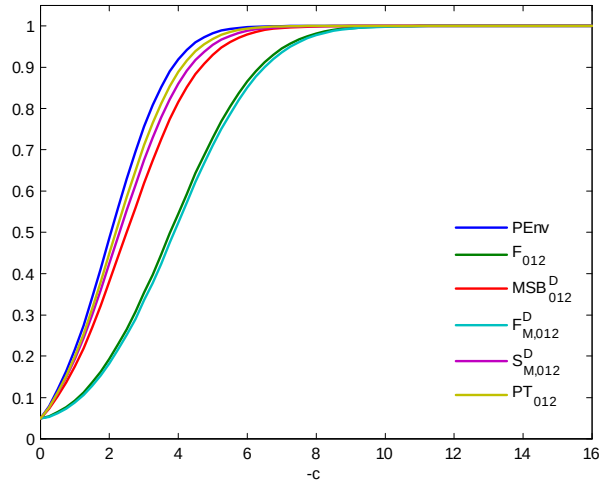

(d) de-trended joint zero and seasonal frequency tests

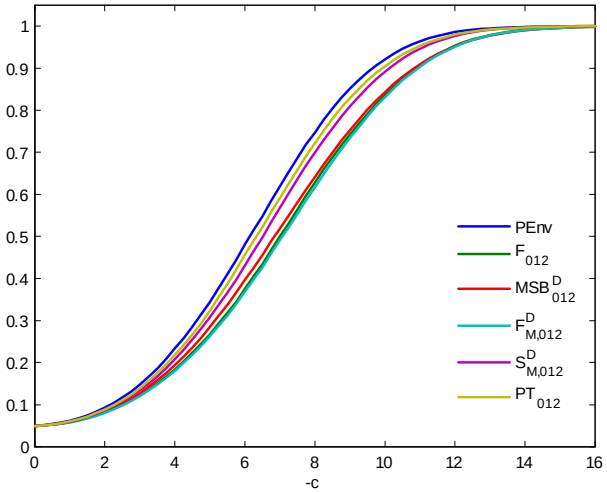

Figure 3: Finite sample size-adjusted power functions of zero frequency unit root tests (quarterly case, $S = 4$)

(a) local GLS de-meaned tests - $N = 50$

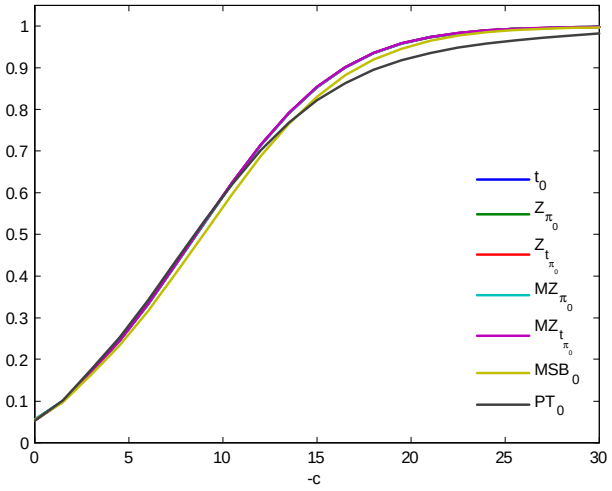

(b) local GLS de-meaned tests - $N = 100$

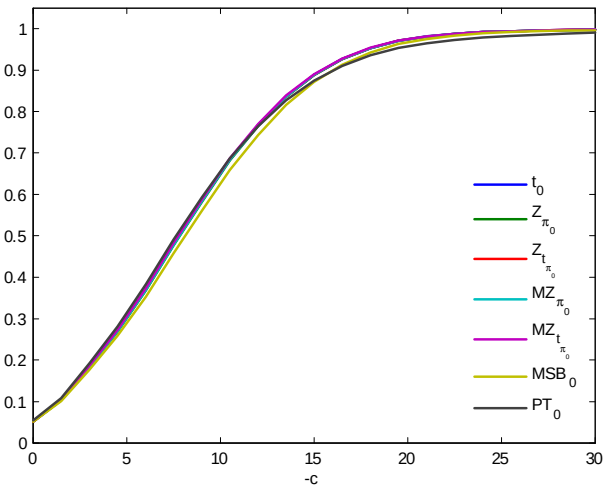

(c) local GLS de-trended tests - $N = 50$

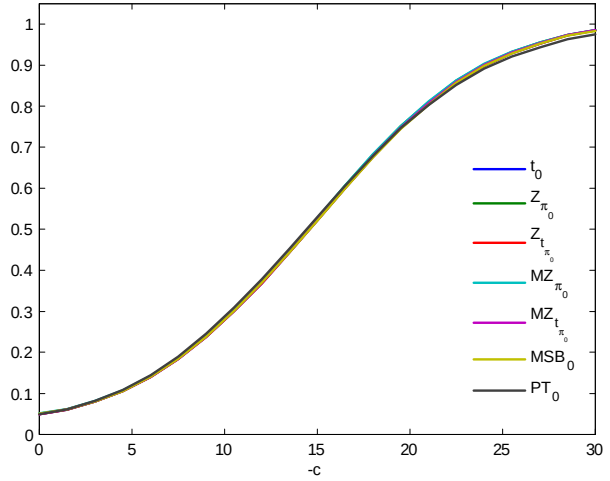

(d) local GLS de-trended tests - $N = 100$

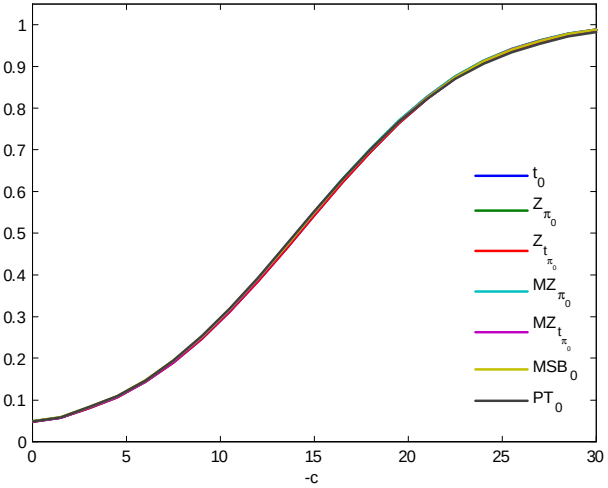

Figure 4: Finite sample size-adjusted power functions of harmonic frequency unit root tests (quarterly case, $S = 4$)

(a) local GLS de-meaned tests - $N = 50$

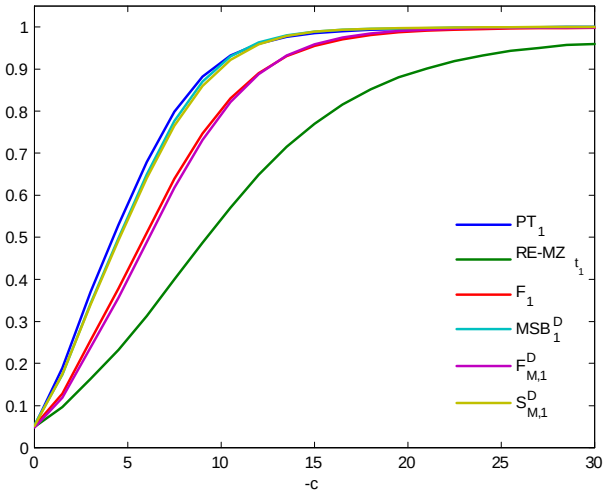

(b) local GLS de-meaned tests - $N = 100$

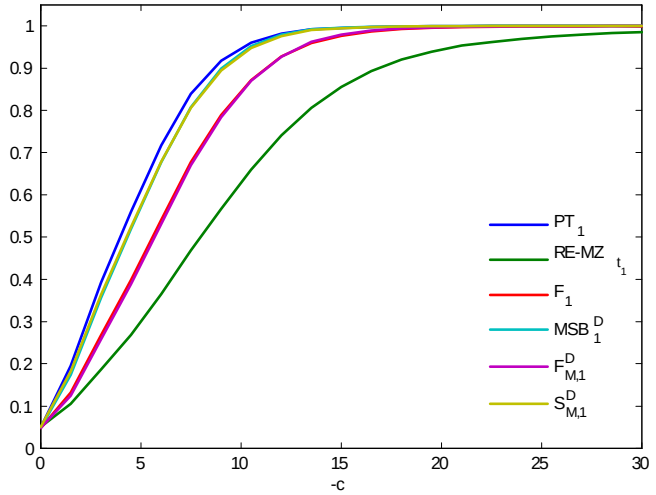

(c) local GLS de-trended tests - $N = 50$

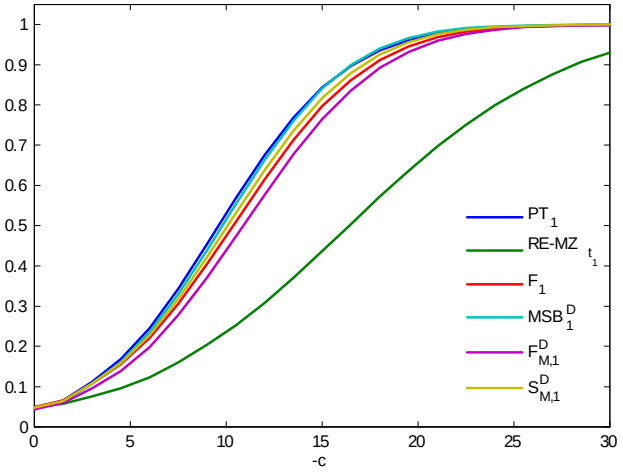

(d) local GLS de-trended tests - $N = 100$

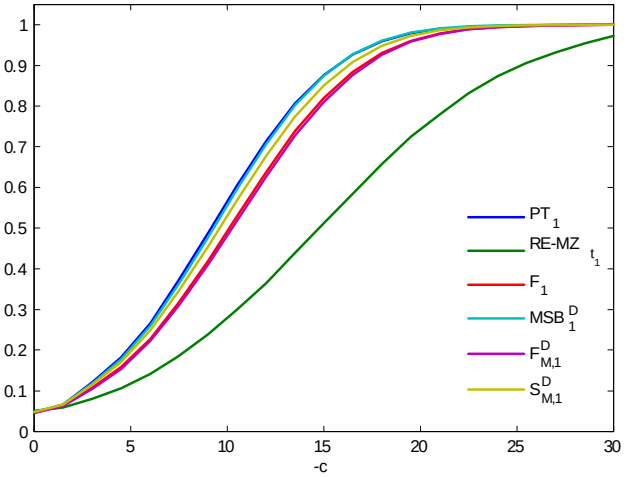

Figure 5: Finite sample size-adjusted power functions of joint seasonal frequency tests (quarterly case, $S = 4$)

(a) local GLS de-meaned tests - $N = 50$

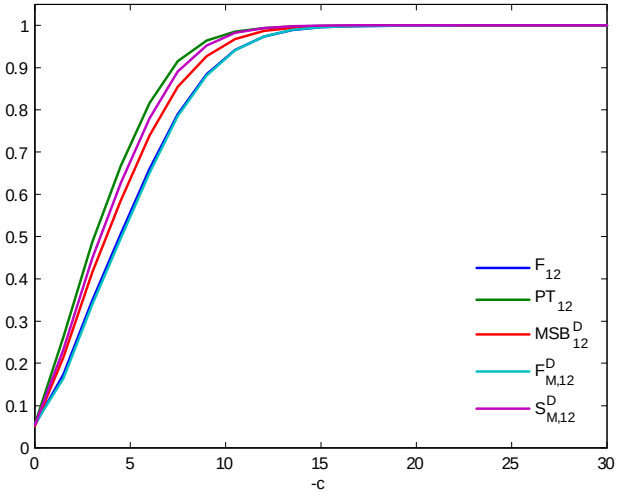

(b) local GLS de-meaned tests - $N = 100$

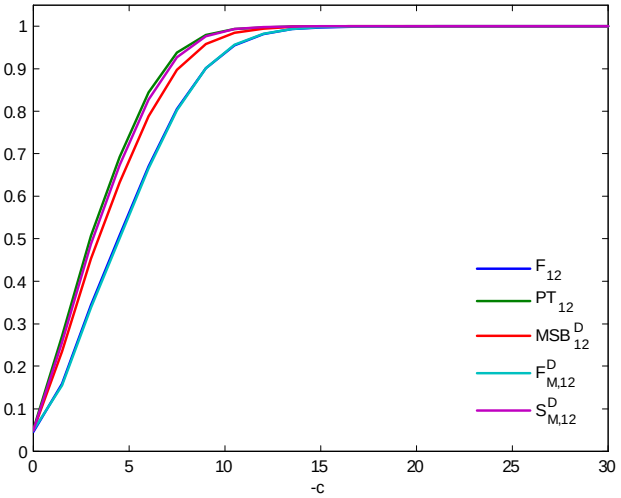

(c) local GLS de-trended tests - $N = 50$

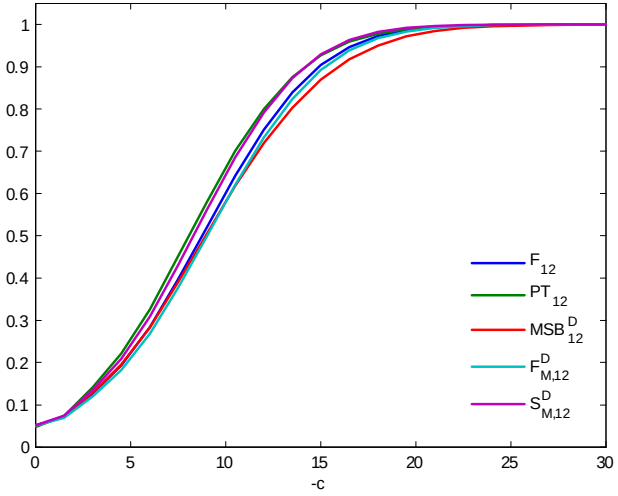

(d) local GLS de-trended tests - $N = 100$

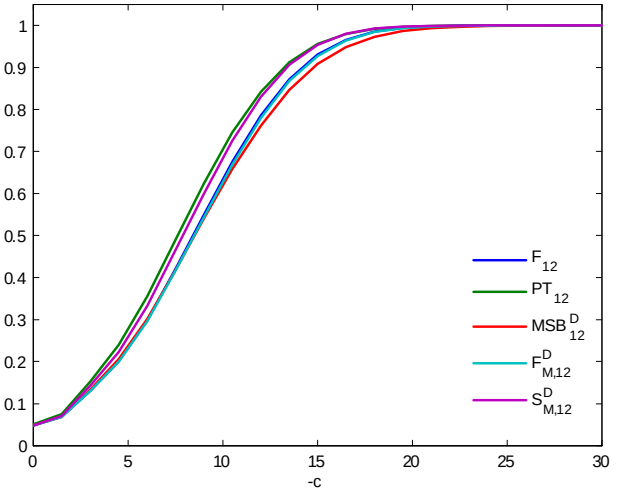

Figure 6: Finite sample size-adjusted power functions of joint zero and seasonal frequency tests (quarterly case, $S = 4$)

(a) local GLS de-meaned tests - $N = 50$

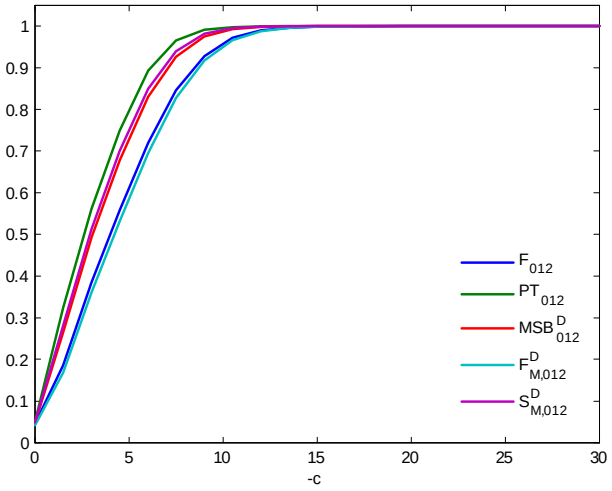

(b) local GLS de-meaned tests - $N = 100$

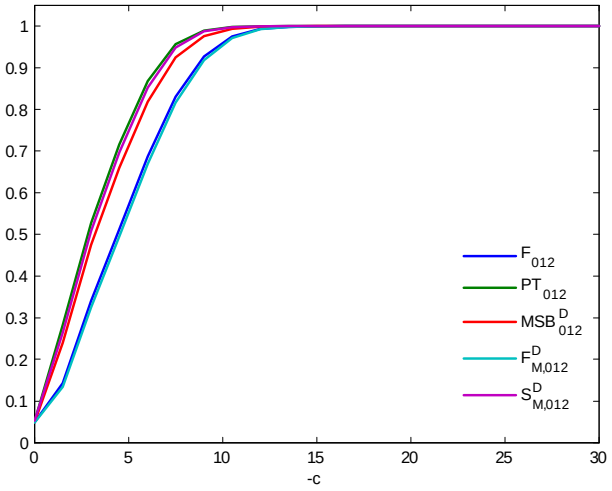

(c) local GLS de-trended tests - $N = 50$

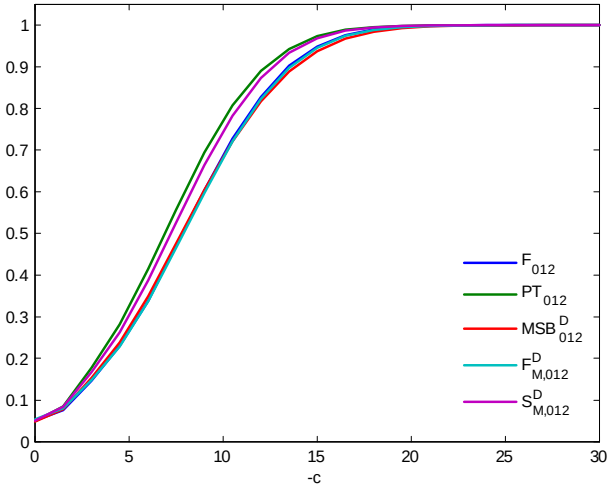

(d) local GLS de-trended tests - $N = 100$